

**OPTIMIZATION OF SCR CONTROL
TECHNOLOGY FOR REDUCED NO_x
EMISSIONS, IMPROVED PERFORMANCE
AND REDUCED OPERATING EXPENSES**

**FINAL REPORT 09-09
APRIL 2009**

**NEW YORK STATE
ENERGY RESEARCH AND
DEVELOPMENT AUTHORITY**





NYSERDA

**New York State Energy Research
and Development Authority**

The New York State Energy Research and Development Authority (NYSERDA) is a public benefit corporation created in 1975 by the New York State Legislature.

NYSERDA derives its revenues from an annual assessment levied against sales by New York's electric and gas utilities, from public benefit charges paid by New York rate payers, from voluntary annual contributions by the New York Power Authority and the Long Island Power Authority, and from limited corporate funds.

NYSERDA works with businesses, schools, and municipalities to identify existing technologies and equipment to reduce their energy costs. Its responsibilities include:

- Conducting a multifaceted energy and environmental research and development program to meet New York State's diverse economic needs.
- The **New York Energy SmartSM** program provides energy efficiency services, including those directed at the low-income sector, research and development, and environmental protection activities.
- Making energy more affordable for residential and low-income households.
- Helping industries, schools, hospitals, municipalities, not-for-profits, and the residential sector, implement energy-efficiency measures. NYSERDA research projects help the State's businesses and municipalities with their energy and environmental problems.
- Providing objective, credible, and useful energy analysis and planning to guide decisions made by major energy stakeholders in the private and public sectors.
- Since 1990, NYSERDA has developed and brought into use successful innovative, energy-efficient, and environmentally beneficial products, processes, and services.
- Managing the Western New York Nuclear Service Center at West Valley, including: overseeing the State's interests and share of costs at the West Valley Demonstration Project, a federal/State radioactive waste clean-up effort, and managing wastes and maintaining facilities at the shut-down State-Licensed Disposal Area.
- Coordinating the State's activities on energy emergencies and nuclear regulatory matters, and monitoring low-level radioactive waste generation and management in the State.
- Financing energy-related projects, reducing costs for ratepayers.

For more information, contact the Communications unit, NYSERDA, 17 Columbia Circle, Albany, New York 12203-6399; toll-free 1-866-NYSERDA, locally (518) 862-1090, ext. 3250; or on the web at www.nyserdera.org

STATE OF NEW YORK
David A. Paterson, Governor

ENERGY RESEARCH AND DEVELOPMENT AUTHORITY
Vincent A. DeIorio, Esq., Chairman
Francis J. Murray, Jr., President and Chief Executive Officer

**OPTIMIZATION OF SCR CONTROL TECHNOLOGY FOR
REDUCED NO_x EMISSIONS, IMPROVED PERFORMANCE
AND REDUCED OPERATING EXPENSES**

Final Report

Prepared for the
**NEW YORK STATE
ENERGY RESEARCH AND
DEVELOPMENT AUTHORITY**

Albany, NY
www.nyserda.org

Barry Liebowitz
Senior Project Manager

Prepared by:
ENERGY RESEARCH CENTER
Bethlehem, PA

Carlos E. Romero
Project Manager

with

Eugenio Schuster
Fengqi Si
Zheng Yao

NOTICE

This report was prepared by the Energy Research Center in the course of performing work contracted for and sponsored by the New York State Energy Research and Development Authority and AES Cayuga (hereafter the “Sponsors”). The opinions expressed in this report do not necessarily reflect those of the Sponsors or the State of New York, and reference to any specific product, service, process, or method does not constitute an implied or expressed recommendation or endorsement of it. Further, the Sponsors and the State of New York, make no warranties or representations, expressed or implied, as to the fitness for particular purpose or merchantability of any product, apparatus, or service, or the usefulness, completeness, or accuracy of any process, methods, or other information contained, described, disclosed, or referred to in this report. The Sponsors, the State of New York, and the contractor make no representation that the use of any product, apparatus, process, method, or other information will not infringe privately owned rights and will assume no liability for any loss, injury, or damage resulting from, or occurring in connection with, the use of information contained, described, disclosed, or referred to in this report.

ABSTRACT

A feasibility project was performed at Cayuga Unit 1 with funding from the New York State Energy Research and Development Authority and AES Cayuga to develop an optimization methodology and demonstrate the combined optimal operation of boiler, selective catalytic reduction (SCR) system, and back-end air preheater (APH). Cayuga Unit 1 is a 560 MW unit, equipped with a low-NO_x firing system and an anhydrous ammonia (NH₃) SCR reduction system for NO_x emissions control. The boiler and low-NO_x system control settings, and SCR and APH operating conditions were tested in a parametric test program. Information from a Breen Energy Solutions ammonium bisulfate (ABS) probe was included for monitoring ammonium salts formation in real-time and as a constraint to the SCR optimization. The parametric test data were used as the basis for the optimization that consisted of an approach, which incorporates accurate on-line support vector regression modeling for adaptive learning, and genetic algorithms for implementation of the multi-objective optimization. Upgrades to the SCR control scheme were proposed using a multi-loop control with proportional-integral-derivative (PID) control tuning and extremum seeking. The results indicate that optimal operating conditions can be achieved for a coordinated boiler/SCR/APH operation that exhibits minimal NH₃ consumption, maximum SCR performance, and optimal net unit heat rate. This optimized operation also results in minimal impact on fly ash unburned carbon content and mitigates ABS formation, and complies with other operational and environmental constraints. The optimal conditions resulted in reduced NH₃ usage of the order of 25 percent, optimal heat rate improvement of approximately 55 Btu/kWh, with improved APH fouling management, and estimated annual cost savings of the order of \$748,000.

Keywords: NO_x Emissions, SCR, Optimization, Control Upgrades.

TABLE OF CONTENTS

| <u>Section</u> | <u>Page</u> |
|---|-------------|
| SUMMARY | S-1 |
| 1 INTRODUCTION..... | 1-1 |
| 2 UNIT DESCRIPTION..... | 2-1 |
| 3 ABS MONITORING..... | 3-1 |
| 4 PARAMETRIC FIELD TESTS | 4-1 |
| 5 DATA ANALYSIS RESULTS AND DISCUSSION | 5-1 |
| DATA ANALYSIS RESULTS..... | 5-1 |
| MODELING RESULTS | 5-15 |
| OPTIMIZATION RESULTS..... | 5-16 |
| 6 UPGRADED SCR CONTROL STRATEGY | 6-1 |
| UPGRADED SCR/APH CONTROL SCHEME..... | 6-1 |
| SCR Control..... | 6-1 |
| Air Preheater Control..... | 6-7 |
| Integrated SCR/APH Control..... | 6-11 |
| NON-MODEL-BASED OPTIMAL ADAPTIVE CONTROL | 6-14 |
| Extremum Seeking..... | 6-14 |
| Real-Time Boiler Optimization..... | 6-16 |
| 7 EVALUATION OF BENEFITS | 7-1 |
| 8 CONCLUSIONS AND RECOMMENDATIONS | 8-1 |
| 9 REFERENCES..... | 9-1 |
| APPENDIX A: CALCULATIONS OF THE EFFECT OF BOILER OPERATING CONDITIONS ON UNIT THERMAL PERFORMANCE FROM TEST DATA | A-1 |
| BACKGROUND..... | A-1 |
| HEAT RATE DIFFERENCE METHOD..... | A-2 |
| Description of the Method | A-2 |
| CALCULATION PROCEDURE..... | A-2 |
| RELEVANT OPERATING PARAMETERS | A-3 |
| Cycle Operating Parameters in Group 1 | A-3 |
| Cycle Operating Parameters in Group 2 | A-3 |
| NUMERICAL EXAMPLE | A-3 |
| RESULTS | A-5 |
| APPENDIX B: CAYUGA UNIT 1 TEST MATRIX..... | B-1 |
| APPENDIX C: FUNDAMENTALS OF EXTREMUM SEEKING | C-1 |

FIGURES

| <u>Figure</u> | <u>Page</u> |
|---------------|--|
| 2-1 | Cayuga Unit 1 – Boiler Configuration 2-1 |
| 3-1 | Representation of APH Temperature Controller Performance..... 3-2 |
| 3-2 | Performance of the APH Temperature Controller..... 3-3 |
| 3-3 | Performance of Ammonia Injection Controller..... 3-3 |
| 5-1 | Contour Plots of O ₂ and NO _x Concentration at the SCR Inlet 5-2 |
| 5-2 | Impact of Boiler Excess O ₂ on Unit Heat Rate Penalty 5-2 |
| 5-3 | Impact of Boiler Excess O ₂ on ABS Formation Temperature..... 5-3 |
| 5-4 | Impact of SOFA Registers on NH ₃ Flow Requirement..... 5-4 |
| 5-5 | Impact of SOFA Registers on ABS Deposition Depth..... 5-4 |
| 5-6 | Impact of SOFA Registers on SCR Removal Efficiency 5-5 |
| 5-7 | Impact of SOFA Registers on Unit Heat Rate Penalty..... 5-5 |
| 5-8 | Impact of 1A1-Mill Coal Flow Rate on SCR Inlet NO _x Emissions 5-6 |
| 5-9 | Impact of Economizer Bypass Damper on SCR Gas Inlet Temperature..... 5-8 |
| 5-10 | Impact of Economizer Bypass Damper on SCR Removal Efficiency..... 5-8 |
| 5-11 | Impact of Ammonia Flow on ABS Formation Temperature and Deposition..... 5-9 |
| 5-12 | Impact of NSR on ABS Formation Temperature and Ammonia in Ash..... 5-10 |
| 5-13 | Impact of APH Bypass Damper Position on ABS Deposition Depth 5-11 |
| 5-14 | Impact of APH Bypass Damper Position on APH Flue Gas Exit Temperature 5-11 |
| 5-15 | Impact of APH Bypass Damper Position on Unit Heat Rate Penalty 5-12 |
| 5-16 | Results of Sootblowing Tests..... 5-13 |
| 5-17 | Proposed Sootblowing Schedule 5-13 |
| 5-18 | Modified AOSVR NO _x Emissions Model Prediction Results..... 5-16 |
| 5-19 | Trained AOSVR Model Results for Boiler Heat Rate Penalty..... 5-17 |
| 5-20 | Lowest NH ₃ Flow Rate vs. SCR Inlet NO _x 5-18 |
| 5-21 | GA Optimization Results for Boiler Outlet NO _x – (a) Initialization Dataset, (b) 1 st Generation, (c) 15 th Generation, (d) 30 th Generation 5-20 |
| 5-22 | GA Optimization Solutions for the Total Cost Function..... 5-21 |
| 5-23 | Cost Components as a Function of Boiler Outlet NO _x 5-22 |
| 6-1 | System Configuration Used for the Control Strategy Upgrade 6-1 |
| 6-2 | SCR Manufacturer’s Typical Control Architecture..... 6-2 |
| 6-3 | SCR Control Architecture Based on the CEM NO _x Input..... 6-2 |
| 6-4 | Multi-Loop SCR Control Architecture Based on CEM NO _x , SCR Inlet NO _x and SCR Outlet NO _x 6-3 |
| 6-5 | SIMULINK SCR Control Configuration 6-3 |
| 6-6 | Simplified SCR Model..... 6-4 |
| 6-7 | SCR Efficiency as a Function of NH ₃ /NO _x _in Ratio 6-4 |
| 6-8 | Transport Channel Simplified Model..... 6-5 |
| 6-9 | SCR Controller..... 6-5 |
| 6-10 | Evolution of the Cost Function 6-6 |
| 6-11 | Evolution of the Controller Gains 6-7 |
| 6-12 | Illustration of the Time Response of the Optimized Multi-Loop Scheme 6-8 |
| 6-13 | APH Control Configuration 6-8 |
| 6-14 | SIMULINK APH Control Configuration 6-9 |
| 6-15 | Simplified APH Model 6-9 |
| 6-16 | ABS Formation Temperature as a Function of NH ₃ /NO _x _in 6-10 |
| 6-17 | ABS Formation Temperature Simplified Model..... 6-10 |
| 6-18 | APH Deposition Depth Controller 6-10 |
| 6-19 | Coordinated SCR and APH PID-Based Control 6-11 |
| 6-20 | SIMULINK Coordinated SCR and APH PID-Based Control..... 6-12 |
| 6-21 | Modification of NO _x _CEM Setpoint..... 6-12 |
| 6-22 | Effect of Modification of NO _x _CEM Setpoint..... 6-13 |

FIGURES (continued)

| <u>Figure</u> | | <u>Page</u> |
|---------------|--|-------------|
| 6-23 | Two-Loop Adaptive Control Strategy with Extremum Seeking | 6-14 |
| 6-24 | Extremum Seeking Approach | 6-15 |
| 6-25 | Example of Extremum Seeking Minimized Cost Function..... | 6-16 |
| 6-26 | Simplified Boiler Dynamic Model | 6-17 |
| 6-27 | Cost Function of O ₂ when SOFA = 0%, Burner Tilt = -4 degrees, SOFA tilt = 1 degree and 1A1 Coal Flow = 15 ton/hr..... | 6-18 |
| 6-28 | SIMULINK Extremum Seeking Boiler Control Configuration | 6-19 |
| 6-29 | Extremum Seeking Implementation for Excess O ₂ Optimal Modulation..... | 6-19 |
| 6-30 | Extremum Seeking Simulation Results (a to e from left to right, top to bottom)..... | 6-20 |
| 6-31 | SIMULINK Extremum Seeking SCR/APH Control Configuration..... | 6-21 |
| 6-32 | Extremum Seeking Implementation for NH ₃ Optimal Modulation..... | 6-22 |
| 6-33 | Extremum Seeking Simulation Results | 6-23 |

TABLES

| <u>Table</u> | <u>Page</u> |
|--------------|--|
| 4-1 | List of Testing Parameters and Their Limits 4-2 |
| 5-1 | Mercury Emissions Estimates for Different Boiler Operation Conditions 5-14 |
| A-1 | Parametric Test Data A-1 |
| A-2 | Sample Test Data A-4 |
| A-3 | Turbine Cycle Corrections and Cycle Performance A-5 |
| A-4 | Effect of Boiler Test Parameters on Unit Heat Rate A-5 |
| B-1 | Cayuga Unit 1 Test Matrix B-2 |

LIST OF ABBREVIATIONS

| | |
|------------------------|---|
| α_T | SOFA Tilt |
| α_{BT} | Burner Tilt |
| θ | Fly Ash Unburned Carbon |
| a_{depth} | ABS Deposition Depth Limit |
| η_B | Boiler Efficiency |
| η_{SCR} | SCR efficiency |
| τ_{SCR} | SCR time constant |
| τ_{TRANSP} | Transport channel time constant |
| ABS | Ammonium Bisulfate |
| AFP | Anti-Fouling Probe |
| A/I | Artificial Intelligence |
| AOSVR | Accurate On-Line Support Vector Regression |
| APH | Air Preheater |
| BL | Baseline |
| C | Cost |
| C_{SCR} | SCR controller transfer function |
| $C_{SCR,OUT}$ | SCR outer-loop controller transfer function |
| $C_{SCR,IN}$ | SCR inner-loop controller transfer function |
| $C_{SCR,FEED}$ | SCR feedforward controller transfer function |
| CCOFA | Closed-Couple Overfire Air |
| CE | Combustion Engineering |
| CF | Correction Factor |
| CFS | Concentric Firing System |
| CO | Carbon Monoxide |
| d_{ABS} | ABS Deposition Depth |
| $D(x)$ | Depth function |
| D | Damper Opening |
| D_{APH} | Air Preheater Bypass Damper Position |
| DCS | Distributed Control System |
| ERC | Energy Research Center |
| ESP | Electrostatic Precipitator |
| $E(x)$ | APH-SCR coordinator |
| f | Function |
| $f(x)$ | SCR feedforward gain |
| F_{coal} | Coal Flow to 1A1-Mill |
| FGD | Flue Gas Desulphurization |
| G_{SCR} | SCR transfer function |
| GA | Genetic Algorithm |
| G_{TRANSP} | Transport channel transfer function |
| G_{APH1} | APH transfer function relating T_{form} and NH_3/NO_x |
| G_{APH2} | APH transfer function relating T_{APH} and damper |
| HR | Net Unit Heat Rate |
| I/S | In-Service |
| J | Extremum-seeking cost function |
| K_D | Extremum-seeking D weight factor |
| $K_{NO_x \text{ in}}$ | Extremum-seeking NO_x in weight factor |
| $K_{NO_x \text{ out}}$ | Extremum-seeking NO_x out weight factor |
| $K_{NO_x \text{ CEM}}$ | Extremum-seeking NO_x CEM weight factor |
| K_{NH3} | Extremum-seeking NH_3 weight factor |
| K_{HR} | Extremum-seeking HR weight factor |
| KZ | SCR gain |

| | |
|------------------------------|--|
| $K_{P,OUT}$ | Outer-loop proportional gain |
| $K_{I,OUT}$ | Outer-loop integral gain |
| $K_{D,OUT}$ | Outer-loop derivative gain |
| $K_{P,IN}$ | Inner-loop proportional gain |
| $K_{D,IN}$ | Inner-loop derivative gain |
| $K_{D,FEED}$ | Feedforward derivative gain |
| $K_{APH} * C_{APH}$ | APH controller transfer function |
| $K_{P,OUT}$ | Outer-loop proportional gain |
| LOI | Loss on Ignition |
| LNCFS | Low-NO _x Concentric Firing System |
| $M_{aux, extr}$ | Auxiliary Extraction Flow Rate |
| $M_{make-up}$ | Make-Up Flow Rate |
| M_{MST} | Main Steam Flow Rate |
| $M_{MST, Spray}$ | Main Steam Attemperating Spray Flow Rate |
| $M_{RHT, Spray}$ | Hot Reheat Attemperating Spray Flow Rate |
| MAE | Mean Absolute Error |
| NPGA | Niched Pareto Genetic Algorithm |
| NH ₃ | Ammonia |
| NN | Neural Network |
| NO _x | Nitrogen Oxides |
| NO _x in | NO _x at the SCR inlet |
| NO _x out | NO _x at the SCR outlet |
| NO _x CEM | NO _x at the CEM |
| NO _x CEM setpoint | Setpoint for NO _x at the CEM |
| NSR | Normalized Stoichiometric Ratio |
| NYSERDA | New York State Energy Research and Development Authority |
| O/S | Out-of-Service |
| O ₂ | Oxygen |
| O&M | Operational and Maintenance |
| OFA | Overfire Air |
| OLE | Object Linking and Embedding |
| OPC | OLE for Process Control |
| P_{cond} | Condenser Back Pressure |
| $P_{throttle}$ | Throttle Pressure |
| P_g | Unit Generation or Load |
| P_{aux} | Auxiliary Power |
| PID | Proportional-Integral-Derivative Controller |
| PLC | Programmable Logic Controller |
| q | Heat Rate Penalty |
| Q_{fuel} | Fuel Heat Rate |
| Q_{steam} | Steam Heat Rate |
| SCR | Selected Catalytic Reduction |
| SIP | State Implemented Plan |
| SOFA | Separated Overfire Air |
| T_{APH} | APH temperature |
| $T_{APH,go}$ | Air Preheater Gas Outlet Temperature |
| T_{form} | ABS formation temperature |
| T_{MST} | Main Steam Temperature |
| T_{HRT} | Hot Reheat Temperature |
| T_{SCR} | SCR time delay |
| T_{TRANSP} | Transport channel time delay |

LIST OF UNITS

| | |
|---------------------------|---------------------------|
| ABS Deposition Depth | Ft |
| Coal Flow Rate | t/h |
| Condenser Pressure | In. Hg. |
| Cost | \$/h |
| Dust Loading | lb/Nft ³ |
| Excess Oxygen | % |
| Fly Ash LOI | % |
| Heat Rate | Btu/hr |
| NH ₃ Slip | ppm _v |
| NH ₃ Flow Rate | lb/h |
| NH ₃ in Ash | Mg/kg (ppm _w) |
| NO _x | lb/MBtu |
| Register/Damper Position | % |
| Residence Time | sec |
| SCR Efficiency | % |
| Stack Opacity | % |
| Steam Cycle Flow Rate | lb/h |
| Steam, Spray Flows | lb/hr |
| Temperatures | °F |
| Throttle Pressure | psia |
| Tilts | Degree |
| Time Delay | sec |
| Unit Heat Rate | Btu/kWh |
| Unit Load | MW |
| Volume | ft ³ |

SUMMARY

A study funded by the New York State Energy Research and Development Authority (NYSERDA) and AES Cayuga was performed to investigate the feasibility of developing an optimization methodology and demonstrate the benefit of operating in an optimal mode that achieve maximum boiler NO_x emissions reductions, maximum selected catalytic reduction (SCR) system performance, minimal unit heat rate penalties, and lower cost of operation at Cayuga Unit 1. Cayuga Unit 1 is a 150 MW_{net} unit, equipped with a low-NO_x firing system and an anhydrous ammonia (NH₃)-based SCR system. Process optimization is a cost-effective approach to improve the cost of NO_x compliance at coal-fired boilers, while meeting other operational and environmental constraints. In boilers equipped with SCRs, this is a classic multi-objective optimization problem to balance boiler thermal performance, NO_x emissions, the cost of reagent and air preheater (APH) maintenance costs. The specific objectives of this study included:

- Provide upgraded instrumentation and control capabilities of ammonium bisulfate (ABS) fouling at the APH.
- Develop a methodology for a combined boiler combustion/SCR/APH optimization.
- Perform field testing at Cayuga Unit 1, and modeling and data analysis to support the demonstration of a combined optimization.
- Develop upgraded control strategy for minimum boiler NO_x emissions, optimal SCR operation, minimal NH₃ consumption, optimal APH operation and minimal overall cost of operation.

Long-term operation of a SCR system at optimal conditions should:

- Improve reagent utilization.
- Minimize catalyst deterioration and reduce operational and maintenance (O&M) costs.
- Operate at tighter stack NO_x levels with minimal standard deviation.
- Maintain SCR constraints such as design NH₃ slip and SO₂-to-SO₃ conversion.
- Minimize SCR impact on balance of plant equipment, such as ABS formation, and unit heat rate.

The following conclusions and recommendations were achieved from the results of this study:

- SCR tuning is an important aspect that should be considered when optimizing the operation of SCR systems. This involves the adjustment of the SCR injection grid

for uniform reagent treatment. However at Cayuga Unit 1, the as-found conditions and NH₃ injection tuning capability rendered this step unnecessary.

- A Breen Energy's AbSensor – Anti-Fouling Probe (AFP) was installed at one of the APH inlets at Cayuga Unit 1 for on-line monitoring of ABS and real-time determination of the ABS deposition axial location in the APH. This probe was found very reliable and an excellent tool to be used in an upgraded optimal SCR system operation.
- Parametric field tests were performed at Cayuga Unit 1. From these tests, it was found that economizer excess O₂, the top two separated overfire air (SOFA) register openings, burner tilt, SOFA tilt, the coal flow to the top pulverizer (1A1-Mill), and the NH₃/NO_x ratio, all have an impact on SCR inlet NO_x, NH₃ requirement for a target stack NO_x emissions level, SCR NO_x removal efficiency, net unit heat rate and ABS deposition. Lower flue gas temperatures were found to improve SCR performance; hence, manipulation of the economizer bypass damper was found ineffective to improve SCR performance at full load. It was found that increasing the NH₃ flow rate in excess of 130 lb/hr, increases the likelihood of exceeding a 2.75 ft. threshold distance from the APH cold-end for ABS deposition. Within this 2.75 ft. distance, ABS removal by sootblowing is greatly enhanced.
- Sootblowing tests were performed to investigate the impact of different sootblowing routines on the operation of the SCR system and associated NO_x reduction and NH₃ consumption. It is recommended a sootblowing schedule that introduces activation of wall blowers (Model IR) at the waterwalls every 10 min., alternating blowers from each ring (A, B and C), and retractable blowers (Model IK) every shift; as well as cleaning of the SCR once a shift, and of the APH three times per shift.
- Artificial intelligence techniques were used to model the test data and provide a tool for mathematical optimization. A modified accurate on-line support vector regression (AOSVR) was implemented on the parametric test data to build artificial intelligence-based, functional relationships between the boiler outlet or SCR inlet NO_x level and heat rate penalty. The prediction performance of proposed AOSVR model was adequate. Genetic algorithms (GAs) were used to solve the constrained multi-objective optimization problem with success. An optimal solution is recommended for the lowest cost of compliance, which corresponds to the following control setting: Economizer excess O₂ = 3.2%, average SOFA register opening = 51% (both top- and mid-SOFA registers open equally), average burner tilt angle = -8 degrees, average SOFA tilt angle = +6 degrees, top 1A1-Mill coal flow rate = 6 ton/hr, APH bypass damper = 0% opens (completely shut) and an NH₃ injection rate = 125 lb/hr. The optimal NH₃ injection rate represents a reduction in NH₃ flow rate

from baseline conditions of approximately 22 percent. The combination of optimal settings should result in NO_x emissions at the boiler outlet of 0.188 lb/MBtu, while limiting ABS deposition to at less than 2.5 ft. from the APH cold-end, and producing fly ash unburned carbon below 4 percent, at a differential cost of \$41.2/hr. This is the lowest combined (heat rate penalty – and NH_3 -related) cost of operation, as compared to a highest cost of close to \$200.00/hr. The savings in net unit heat rate from operation at optimal boiler and APH conditions equate to 54 Btu/kWh as 0.6% from the baseline net unit heat rate.

- A multi-loop control upgrade was proposed to enhance the boiler/SCR/APH control strategy. The multi-loop control approach was complemented with a systematic method for optimal tuning of proportional–integral–derivative (PID) control gains. The SCR control logic that was in use at Cayuga Unit 1 was partially modified to include a scheme that incorporates the feedback measurements implemented in this project (viz, real-time ABS monitoring and deposition tracking). The control system upgrade includes a control strategy provision for the APH bypass damper, by controlling the average cold-end APH temperature to minimize APH fouling/plugging. Additionally, simple dynamic models for the boiler, SCR system, and APH system were identified from the data and proposed to provide coordination of both the SCR and APH control systems to enhance the overall performance of the system. This coordination approach led to the definition of tradeoffs, resolved using extremum-seeking control techniques.
- For future work, two extremum-seeking loops are proposed for real-time optimization at Cayuga Unit 1. The first non-model-based adaptive extremum-seeking controller is proposed to regulate the boiler inputs (O_2 , SOFA register opening, burner tilt, SOFA tilt, top mill coal flow) to minimize both NO_x at the SCR inlet and the boiler heat rate penalty. Non-model-based controllers learn from dynamic operating data of the process. This compares to model-based controllers that utilize dynamic models to obtain mathematical conditions between the controller design parameters and tuning rates. The second non-model-based adaptive extremum-seeking controller is proposed to regulate the NH_3 flow to the SCR system and the APH bypass damper opening in order to optimally control in real-time and in a coordinated fashion both, the NO_x at the stack and ABS deposition within the APH. Based on the results obtained during this project, the proposed approach has the potential for further reducing stack NO_x emissions, unit heat rate, NH_3 usage, and provide savings from reduced APH washing frequency.
- Based on the results of this study, it is indicated that modifying the combined operation of the boiler and SCR system can result in savings in reagent usage, heat

rate improvements, and corresponding O&M costs. Estimates were run to calculate the economic benefits of an optimal operation. In addition, other indirect benefits would result from these improvements. These include catalyst life extension, reduction in APH cleaning frequency and costs associated with the loss of unit availability. Other added benefits not considered in the evaluation of benefits include savings due to optimal sootblowing system operation, reduction in fly ash NH₃ contamination, and reduction of sulfur related problems, such as sulfuric acid corrosion and stack visible plume. The estimated annual cost savings for Cayuga Unit 1, due to optimized operation of the boiler/SCR/APH system is on the order of \$748,000. The estimates do not consider that it might be practical for utilities to “over-control” NO_x to sell allowances into the NO_x allowance market.

The results of this analysis are based on a single limited data set. However, these results indicate that there is a significant potential to optimize the combined operation of boiler combustion, SCR system and APH to achieve reduced operating costs.

Section 1 INTRODUCTION

Responding to environmental regulations mandated by the EPA's State Implementation Plan (SIP) Call Rule, the U.S. power industry has embraced application of the Selective Catalytic Reduction (SCR) technology for nitrogen oxide (NO_x) emission control. This has resulted in 191 SCR installations on U.S. utility boilers by 2004, representing approximately 150 GW of coal-fired capacity. SCR is considered a "mature" technology, which has been extensively applied in Europe and Japan since 1986. SCR systems rely on the chemical reduction of NO_x with ammonia (NH₃) over the surface of a catalyst. A theoretical one-to-one NH₃/NO_x molar ratio would result in conversion of these reactants to environmentally benign molecular nitrogen and water vapor. There is a good deal of care devoted by the equipment supplier to the design and initial operational setup of SCR systems, which is dictated by the particular application and related to boiler configuration and type, coal and fly ash composition, and target NO_x emission level or NO_x removal efficiency. Other constraints that influence SCR design specifications include catalyst life, ammonia (NH₃) slip, SO₂-to-SO₃ conversion, and maximum pressure drop across the SCR reactor.

Once the SCR system is retrofitted to a boiler, however, continuous, efficient, long-term operation of the SCR system requires the appropriate interaction between the flue gas, reagent and catalyst, which really indicates how integral the SCR reactor is to the combustion process it serves. As described in an article in the journal POWER: "while it may be down there, success of a SCR has everything to do with what is happening upstream." This is accentuated by the situation with the NO_x SIP Call requirements, which provide incentive for operating SCR process equipment to deliver greater than the typical 75-85% European performance levels. Many U.S. utilities' NO_x strategic plans are based on SCR performance at key units with 90⁺% NO_x removal and control of NH₃ slip at 2 ppm. Consistently achieving those targets (at the lowest available reagent consumption levels) over the 5-month period of the Ozone Season or over the length of the year to meet generating system NO_x caps, is affected by normal changes in the boiler and associated firing system, which distort process conditions from assumed design targets. Additionally, SCR process instrumentation and controls, and reagent delivering systems suffer from inherent deficiencies, particularly under a variety of operational regimes (i.e., low-loads, varying load ramp rates, fluctuating coal sources), which result in deviations from optimal SCR operation and, consequently, increased operational and maintenance (O&M) costs and deteriorated catalyst life.

Optimal, cost-effective operation of the SCR system is mainly affected by changes to the flue gas conditions, the amount of NO_x generated in the furnace, and the NH₃/NO_x preparation and use in the catalyst bed. Most operators of SCR systems recognize these effects and try to modify combustion in the furnace for lower inlet NO_x to the SCR system, as well as periodically tune the SCR unit for best reagent utilization and minimal O&M costs. The SCR tuning targets provide relatively uniform NO_x, temperature,

and flue gas flow conditions at the reagent point of injection at the SCR reactor inlet and maintain uniform distributions of NO_x and ammonia slip at the outlet of the SCR reactor. Typical target ranges for the variables of interest are: inlet temperature distribution, ± 30°F from the mean; inlet flow distribution, ± 15 percent from the mean; and NH₃/NO_x molar ratio, ± 5 percent from the mean.

In addition to periodical tuning of the SCR system, optimization of the combined furnace combustion/SCR system/boiler back-end is of significant importance to obtain the maximum NO_x reduction benefit from the post-combustion emissions control system at the lowest O&M cost, on a consistent basis. Optimization of combined boiler and SCR operation requires consideration of all operating parameters that impact the combustion side, SCR performance and the air preheater (APH). The SCR post-combustion NO_x control technology is usually retrofit on boilers equipped with low-NO_x firing systems and on high-dust, high-temperature configurations, with the SCR system located in front of the APH and the dust collection equipment. SCR systems designed and operated to achieve high NO_x reduction efficiencies of over 90%, are challenged to perform at the optimal level, while achieving less than 2 ppm of NH₃ slip, resulting in over-feeding of NH₃, with associated operating cost penalties. The price of NH₃ has more than doubled in recent years (currently at approximately \$500/ton NH₃). Additionally, in coal-fired boilers, high NH₃ slip has an adverse impact on cold-end equipment located downstream of the SCR reactor. The concerns include ammonium bisulfate (ABS) deposition, and plugging and corrosion potential of APHs. Controlling and mitigating APH fouling is imperative in coal-fired boilers, since it precludes continued operation of the unit, requiring forced shutdowns for APH cleaning, with the associated loss in unit availability and financial penalty.

The challenge of the SCR control technology is to achieve cost-effective high levels of NO_x emissions performance, while constraining its detrimental impact at the boiler back-end. An integrated approach for the optimization of the combustion and post-combustion systems, including the APH, offers an alternative to meet this challenge. Such an approach should consider, in a coordinated fashion, the optimal operation of the boiler firing system, SCR reactor (including the reagent injection system), APH, and net unit thermal performance. To investigate the feasibility of developing an optimization methodology and demonstrate the benefit of operating in an optimal mode that achieves maximum boiler NO_x emissions reductions, maximum SCR system performance, minimal unit heat rate penalty, and lower cost of operation, a study was conducted by the Energy Research Center, under funding from the New York State Energy Research and Development Authority (NYSERDA) and AES Cayuga. The specific objectives of this study include:

- Provide upgraded instrumentation and control capabilities of ABS fouling at the APH.
- Develop a methodology for a combined boiler combustion/SCR/APH optimization.
- Perform field testing at Cayuga Unit 1, and data analysis and modeling to support the demonstration of a combined optimization.

- Develop upgraded control strategies for minimum boiler NO_x emissions, optimal SCR operation, minimal NH₃ consumption, optimal APH operation, and minimal overall cost of operation.

This report contains a description of the test unit used for this project, instrumentation retrofit to monitor ABS formation in the APH, and a summary of the parametric tests, data analysis results, control system upgrade, as well as an evaluation of the benefits of this optimization, and conclusions and recommendations obtained from this project.

Section 2
UNIT DESCRIPTION

This project was performed at AES's Cayuga Station Unit 1. Cayuga Unit 1 is a 150 MW_{net}, single-reheat, tangentially-fired Combustion Engineering (CE) boiler, equipped with a low-NO_x concentric firing system (LNCFS) level III. The LNCFS-III system consists of four elevations of burners arranged in four corners (see Figure 2-1). Four pulverizers (1A1, 1B2, 1A3 and 1B4, from top to bottom) supply coal to the burner system, one mill per elevation. Cayuga Station typically fires Northern Appalachian coal; however, blending with lower quality fuels is common at this station. The windbox compartment at each corner is composed of fuel air registers (coaxial with the burner nozzle), auxiliary air registers and concentric fire system (CFS) air registers that are used to divert combustion secondary air at an offset, with respect to the burner centerline. In addition to the secondary air ports, the LNCFS-III arrangement at Cayuga Unit 1 incorporates overfire (OFA) in two set of registers, two closed coupled overfire air (CCOFA) registers, and a separated OFA (SOFA) compartment with three registers. All the burner buckets and CCOFAs are connected to tilt in unison for controlling of steam temperatures. The SOFA compartments are also tiltable for combustion staging. Cayuga Unit 1 is equipped with two Ljungstrom type rotating APHs. These APHs are equipped with air bypass capabilities for average cold-end temperature control and acid dewpoint mitigation at the APH cold-end. The Cayuga Unit 1 APHs are equipped with rake type sootblowers, which can reach and remove deposits from the cold-end approximately 2.75 ft. into the cold-end baskets. The rest of the boiler back-end configuration includes an electrostatic precipitator (ESP) for particulate removal, and a flue gas desulphurization unit (FGD).

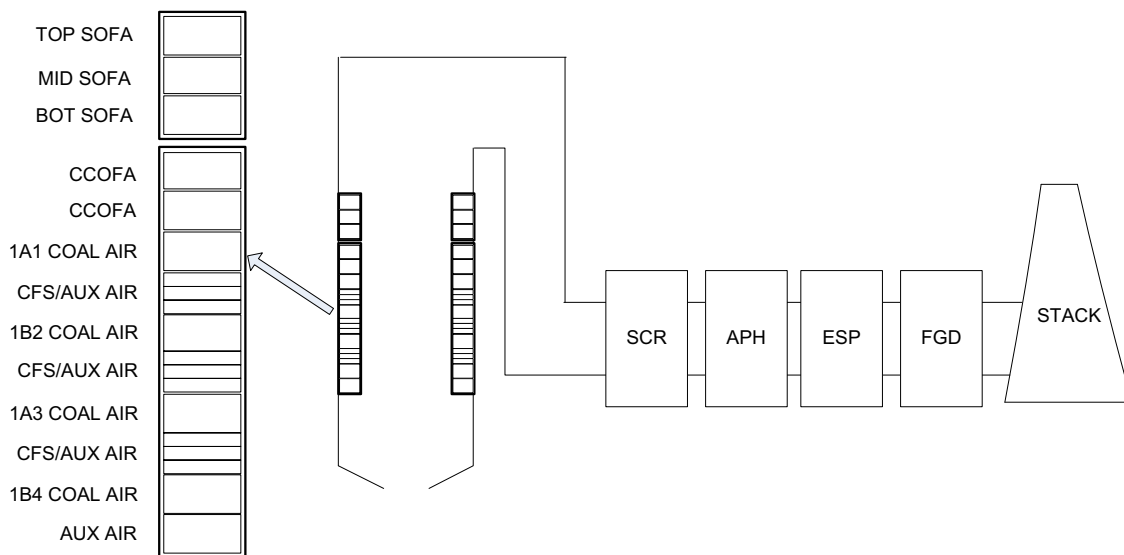


Figure 2-1: Cayuga Unit 1 – Boiler Configuration.

Combustion control at Cayuga Unit 1 is based on the typical parallel air/fuel control scheme. An excess air or percent oxygen (O₂) trim control loop is available in the combustion control system. The excess O₂ bias is applied at Cayuga Unit 1 on-manual operation by the boiler operators to balance furnace outlet or SCR inlet NO_x emissions and fly ash unburned carbon (or loss on ignition, LOI). A bias is an adjustment applied to a controllable parameter to eliminate the deviation in the value of the parameter with respect to a prescribed set point. Due to fly ash sale and landfilling restrictions, fly ash LOI at Cayuga is maintained at below 4 percent. Periodical samples of fly ash are taken throughout the day at Cayuga Unit 1 and analyzed on-site for LOI. Boiler excess O₂ is adjusted according to maintain the fly ash below the required threshold. Steam temperatures are controlled by tempering sprays, burner tilts and sootblowing. Design steam temperatures are 1,000°F, for both main steam and hot reheat steam temperatures.

Cayuga Unit 1 is equipped with a 2-layer, anhydrous NH₃-based SCR system, with a TiO₂/V₂O₅/WO₃ formulation and total catalyst volume of 5,890 ft³ for additional NO_x control. Design requirements for the SCR system at Cayuga Unit 1 included 90% NO_x reduction based on an inlet NO_x emission rate for the specified coals of 0.42 lb/MBtu, and an NH₃ slip of less than 2 ppm at actual excess O₂. Other design considerations include an operating SCR temperature in the range between 608 and 700°F, with a normal operating temperature at full unit load of 627°F, limited sulfur dioxide (SO₂) to sulfur trioxide (SO₃) oxidation of less than 1%, and dust loading of 0.00037 lb/Nft³, (normal ft³ or a standard temperature of 68°F and standard pressure of 1 atm.) with a catalyst pitch of 0.2 in. The SCR reactor houses the catalyst in a downflow orientation and it is equipped with economizer bypass for SCR inlet temperature control at low load operation. The economizer bypass dampers allow hotter flue gas from the middle of the primary superheater to mix with the economizer outlet gas to maintain a minimum catalyst inlet temperature of 608°F. Additional dampers are provided for SCR reactor isolation and flow modulation. SCR cleaning is achieved with six air-based retractable sootblowers. The anhydrous NH₃ system includes an evaporation/air dilution skid and injection grid. Ammonia concentration in the ammonia/air mixture is maintained at approximately 5%. Ammonia injection and mixing with the flue gas is achieved with an injection pipe manifold that traverses the flue gas and two sets of static mixers. SCR gas side instrumentation includes NO_x analyzers at the inlet and outlet of the reactor, and a zirconium dioxide O₂ analyzers. Ammonia injection control is performed using a combined feedforward and feedback control scheme. In this scheme, the unit distributed control system (DCS) calculates the total NO_x in the flue gas at the SCR inlet. This determines the feedforward portion of the injection signal to the NH₃ flow control valve. The DCS is also allowed to trim the NH₃ injection rate based on the feedback from the NO_x analyzer located at the SCR outlet and to maintain a constant NO_x removal efficiency across the SCR. A value of 90% NO_x removal is used for NH₃ trimming.

Section 3

ABS MONITORING

As part of this project Cayuga Unit 1 was retrofit with instrumentation for monitoring of ABS. An ABS monitoring sensor, manufactured by Breen Energy, Inc., was installed at one of the APH inlets of Cayuga Unit 1. The intention was to use one single sensor as indication of the fouling condition of both rotating preheaters. The Breen Energy's AbSensor - Anti-Fouling Probe (AFP) is a probe that measures the conduction of electrical current across the probe's tip that results from condensed hydrated ammonium bisulfate below its dewpoint. The instrument reports both the ABS formation or condensation, and evaporation temperature via object linking and embedding (OLE) for process control (OPC). The detection process consists of cooling the initially hot detector tip by controlled application of cooling air. The presence of a condensed ABS liquid phase is determined by the change in electrical resistance/current between the probe's electrodes. Following detection of condensate, the cooling air stream is removed and the probe is allowed to return to the flue gas temperature. As the probe heats, the change in electrical resistance is measured again to detect the liquid evaporation temperature of the deposit. The ABS monitoring capability also included programmable logic controllable (PLC) hardware, integrated APH model and temperature controller, and NH₃ injection controller. The NH₃ injection controller can provide closed loop control to the SCR reagent injection process by estimating the mismatch between a unit NO_x emissions setpoint and the actual stack NO_x indication, to produce a NH₃ bias that is applied to the DCS programmed SCR NH₃ flow vs. unit load curve. More description of the NH₃ injection controller will be provided in the Upgraded SCR Control Strategy Section.

The Breen's APH temperature controller includes an APH heat transfer calculation, and a control scheme that provides a bias to the plant DCS' APH cold-end average temperature (the average of APH flue gas out and APH air inlet temperatures) setpoint. This setpoint has traditionally been used to control for the impact of sulfuric acid dewpoint deposition. The APH heat transfer calculation is based on a comprehensive metal/gas matrix model developed by Lehigh University, which provides real time information on the maximum APH metal temperature as a function of the axial distance from the APH cold-end. The input parameters used by the first-principle APH heat transfer calculation include flue gas and air inlet temperatures, and gas and air flow rates. This information and the measured AbSensor evaporation temperature are used by the APH temperature control scheme to estimate a potential ABS condensation depth from the APH cold-end (the intersection of these two temperatures). The controller is then manipulated to maintain an operational condensation depth within a setpoint ABS deposition depth that represents the cleanable range of the sootblowers located (only) at the APH cold-end. In case, the actual condensation depth is found to penetrate beyond the allowed condensation depth setpoint, an APH cold-end average temperature bias is introduced by the controller to the DCS. This bias results in a manipulation of the APH air bypass damper, which changes the internal APH heat transfer patterns and modifies the APH

cold-end average temperature to a new biased setpoint, within the ABS deposition setpoint. Limits for this bias are imposed to prevent the controller from operating at excessive heat rate penalties and exceeding the acid dew point of the flue gas. Figure 3-1 includes a representation of the APH temperature controller performance.

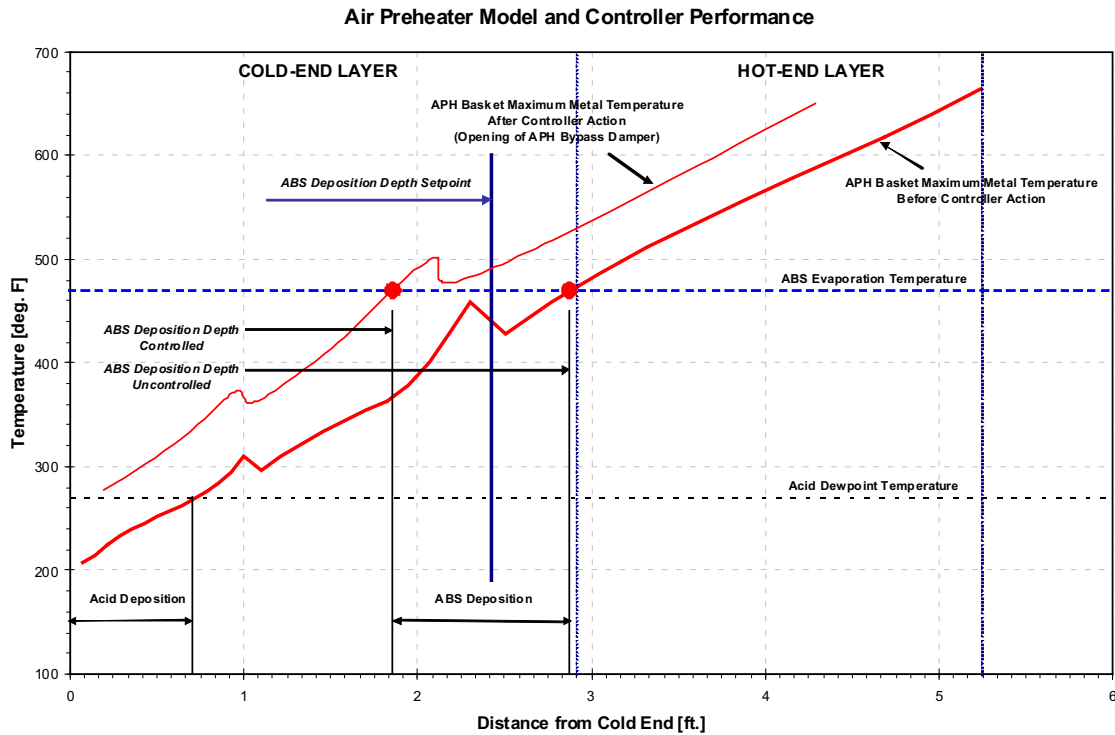


Figure 3-1: Representation of APH Temperature Controller Performance.

Tuning of the installed Breen Energy’s technology was performed between August 29-30 and September 26-27, 2007. The tuning consisted of off-line manipulation of the controllers’ input parameters to verify the adequacy of the different variable setpoints. Additionally, a series of tests was performed to adjust the APH condensation depth setpoint and assure that the APH temperature controller would operate the APH back-end temperature within a controllable range. Figure 3-2 shows the results of testing performed to investigate the APH temperature controller response to changes to the APH condensation depth. In the particular tests of Figure 3-2, the APH condensation depth setpoint was adjusted from 2.8 ft. from the APH cold-end to 2.6 ft. The response of the APH temperature controller was adequate, with the APH bypass damper opening to adjust the APH cold-end average temperature to a higher level, and the subsequent displacement of the actual ABS condensation depth toward the cold-end. The time delay for this response is of the order of 4 min. It was decided to implement an APH condensation depth setpoint at 2.75 ft. from the cold-end.

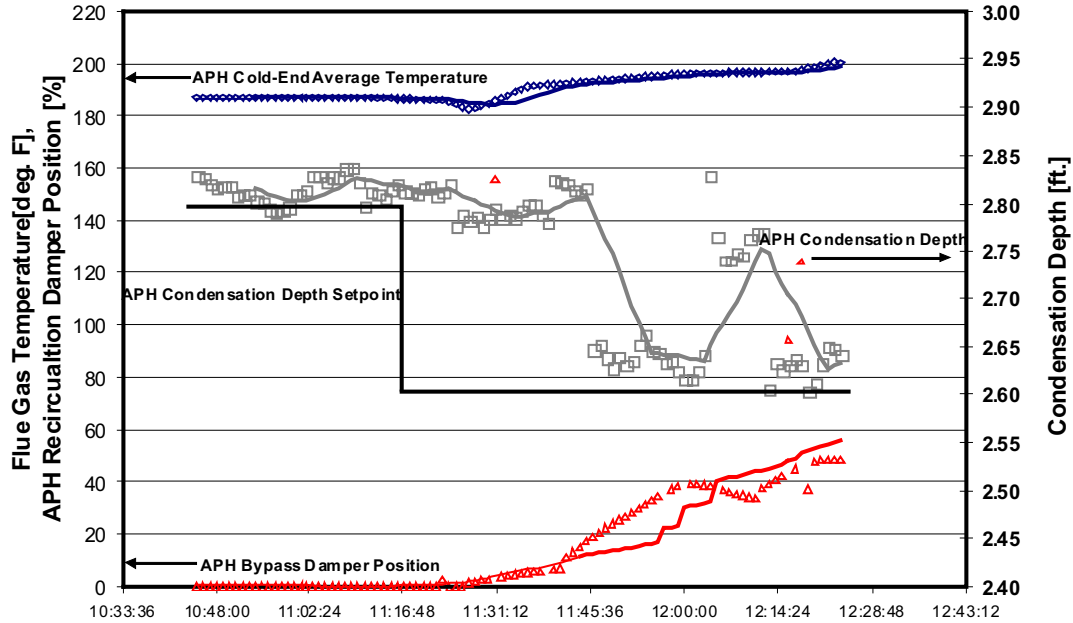


Figure 3-2: Performance of the APH Temperature Controller.

Figure 3-3 shows results of testing performed to investigate the NH₃ flow injection controller response to changes in SCR inlet NO_x. In the particular tests of Figure 3-3, a boiler outlet NO_x decrease was followed by a corresponding decrease in reagent flow rate to compensate for the lower inlet NO_x emissions, and maintain the stack NO_x setpoint at a pre-determined value of 0.095 lb/MBtu. The average stack NO_x emission level for this period was 0.093 ± 0.003 lb/MBtu. The drastic changes in NH₃ flow in Figure 3-3 are most likely due to the delays associated with the NH₃ controller.

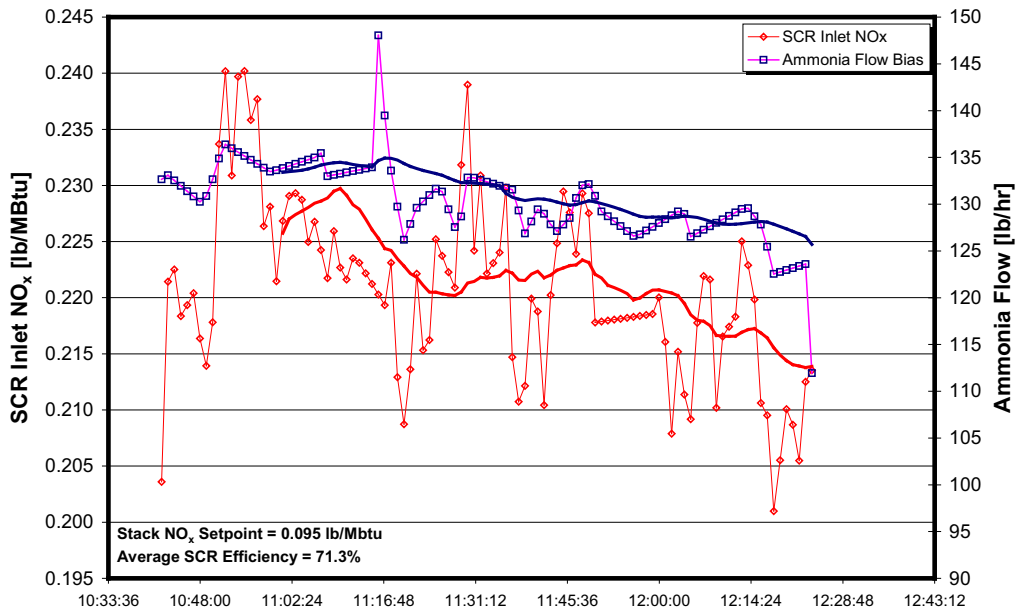


Figure 3-3: Performance of Ammonia Injection Controller.

Section 4

PARAMETRIC FIELD TESTS

Parametric field tests were performed at Cayuga Unit 1. Due to unit availability and station scheduling, these tests were performed during the weeks of November 26, December 3 and 10, 2007, and January 14, 2008. Testing was conducted by two ERC engineers with support from the station. Testing was performed at three unit loads, 150 (full load), 100 and 75 MW, while firing a baseline coal (as much as possible). The load level of 75 MW is the minimum operating load for Cayuga Unit 1. The objective of these tests was to obtain enough data, under controlled conditions, for characterizing the impact of boiler and low-NO_x firing system control settings, sootblowing, and SCR system and APH, on SCR and APH performance, boiler outlet NO_x (SCR inlet NO_x), NH₃ injection requirement, unit heat rate, and ABS formation. Additionally, the parametric tests investigated the impact of SCR system operation, APH bypass damper and sootblowing scheduling on these same parameters of interest. Test results were also used to build a database to be used for artificial intelligence (AI) modeling and to obtain the best combinations of boiler firing system, SCR and APH operational settings for SCR system optimal control strategy and upgrades. This report concentrates on the results achieved at full load, since that Cayuga Unit 1 is a base-loaded unit and it stays most of the time at full load.

Previous to the field tests, a test plan was developed in collaboration with AES Cayuga engineers. The plan was reviewed and approved by the station. The first planned step consisted of a survey of the boiler and low-NO_x and SCR system to determine baseline (as-found) conditions and control settings. Also, the first step included performing an extended test at baseline settings. Baseline settings are those as-found settings commonly used by the operators. The second planned step consisted of combustion and SCR tuning. For this tuning, a permanently installed gas sampling grid and a portable gas analyzer was used to sample the flue at the economizer exit or SCR inlet location. The purpose of this tuning is typically to perform adjustments to the boiler, low-NO_x firing system and NH₃ injection to achieve balanced combustion conditions at the boiler convective pass before the SCR inlet, as well as balanced SCR performance.

Additionally, a series of parametric tests was planned in which one or two boiler/low-NO_x system parameter was tested at a time, while all other operating parameters were held constant. The parameters used for testing and their available operating ranges are included in Table 4-1. Additional testing was performed to characterize the impact of CCOFA registers, different pulverizers out-of-service (O/S) configurations, the SCR economizer bypass dampers and boiler sootblowing.

Six to seven tests were scheduled per day, including a baseline test at the beginning of each day, followed by a series of parametric tests. The duration of each test was dictated by the requirements of collecting a

Table 4-1: List of Testing Parameters and Their Limits.

| No. | Symbol | Variable description | Unit | Upper limit | Lower limit |
|-----|---------------|----------------------------|------|-------------|-------------|
| 1 | O_2 | Excess O_2 | % | 4.0 | 2.5 |
| 2 | $SOFA$ | Average top SOFA Opening | % | 100 | 0 |
| 3 | α_{ST} | SOFA Tilt | Deg. | 25 | -15 |
| 4 | α_{BT} | Burner Tilt | Deg. | 15 | -15 |
| 5 | F_{coal} | Coal flow rate of top mill | t/h | 19 | 0 (OFF) |
| 6 | NH_3 | Ammonia flow rate | lb/h | 250 | 0 |
| 7 | D_{APH} | APH bypass damper position | % | 100 | 0 |

sufficient quantity of fly ash sample and sufficient steady-state data. Steadiness of data was recognized, after changes in control settings and the associated transient that occurs after the upset, by flat trending in emissions, NH_3 consumption, steam temperatures and attemperation, and flue gas temperatures at the boiler back-end. Economizer excess O_2 was measured at the economizer outlet and was used as an indication of the amount of excess air fed to the boiler, the average of the top and middle SOFA register openings was used as an indication of combustion staging. The average burner and SOFA tilt angles, and the coal flow rate to the top 1A1-Mill were included in the parametric list to fully characterize the relationship between boiler control settings and boiler outlet or SCR inlet NO_x and unit thermal performance. The NH_3 flow rate was measured at the SCR injection point, and together with the APH bypass damper position, was used to characterize parametric relationships for the SCR and APH, respectively. Coal and fly ash was sampled daily and for each test run, respectively, and analyzed off-line. Fly ash samples were collected from the first row of ESP hoppers and combined into a composite sample, and analyzed for unburned carbon or loss on ignition (LOI). For fly ash sample collection, ESP tests hoppers were evacuated as part of their operational cycle and put on bypass to accumulate samples for each corresponding test run.

Average data on SCR inlet and outlet NO_x , and SCR NO_x removal efficiency (defined as the normalized NO_x reduction across the SCR with respect to the inlet NO_x), main steam and hot reheat steam temperatures, attemperating flow rates, boiler flue gas and air temperatures were acquired from the plant OSI soft PI data acquisition system for each test point. ABS formation temperature was measured at the APH inlet, as indicated by the Breen's probe and its signal incorporated into the OSI soft PI system. Indication of net unit heat rate deviation or penalty for each test point, or combination of test parameters, with respect to baseline conditions, was estimated from a heat and mass balance model of the unit. A description of the procedure used to estimate the heat rate difference with respect to baseline conditions is include in Appendix A. Sootblowing tests were performed to characterize the impact of different groups of sootblowers on the parameters of interest. For these tests, activation of selected group of blowers was carried out, at steady boiler, low- NO_x firing system and SCR system control settings.

Table B-2, in Appendix B, contains the matrix of the field tests that were performed at Cayuga Unit 1. Table B-2 describes the particular conditions of the parameters of interest. A total of 102 tests were performed. These tests involved manipulation of combustion and the low-NO_x firing system, the SCR system, the APH, and sootblowing. The maximum level of manipulation of each particular parameter was determined in conjunction with the plant staff, in terms of having enough data to characterize the effect of each parameter on the variables of interest (i.e., NH₃ consumption, SCR NO_x reduction efficiency, unit heat rate, etc.) and in accordance with the unit operational and environmental constraints (i.e., minimum windbox pressure, maximum allowable ABS penetration depth, maximum stack opacity, maximum fly ash LOI level, etc.).

Section 5
DATA ANALYSIS RESULTS AND DISCUSSION

DATA ANALYSIS RESULTS

Before performing any parametric field tests, sampling of the flue gas was performed. A permanently installed 8 x 4 gas sampling grid and a portable gas analyzer was set up to sample the flue at the SCR inlet location. The purpose of this sampling is to determine the level of NO_x stratification in the input flue gas to the SCR, and injected NH₃ stratification at the SCR inlet. Guided by the results of this activity, adjustments to the boiler and low-NO_x firing system are typically planned (i.e., corner-to-corner combustion balancing) to achieve balanced combustion conditions at the boiler convective pass before the SCR inlet. Additionally, signs of NH₃ stratification are corrected by adjustment to the NH₃ injection valves. However, this was not an option at Cayuga Unit 1, since no modulation valves are available for localized NH₃ flow manipulation. Figure 5-1 shows a contour plot of the measured excess O₂ and NO_x concentration at the SCR inlet. The most important data, NO_x emissions (corrected to 3.0% O₂), indicate that the range of NO_x concentration is from 297 to 313 ppm at 3% O₂. This is approximately a 5.2% deviation of the mean, which is within recommended flue gas stratification for SCR applications. No further action was taken on manipulating combustion for homogenizing the flue gas at the SCR inlet.

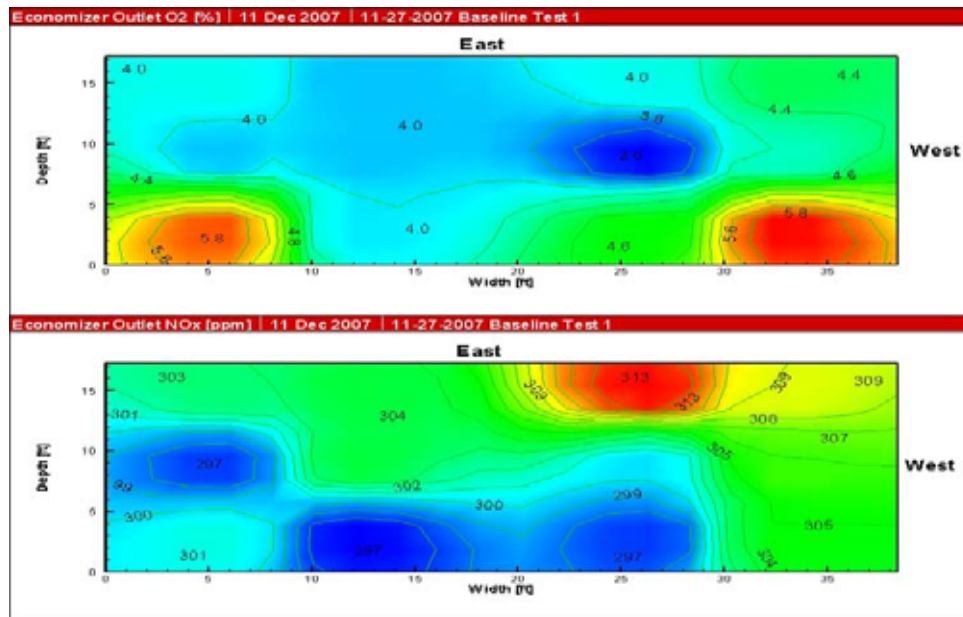


Figure 5-1: Contour Plots of O₂ and NO_x Concentration at the SCR Inlet.

Data obtained from the parametric field tests were reduced and analyzed to determine trending relationships between independent or controllable parameters and the boiler, SCR and APH dependent parameters. The independent parameters investigated for the boiler included excess O₂, SOFA settings,

burner and SOFA tilt positions, and the coal flow rate to the top 1A1-Mill. The dependent parameters included boiler outlet or SCR inlet NO_x emissions rate, the NH_3 flow requirement to achieve 0.095 lb/MBtu NO_x at the stack, the SCR NO_x removal efficiency (calculated as the normalized NO_x reduction across the SCR, with respect to the inlet NO_x level), the SCR inlet gas temperature and APH gas outlet gas temperature, the main and hot reheat steam temperature and attemperating spray flows, the ABS formation temperature and condensation depth in the APH, fly ash LOI, and the calculated heat rate deviation or penalty.

From the data analysis it was estimated that the impact of excess O_2 on boiler NO_x emissions level is approximately a 0.055 lb/MBtu drop per percent reduction in excess O_2 . This translates in a reduction in NH_3 flow requirement of approximately 41 lb/hr of NH_3 to maintain the stack NO_x constraint of 0.095 lb/MBtu at the stack. Excess O_2 was also found to modestly increase SCR removal efficiency for the particular SCR system at Cayuga Unit 1. This impact on SCR efficiency correlated to the inverse relationship between excess O_2 and flue gas flow rate, and SCR residence time. The impact of excess O_2 in flue gas temperature was found to be of approximately $-8^\circ\text{F}/\% \text{O}_2$ at the SCR inlet and insignificant at the APH outlet. Excess O_2 increase was found to increase steam temperatures and the attemperating spray requirement, if the steam temperatures exceed the design values, by approximately $+15^\circ\text{F}/\% \text{O}_2$. Fly ash LOI increases almost a percent, per reduction of a percent point in excess O_2 . The impact of O_2 on these performance parameters results in a parabolic trend with respect to boiler heat rate penalty, resulting in a minimum in heat rate at approximately 3.15% (see Figure 5-2). The reduction in excess O_2 for boiler emissions reduction also helps reduce ABS formation temperature by approximately 12.5°F per percent reduction in O_2 (see Figure 5-3). The ABS probe evaporation temperature was used as the best indication of ABS formation temperature, based on the experience of Breen Energy. Opacity was noticed to increase by only 0.7% for the range of O_2 used in the excess air tests (2.5-4.0% O_2).

The impact of the overfire air registers on the variables of interest was found to be of first order. The CCOFA and SOFA registers were manipulated at different opening levels and vertical biases. It was found that the effect of CCOFAs and the lower elevation SOFA register on boiler NO_x , and flue gas and steam temperatures was of second order. The top two elevations of SOFA, opened at identical setting, were found to be most effective in reducing boiler outlet NO_x . Hence, these two registers were used in the SOFA tests. Figures 5-4 to 5-7 show some of the results obtained from the data analysis in relation to the SOFA register openings. Figure 5-4 shows the reduction in required NH_3 flow to comply with a stack NO_x constraint of 0.095 lb/MBtu as a function of SOFA register opening. The SOFA indication used in the plots corresponds to the average position of the top two SOFA registers. It was found that reductions of the order of 35% can be achieved from baseline NH_3 injection flow rates, over the physical range of the SOFA registers. This level of NH_3 flow consumption (and SOFA opening) impacts the deposition of ABS and the location of the ABS deposition depth along the APH axis (see Figure 5-5). The goal is to keep the ABS

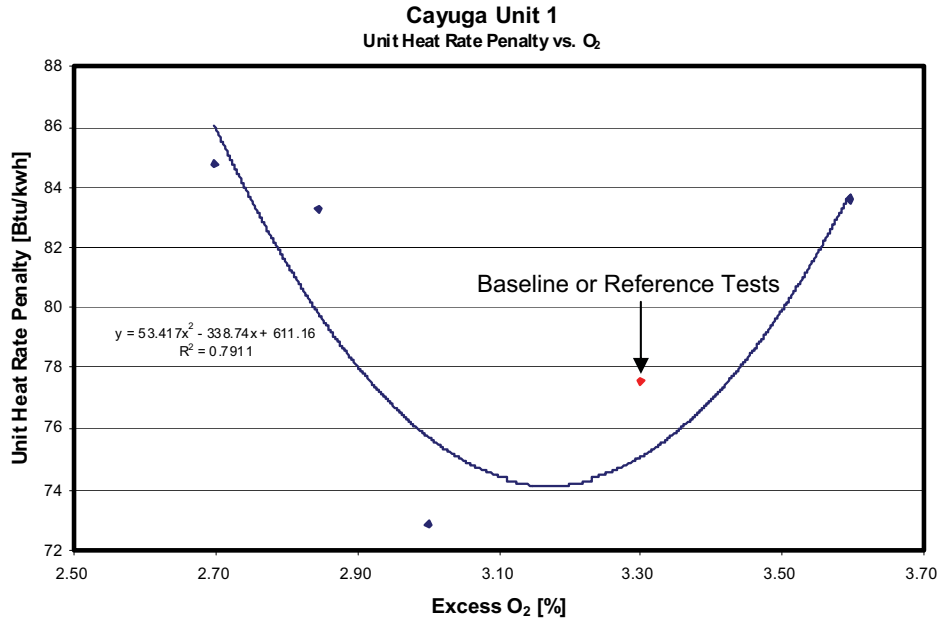


Figure 5-2: Impact of Boiler Excess O₂ on Unit Heat Rate Penalty.

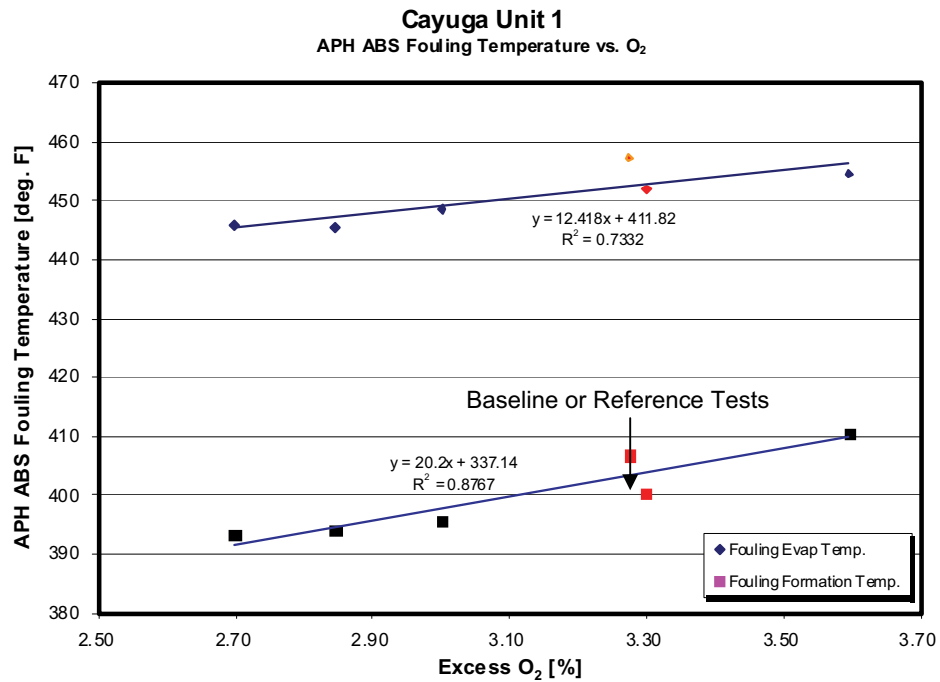


Figure 5-3: Impact of Boiler Excess O₂ on ABS Formation Temperature.

deposition depth closer to the APH cold-end, where sootblowers can reach the deposits and clean them. An ABS deposition depth setpoint was set at Cayuga Unit 1 at 2.75 ft. from the APH cold-end. Also impacted by the SOFA registers is the SCR efficiency and net unit heat rate. Figures 5-6 and 5-7 show the effect of OFA opening on SCR NO_x reduction efficiency and unit heat rate penalty, respectively. The negative impact on SCR efficiency is associated to the changes in flue gas temperature. The negative impact on unit

heat rate is associated to the increase in fly ash LOI and increase in flue gas temperature. The impact of SOFA registers on fly ash LOI was more noticeable at openings in excess of 60%, where the LOI increases up to 6%. The impact of SOFA on stack opacity is negligible.

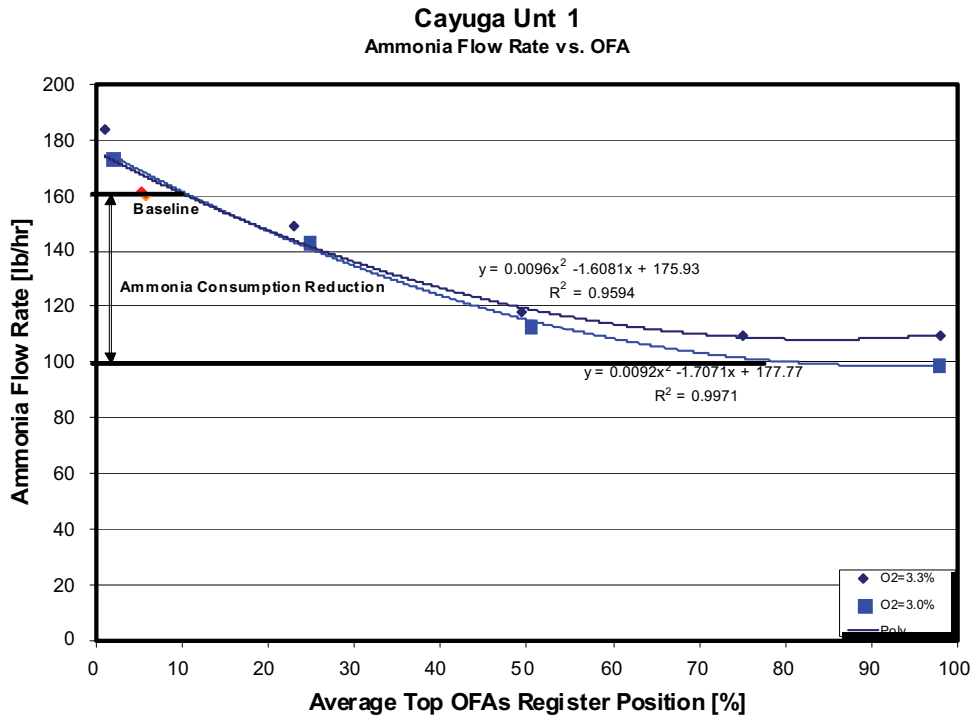


Figure 5-4: Impact of SOFA Registers on NH₃ Flow Requirement.

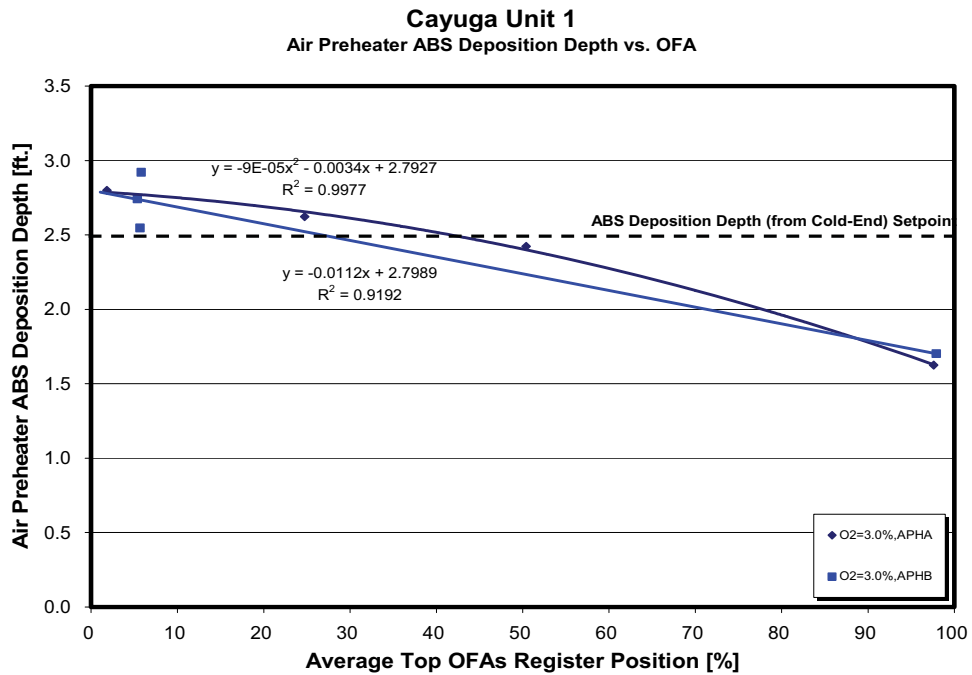


Figure 5-5: Impact of SOFA Registers on ABS Deposition Depth.

Cayuga Unt 1
SCR Efficiency vs. OFA

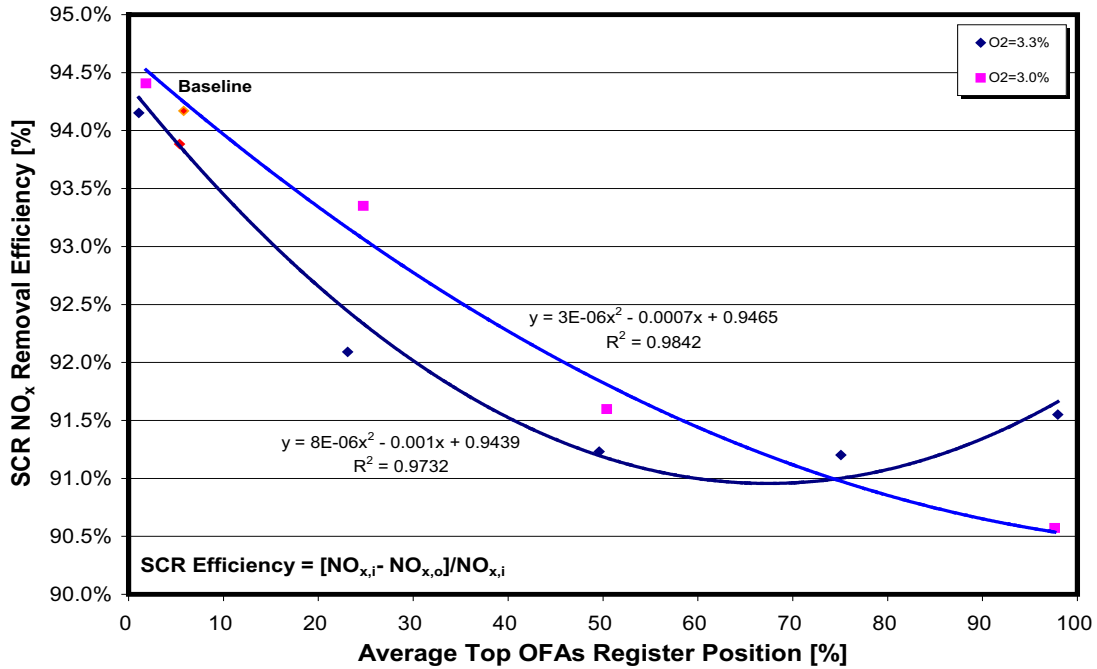


Figure 5-6: Impact of SOFA Registers on SCR Removal Efficiency.

Cayuga Unt 1
Unit Heat Rate Penalty vs. OFA

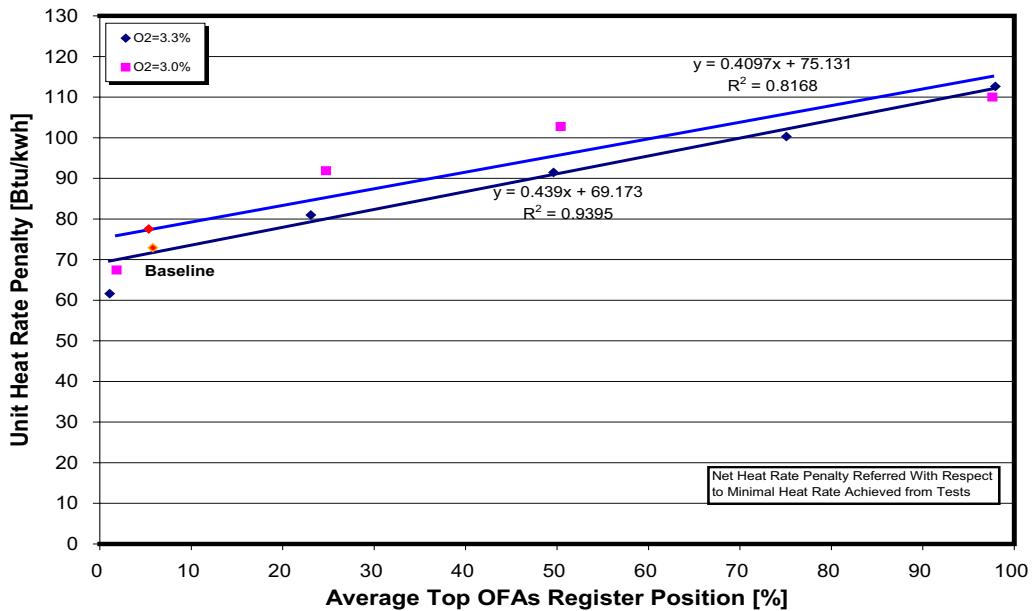


Figure 5-7: Impact of SOFA Registers on Unit Heat Rate Penalty.

Testing was performed to investigate the effect of biasing coal flow and taking selective mills O/S on boiler outlet NO_x emissions. It was found that the most significant impact is introduced by the top 1A1

pulverizer. Special effort was devoted to perform systematic tests on the 1A1-Mill, by biasing its coal flow until taking the mill completely off. While this was done, the other bottom mills were loaded equally. Figure 5-8 shows the relationship between 1A1-Mill coal flow and SCR inlet NO_x emissions. The reduction in coal flow from its maximum flow rate of 19 ton/hr to the O/S condition represents a reduction in NO_x emissions rate of 0.048 lb/MBtu. The corresponding reduction in NH₃ flow to maintain the target NO_x emissions at the stack, is 27 lb/hr. For this reason, this parameter was included in the optimization list of parameters; however, changes in coal quality that would require a higher total coal flow to produce the same unit load, will preclude biasing of the top mill. Reduction in coal flow to the top 1A1-Mill has a modest detrimental impact on SCR NO_x removal efficiency. No significant impact was found from the top mill biasing on flue gas temperatures. The impact of 1A1-Mill biasing on steam temperatures and attemperation was very significant, representing more than 1°F increase per ton/hr of coal flow reduction. This might be due to the change in heat transfer pattern in the furnace, leading to an increase in furnace exit gas temperature (FEGT). Top mill biasing has only a minor impact on ABS deposition and stack opacity. The impact of 1A1-Mill on fly ash LOI is of approximately 0.5% for the range of fully loaded to O/S. The impact of heat rate deviation represents approximately 4.5 Btu/kWh per ton/hr reduction in coal flow rate. This impact is related to the improvement in combustion in the lower furnace, as well as in steam temperature, in excess of design levels.

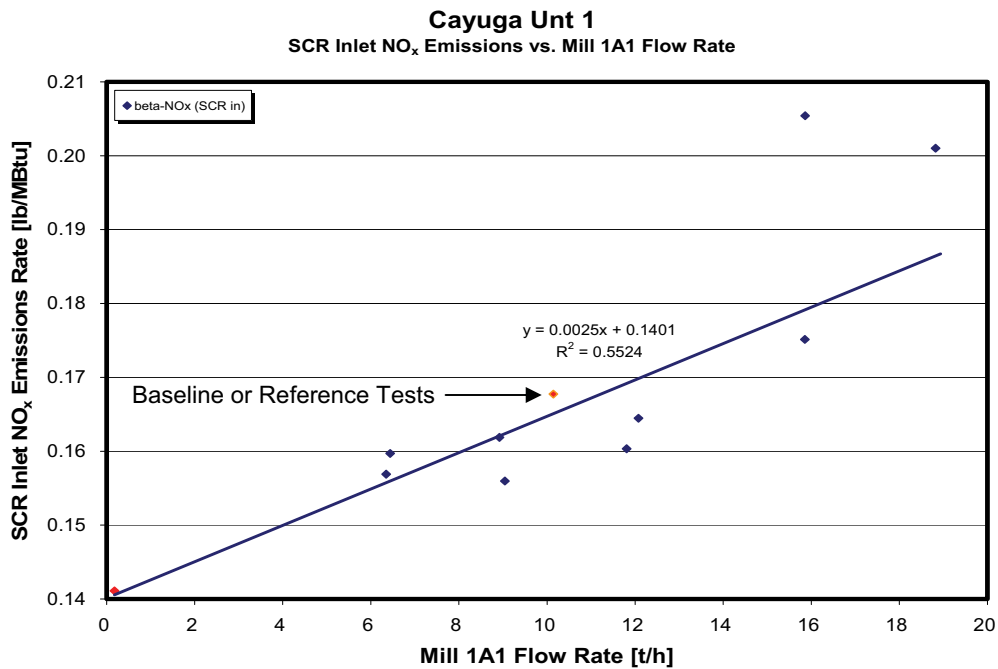


Figure 5-8: Impact of 1A1-Mill Coal Flow Rate on SCR Inlet NO_x Emissions.

The other additional parameters that were investigated at the boiler/combustion side, were the burner and SOFA tilt. One technique that results in reduction in boiler NO_x emissions in tangentially-fired boilers is

the enhancement in combustion staging by stretching the fireball, by lowering the burner tilts and raising the overfire air tilts. This was implemented in a series of parametric tests that included combination of both parameters. It was found that burner tilt helped reduce NO_x emissions, with a minimum emissions level achieved in the range from -5 to -8 deg. Improvements in NO_x emissions were also found with upward tilting of the SOFA registers, with the most reduction achieved at SOFA tilts between 0 and +6 deg.

Moving down the convective pass, trending relations and trade-offs were investigated for the SCR and APH. The independent parameters investigated for the SCR included the economizer bypass damper and the NH_3 treatment in the catalyst, also indicated by the normalized stoichiometric ratio (NSR), or the molar ratio of NH_3 to NO_x . The dependent parameters affected by those independent parameters at the SCR include the SCR inlet gas temperature, the SCR performance efficiency, and ABS formation temperature and deposition, as applicable. Tests that involved manipulation of the economizer bypass dampers were performed in the range from fully closed to 40% open. The economizer bypass damper vs. SCR inlet temperature resulting trend is included in Figure 5-9. As it can see from Figure 5-9, an increase in economizer bypass damper results in a steep increase in flue gas temperature of about +1 °F per percent opening, and at about 40% open the SCR inlet gas temperature approaches the 700 °F limit recommended by the SCR manufacturer. However, when plotting the opening of the economizer bypass damper vs. the SCR NO_x reduction efficiency, it was found that the efficiency has an inverse relationship with the economizer bypass damper opening. This indicates that the SCR catalyst formulation is such that works on the right-hand side of the SCR vs. temperature curve, reducing NO_x conversion efficiency as the catalyst temperature increases (see Figure 5-10). For this reason, this parameter was excluded from the optimization list of parameters. From the economizer bypass damper testing, it was also found that the ABS deposition is not affected by changes in economizer bypass opening.

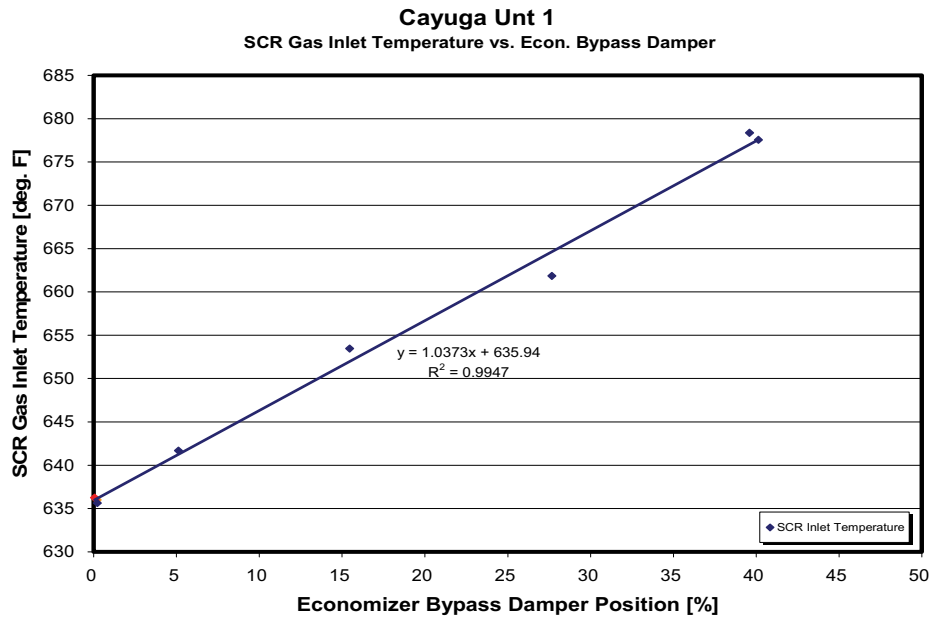


Figure 5-9: Impact of Economizer Bypass Damper on SCR Gas Inlet Temperature.

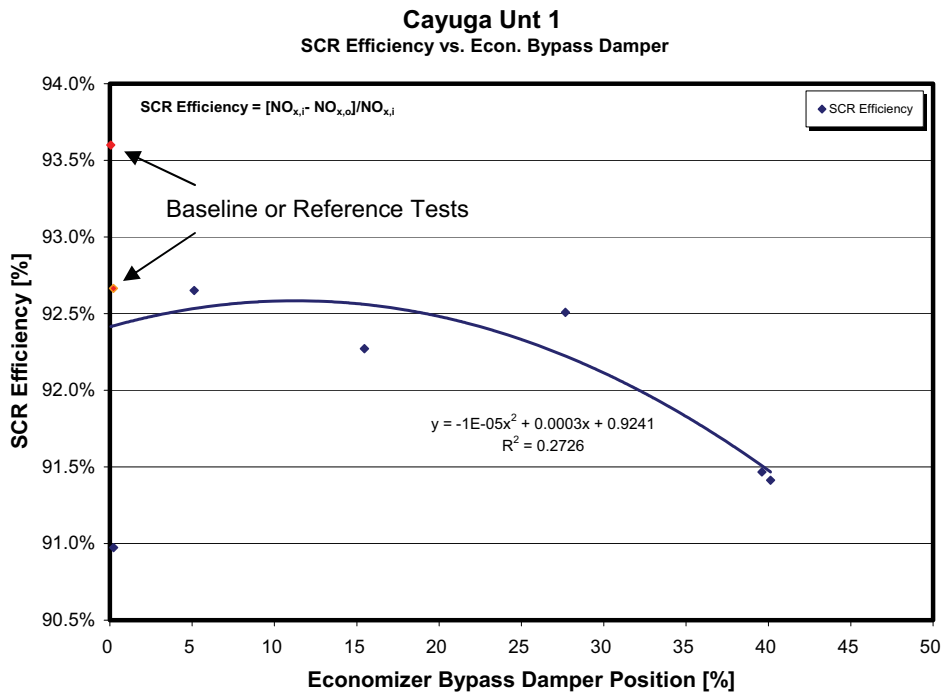


Figure 5-10: Impact of Economizer Bypass Damper on SCR Removal Efficiency.

The impact of NH₃ flow rate on the parameters of interest was also determined from the parametric test data. Figure 5-11 shows the trend for ABS formation and evaporation temperature as a function of NH₃ flow rate. Also included in Figure 5-10 is the axial location of the ABS deposition in the APH. As expected, the increase in NH₃ flow increases the ABS formation temperature, which implies that the

probability of ABS condensing at higher temperatures and, consequently, penetrating toward the APH hot-end is higher. As shown in Figure 5-11, increasing the NH₃ flow rate higher than 110 lb/hr, results in a deposition layer that moves beyond a 2.75 ft. mark from the APH cold-end, and at NH₃ flow rates, in excess of 130 lb/hr, the likelihood of exceeding the 2.75 ft. threshold for sootblowing removal is greatly enhanced. Obviously, these results can be modified by variations in the SO₃ concentration in the flue gas.

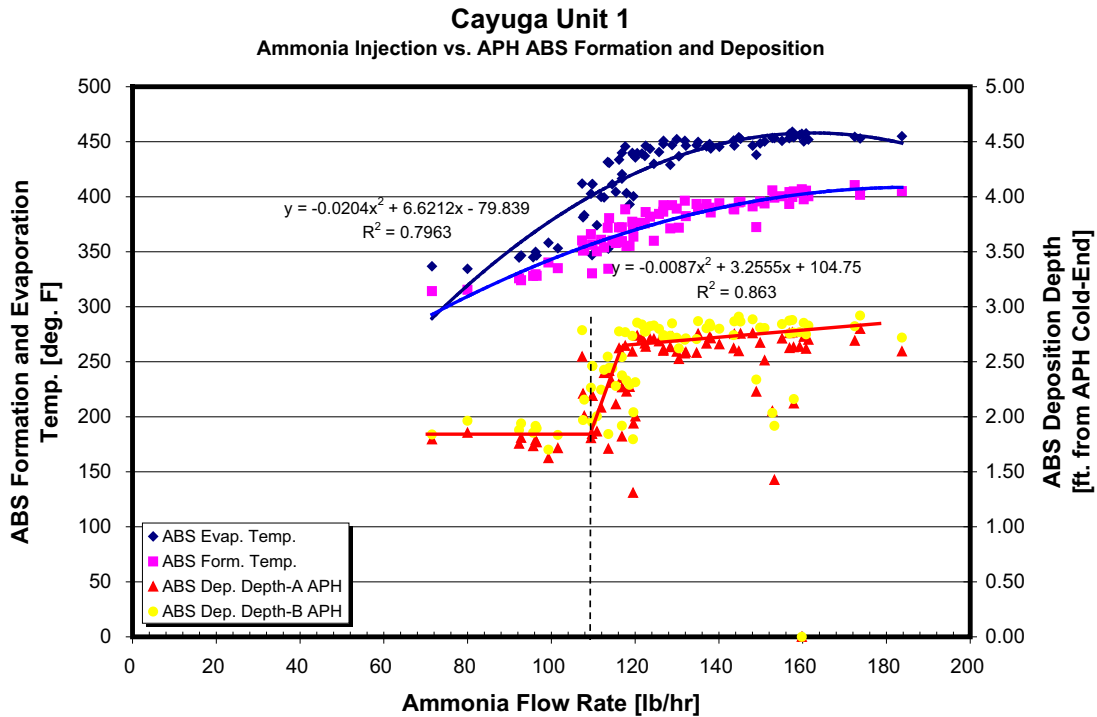


Figure 5-11: Impact of Ammonia Flow on ABS Formation Temperature and Deposition.

Figure 5-12 also shows results of NH₃ treatment with respect to ABS formation temperature, expressed as NH₃/NO_x ratio or NSR. For the particular SCR at Cayuga Unit 1, the ABS formation temperature tends to increase with NH₃ treatment. Similarly, the concentration of NH₃ in the fly ash increases with NSR. However, the NH₃ concentration in the ash is relatively small (less than 60 ppm_w) for NSR levels as high as 1.15. This is considered a very low level of NH₃ contamination, with values larger than 100 ppm_w considered of importance when using the fly ash for concrete applications.

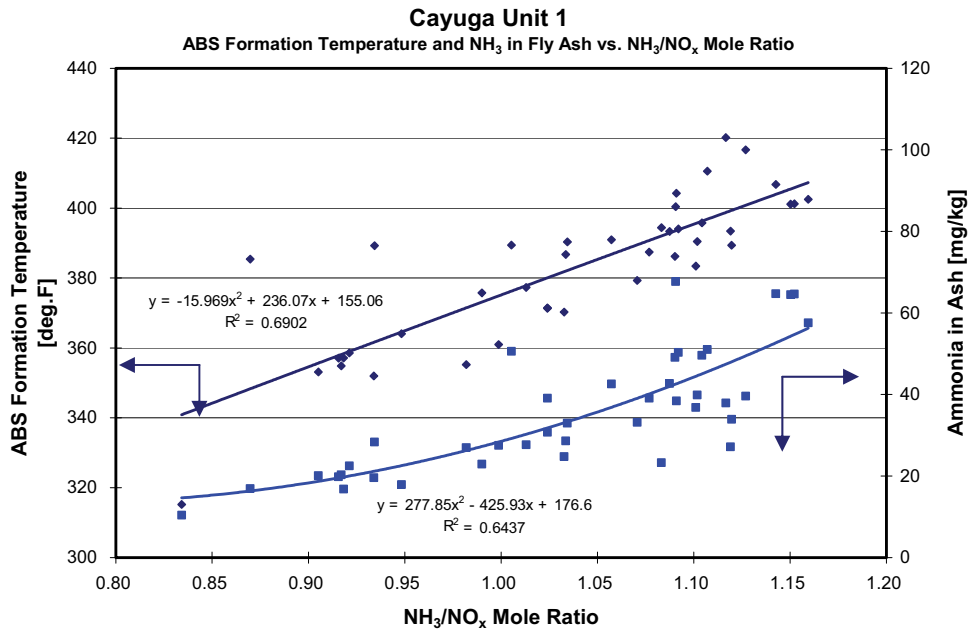


Figure 5-12: Impact of NSR on ABS Formation Temperature and Ammonia in Ash.

The independent parameter investigated for the APH was the air bypass damper. This parameter is used in the winter to increase the temperature at the APH cold-end to avoid acid dewpoint condensation. A similar approach works for ABS, where the APH air bypass damper can be used to maintain the ABS deposition location toward the cold-end and outside a previously determined limit of 2.75 ft., where the sootblowers located at the APH cold-end can reach and clean the ABS deposit. Manipulation of the APH air bypass dampers (one for each rotating APH) has an impact on the APH metal temperatures, which helps mitigate the ABS deposition, but also on the gas outlet temperature, which detrimentally impact unit heat rate. Tests that involved manipulation of the APH air bypass damper were performed in the range from fully closed to 75% open, as allowed by the plant. Figures 5-13 to 5-15 show the trends between the APH bypass damper position vs. ABS deposition depth, APH gas outlet temperature, and resulting unit heat rate penalty. In Figure 5-13, it can be seen that the APH bypass damper is effective in moving ABS formation from inside the 2.75 ft. threshold to the cold-end. However, Figure 5-14 shows that this improvement made in ABS deposition depth is accompanied by a significant increase in APH flue gas outlet temperature of the order of 50°F for the range of APH damper manipulation from 0 to 75%. This increase in stack losses has an impact on the net unit heat rate of as much as 150 Btu/kWh (Figure 5-15). This means that it is very important to control NH₃ injection and maintain an optimal performance at the SCR to minimize NH₃ slip, which adversely impacts ABS formation. When the conditions are such that ABS formation beyond the established threshold is inevitable, manipulation of the APH bypass damper is necessary. However, this should be a last resource, because the cost associated with the heat rate penalty has to be assessed against the cost of washing a fouled APH.

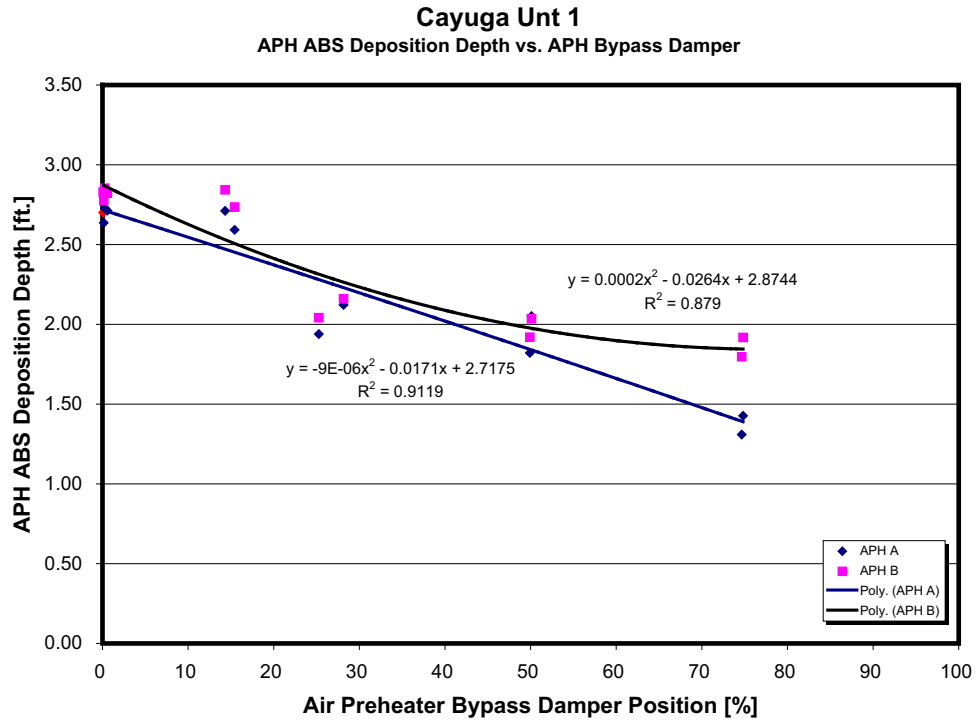


Figure 5-13: Impact of APH Bypass Damper Position on ABS Deposition Depth.

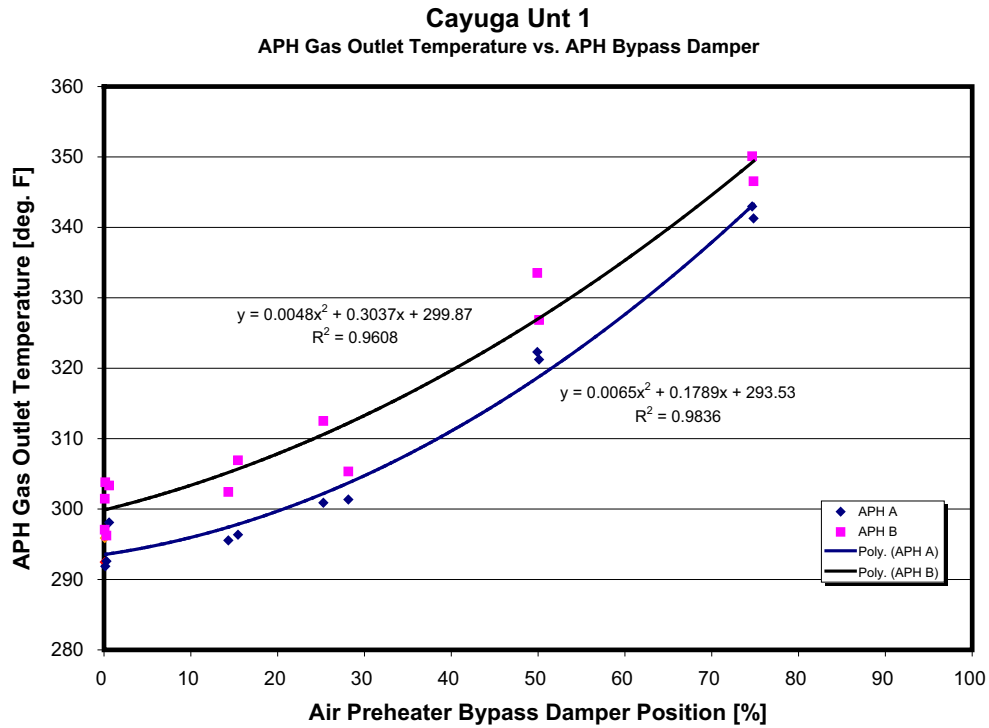


Figure 5-14: Impact of APH Bypass Damper Position on APH Flue Gas Exit Temperature.

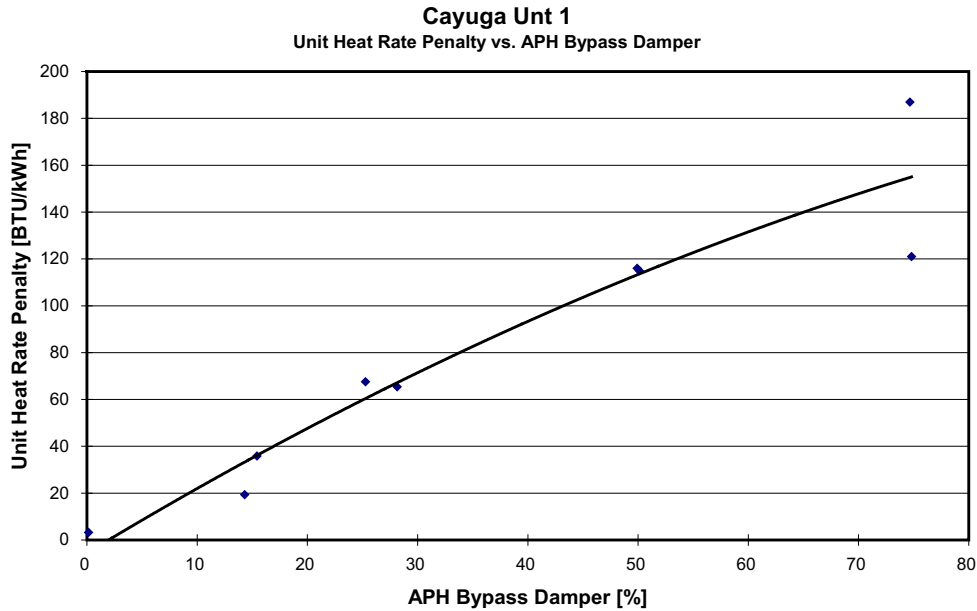


Figure 5-15: Impact of APH Bypass Damper Position on Unit Heat Rate Penalty.

Additionally, sootblowing tests were performed to investigate the impact of different sootblowing routines on the operation of the SCR system and associated NO_x reduction and NH₃ consumption. Sootblowing tests were performed with the unit at steady operating conditions. These sootblowing tests included activation of wallblowers (IRs) and retractables in the convective pass (IKs), including the SCR reactor and the APH. It takes approximately 2 minutes to blow individual IRs, 8 minutes to blow IKs and of the order of 20 minutes to blow individual sootblowers at the SCR and APH. Cayuga Station burns a range of bituminous coals that have a potential for high-temperature slagging and fouling, which has imposed a sootblowing schedule that runs continuously. However, the plant has not optimized its sootblowing practice and each operator blows soot in his/her own preferred way, once all the boiler is cleaned once per 12-hour shift. Some areas that are critical, such as the APH and the boiler slope area might be cleaned at a higher frequency.

The sootblowing tests performed as part of this project, targeted at evaluating the impact of sootblowing scheduling on SCR related variables, while not overlooking the slagging/fouling constraint. Figure 5-16 shows results from one of these tests, where selective IRs, IKs, and the SCR and APH were cleaned sequentially. As a consequence of the sootblowing activation, the flue gas temperature at the SCR declined and the SCR reactor was cleaned. This led, as seen in Figure 5-16, to a drop in ABS formation temperatures and a reduction in the NH₃ flow rate to achieve the prescribed NO_x stack limit. Based on the results of these tests, a sootblowing schedule is proposed that considers the cleaning constraints of selected fouling-sensitive areas, such as the APH. This schedule is included in Figure 5-17, for each shift. The

recommended schedule suggests activation of IR blowers at the waterwalls every 10 min., alternating blowers from each ring (A, B and C), as well as cleaning of the SCR once a shift, and of the APH three times per shift.

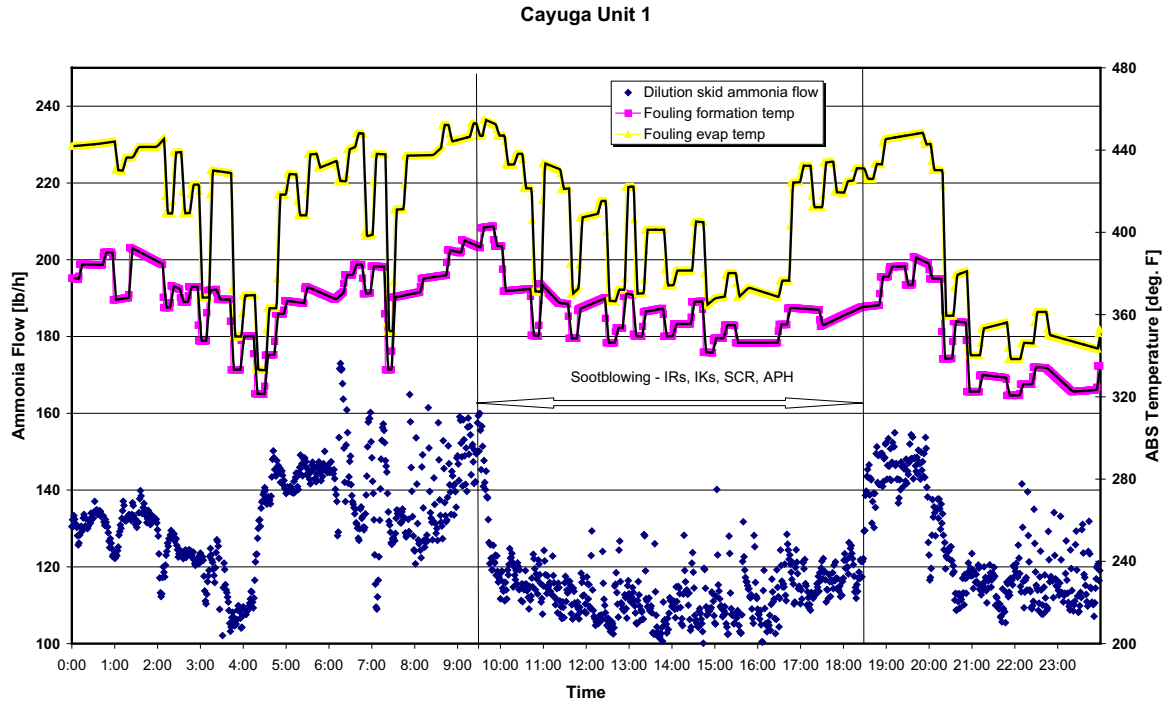


Figure 5-16: Results of Sootblowing Tests.

| Hour | 1 | | | | | | 2 | | | | | | 3 | | | | | | 4 | | | | | | 5 | | | | | | 6 | | | | | | |
|--------|---|----|----|----|----|----|----|----|----|----|----|----|----|----|----|----|----|----|-----|----|----|----|----|----|----|----|----|----|----|----|----|----|----|----|----|----|----|
| Minute | 0 | 10 | 20 | 30 | 40 | 50 | 60 | 10 | 20 | 30 | 40 | 50 | 60 | 10 | 20 | 30 | 40 | 50 | 60 | 10 | 20 | 30 | 40 | 50 | 60 | 10 | 20 | 30 | 40 | 50 | 60 | 10 | 20 | 30 | 40 | 50 | 60 |
| Wall | A | B | C | A | B | C | A | B | C | A | B | C | A | B | C | A | B | C | A | B | C | A | B | C | A | B | C | A | B | C | A | B | C | A | B | C | A |
| IK | | | | | | | 1R | | | | | 6L | | | | | | | 10R | | | | | | | | | | | | | | | | | | |
| Econo. | | | | | | | | | | | | | E2 | | | | | | | E4 | | | | | | | | | | | | | | | E3 | | |
| SCR | | | | | | | | | | | | 6 | | | | | | | 5 | | | | | | | | | | | | | | | | | | |
| APH | A | | | B | | | | | | | | | | | | | | | | | | | | | | | | | | | | | A | | | | |

| Hour | 7 | | | | | | 8 | | | | | | 9 | | | | | | 10 | | | | | | 11 | | | | | | 12 | | | | | | |
|--------|---|----|----|----|----|----|----|----|----|----|----|----|----|----|----|----|----|----|-----|----|----|----|----|----|----|----|----|----|----|----|----|----|----|----|----|----|----|
| Minute | 0 | 10 | 20 | 30 | 40 | 50 | 60 | 10 | 20 | 30 | 40 | 50 | 60 | 10 | 20 | 30 | 40 | 50 | 60 | 10 | 20 | 30 | 40 | 50 | 60 | 10 | 20 | 30 | 40 | 50 | 60 | 10 | 20 | 30 | 40 | 50 | 60 |
| Wall | | B | C | A | B | C | A | B | C | A | B | C | A | B | C | A | B | C | A | B | C | A | B | C | A | B | C | A | B | C | A | B | C | A | B | C | A |
| IK | | | | | | | 1L | | | | | 6R | | | | | | | 10L | | | | | | | | | | | | | | 4R | | | | |
| Econo. | | | | | | | | | | | | | E2 | | | | | | | E4 | | | | | | | | | | | | | | E1 | | | |
| SCR | | | | | | | | | | | | 3 | | | | | | | 2 | | | | | | | | | | | | | | 1 | | | | |
| APH | | | | | | | | | | | | | | | | | | | | | | | | | | | | | | | | A | | B | | | |

Figure 5-17: Proposed Sootblowing Schedule.

As part of this project, theoretical estimates were performed to consider the impact of modifications to boiler, SCR and APH control settings on mercury (Hg) emissions at the boiler back-end. Mercury is a toxic pollutant that has a significant impact on human health. Coal-fired power plants constitute the largest source of anthropogenic Hg emissions in the United States. There is pending (vacated) federal regulation and current stringent limits from some states, including New York for controlling Hg emissions from coal-fired boilers. Based on a numerical model developed by Lehigh University, calculations were performed of selected modified boiler conditions and their impact on Hg. The numerical model includes a gas-phase Hg chemical kinetic model composed of 92 reversible reactions and 35 species. This model is able to simulate homogeneous Hg oxidation in the boiler flue gas and heterogeneous Hg oxidation by the fly ash. Model results have been validated by bench-scale experimental data from the literature and matched with full-scale experimental data obtained from field tests at two power generation units.

Model Hg emissions results are included in Table 5-1. Table 5-1 includes the residence time used for each section of the convective pass, where flue gas temperature data were available, and the corresponding temperatures at the inlet of each section. These sections start at the furnace exit and include the SCR inlet, APH inlet and outlet, and the stack. A linear temperature profile was used for each reactor. A typical Eastern bituminous coal composition and Hg content was used in the simulations. The results included in Table 5-1 indicate changes in boiler conditions that lead to changes in excess O₂ level and fly ash LOI are not sufficient to cause a significant change in Hg emissions. Mercury emissions were expressed in relation to elemental mercury (Hg⁰). For both distinct set of operating conditions, Hg⁰ is reduced in the convective pass to about 79% at the SCR inlet and completely reduced to oxidized mercury (Hg²⁺) after crossing the SCR. The model does not include the impact of Hg oxidation on the SCR catalyst.

Table 5-1: Mercury Emissions Estimates for Different Boiler Operating Conditions.

| Location | Temperature (°F) | Residence Time (sec) | Hg ⁰ Emissions |
|---|------------------|----------------------|---------------------------|
| Excess O ₂ = 3.30%, Fly Ash LOI = 2.5% | | | |
| Furnace Outlet | 2,100 | 0 | 1.25E-09 |
| SCR Inlet | 637 | 1.7 | 9.81E-10 |
| APH Inlet | 636 | 2.3 | 9.45E-11 |
| APH Outlet | 295 | 2.9 | 3.19E-17 |
| Stack | 159 | 3.4 | 5.53E-17 |
| Excess O ₂ = 2.85%, Fly Ash LOI = 3.5% | | | |
| FEGT | 2,080 | 0 | 1.25E-09 |
| SCR Inlet | 638 | 1.7 | 9.99E-10 |
| APH Inlet | 636 | 2.3 | 9.44E-11 |
| APH Outlet | 297 | 2.9 | 3.25E-17 |
| Stack | 159 | 3.4 | 3.09E-17 |

MODELING RESULTS

Artificial intelligence (AI) modeling was performed on the data collected in the parametric testing. The AI modeling consisted of neural networks (NNs) and accurate on-line support vector regression (AOSVR) model development. NNs are mathematical algorithms that use interconnecting artificial neurons that mimic the properties of biological neurons. Support vector regression is a data-driven supervised learning method for classification and regression problems, based on statistic learning theory. AOSVR possesses the ability of being universal approximators of any multivariate function to any desired degree of accuracy. Belonging to the family of Kernel methods, AOSVR transfers the input space to a high dimension feature space by a nonlinear map; thus, original nonlinear relationships can be approximated as a linear function, f :

$$f(\mathbf{w}, \mathbf{x}) = \langle \mathbf{w}, \Phi(\mathbf{x}) \rangle + b$$

Where $\{(\mathbf{x}_i, y_i)\}, i=1,2,\dots,l$, and $\mathbf{x}_i \in R^m$, $y_i \in R$ is the training data set, $\langle \cdot, \cdot \rangle$ is the dot product, b is the threshold, and \mathbf{w} is the weight vector, which can be identified under a given regularized risk function. NN and AOSVR, both provided comparable model result accuracy. However, the AOSVR method overcomes some of the problems of artificial NNs associated with slow training, local minima and poor interpretability of the results. Results on the AOSVR modeling are included in this report.

AOSVR was used to built artificial intelligence-based, functional relationships between the boiler outlet or SCR inlet NO_x level and heat rate penalty (with respect to the design heat rate level), and the first five parameters included in Table 4-1 (O_2 , $SOFA$, α_{ST} , α_{BT} and F_{coal}). The AOSVR model was trained with the database obtained from the parametric tests, and adaptively updated with real-time data sets. Four thousand data points were extracted from real-time data at a 1-minute sample rate and used for AOSVR adapting. Figure 5-18 shows a comparison between the on-line data and the predicted model results for boiler outlet NO_x emissions rate. The AOSVR showed good convergence and acceptable learning efficiency. AOSVR accurate learning results from its efficient data updating and it is well suited for time-varying systems. The prediction performance of proposed AOSVR models was evaluated using a mean absolute percentage error (MAE) as validation criterion, which is defined as:

$$\text{MAE} = \frac{1}{n} \sum_{i=1}^n \frac{|y_i - \hat{y}_i|}{y_i} \times 100\%$$

Where n is the sample size, y_i denotes the sample data, and \hat{y}_i is the modeling output value. The MAE value for the AOSVR boiler outlet NO_x and heat rate penalty was 1.65. Smaller values of MAE indicate better model predicting capabilities.

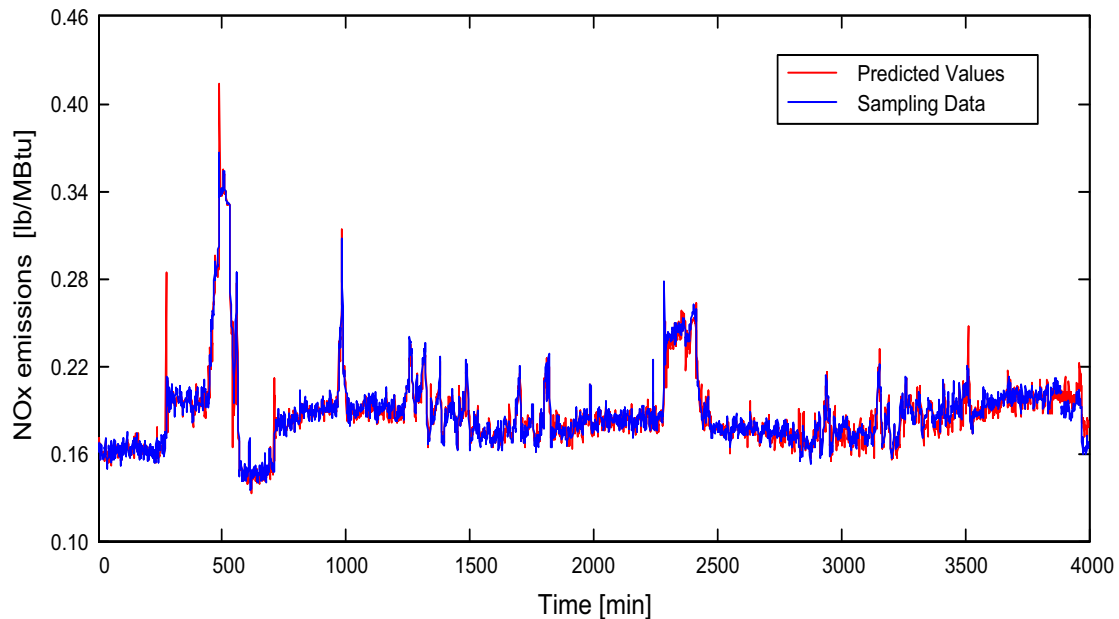


Figure 5-18: Modified AOSVR NO_x Emissions Model Prediction Results.

Figure 5-19 shows AOSVR model trending results for the impact of boiler parameters on heat rate deviation or penalty. The modeling results in Figure 5-19 are consistent with the trending expected from each of the selected boiler control settings. The heat rate penalty vs. excess O₂ exhibits a second order trend, where increase in heat rate to the left is due to increases in fly ash LOI, and to the right due to stack losses. The trending with respect to burner and SOFA tilt angle is related to the enhancement in steam temperatures due to the changes in radiant heat when the burners are modulated. The increased trending in heat rate penalty with respect to increased coal flow to the top elevation mill and the SOFA register opening is due to the decrease in particle burnout residence time that occurs when the upper elevation of burners is in-service (I/S), and to the cooling effect to the fireball caused by the SOFA, respectively. Modeling results obtained from the AOSVR model were compared with actual plant data obtained during the parametric tests, showing a good degree of accuracy.

OPTIMIZATION RESULTS

The functional relationships obtained from the AOSVR modeling were then used to perform a boiler/SCR/APH mathematical optimization. Additionally, relationships for the lowest required NH₃ injection flow rate as a function of SCR inlet NO_x and for heat rate penalty as a function of the APH air bypass level were used in the optimization. Figure 5-20 shows the plot of minimal NH₃ flow rate vs. SCR inlet NO_x. The minimal NH₃ vs. SCR inlet NO_x curve shows a rapid increase when the SCR inlet NO_x level exceeds the 0.26 lb/MBtu, which is characteristic of the catalyzed NO_x reduction process in the SCR

reactor. Maintaining the NH_3 injection rate with the same slope, as the one exhibited at low NO_x levels ($< 0.26 \text{ lb/MBtu}$) would result in violation of the stack NO_x emissions constraint. An increase in NH_3 flow is required at larger SCR inlet NO_x levels. This increase in reagent requirement for elevated SCR inlet NO_x levels is what increases the risk of NH_3 slip and, subsequent formation of ABS in the ducting and equipment, downstream of the SCR.

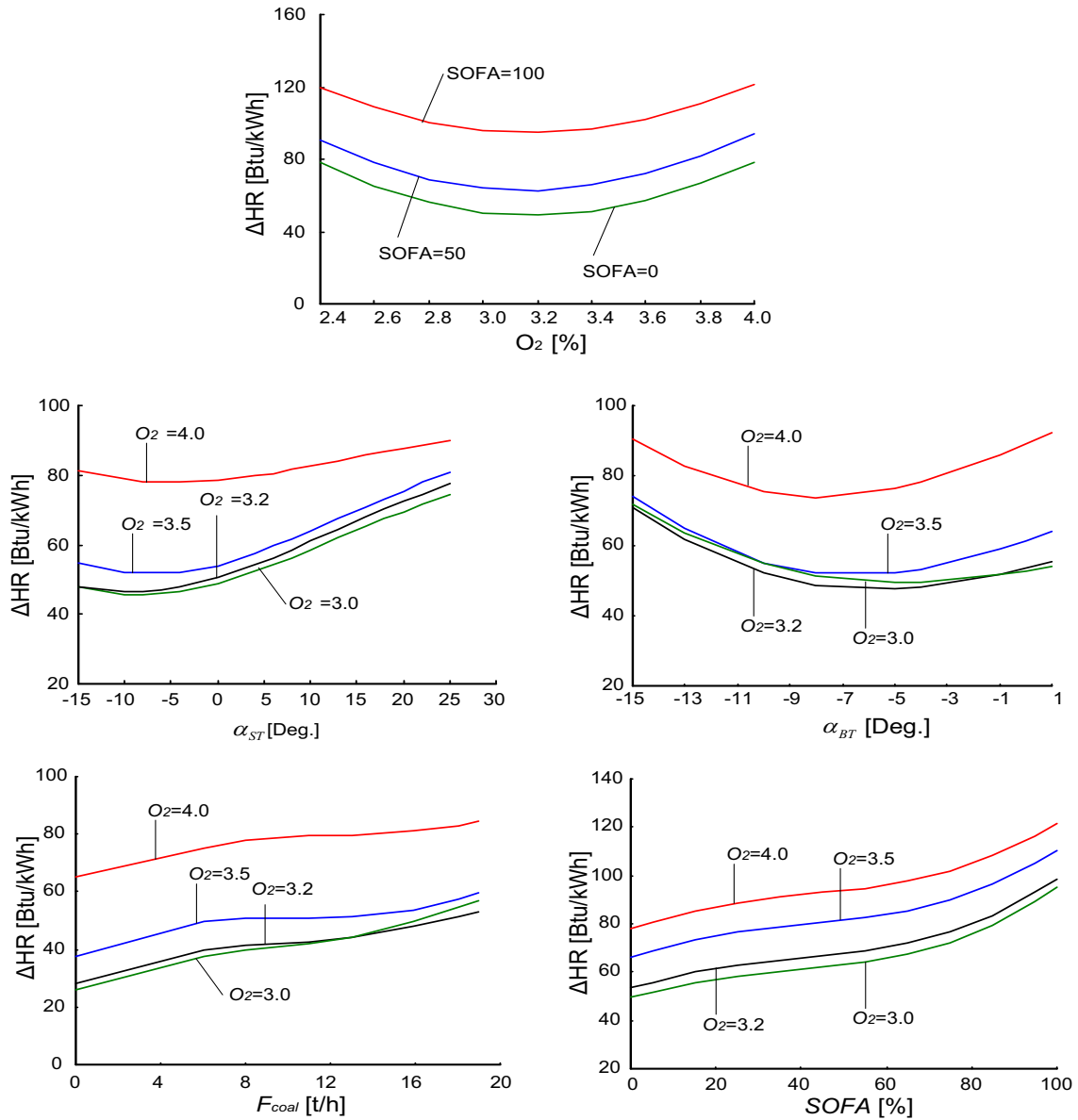


Figure 5-19: Trained AOSVR Model Results for Boiler Heat Rate Penalty.

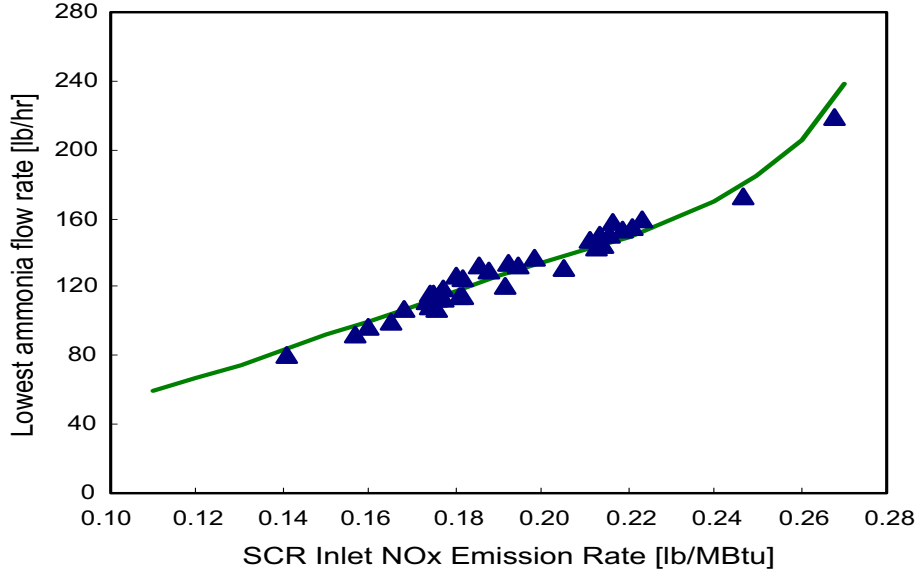


Figure 5-20: Lowest NH₃ Flow Rate vs. SCR Inlet NO_x.

The optimization was performed in two steps, using genetic algorithms (GAs). GA is a class of stochastic search optimization technique, which derives its behavior from the evolutionary theory of natural selection. In this work, the Niche Pareto genetic algorithm (NPGA) was used. A Pareto optimal set is a set of solutions that are non-dominated with respect to each other. In the NPGA approach, a higher number of individuals are involved in competition, resulting in a higher searching efficiency achieved. A solution is Pareto optimal if it is not dominated by any other solution in the solution space. In the GA solution used in this project, a multi-objective optimization (MOO) problem was formulated as:

$$\begin{aligned} \min \mathbf{f}(\mathbf{x}) &= [f_1(\mathbf{x}), f_2(\mathbf{x}), \dots, f_k(\mathbf{x})] \\ \text{s.t. } \mathbf{g}(\mathbf{x}) &\leq 0 \\ \mathbf{h}(\mathbf{x}) &= 0 \end{aligned}$$

Where $\mathbf{x} = [x_1, x_2, \dots, x_n]^T \in \mathbf{X}$ is the vector of decision variables in the decision space,

$\mathbf{X}, f_i : R^n \rightarrow R, i = 1, 2, \dots, k$ is the objective function, and $\mathbf{g}(\cdot)$ and $\mathbf{h}(\cdot)$ are the inequality and equality constraint vectors. The MOO problem was defined to find the particular set, $\mathbf{x}^* \in \mathbf{X}$, which satisfies both constraints and yields the optimum values of all objective functions. Since there is rarely a single point that simultaneously optimizes all object functions, a Pareto optimum is defined to look for trade-offs in these objectives.

In the GA implementation of this study, a population of candidate solutions was first used, based on the parametric test database. This population was then modified (recombined and randomly mutated) to form new iterative populations, from which better fitness or solutions were achieved that fulfill the multi-

objective optimization problem. The GA implementation was done in two steps. In the first step, a GA was used to derive a functional relationship between the minimal or optimal boiler heat rate penalty as a function of target boiler outlet or SCR inlet NO_x. The constrained multi-objective optimization problem was defined by:

$$\begin{aligned} \min \text{NO}_x &= f_{\text{NO}_x}(\text{O}_2, \text{SOFA}, \alpha_{\text{ST}}, \alpha_{\text{BT}}, F_{\text{coal}}) \\ \min q &= f_q(\text{O}_2, \text{SOFA}, \alpha_{\text{BT}}, F_{\text{coal}}) \\ \text{subject to: } \theta &\leq \theta_{\text{max}} \\ \text{O}_{2,\text{min}} &\leq \text{O}_2 \leq \text{O}_{2,\text{max}} \\ \text{SOFA}_{\text{min}} &\leq \text{SOFA} \leq \text{SOFA}_{\text{max}} \\ \alpha_{\text{ST},\text{min}} &\leq \alpha_{\text{ST}} \leq \alpha_{\text{ST},\text{max}} \\ \alpha_{\text{BT},\text{min}} &\leq \alpha_{\text{BT}} \leq \alpha_{\text{BT},\text{max}} \\ F_{\text{coal},\text{min}} &\leq F_{\text{coal}} \leq F_{\text{coal},\text{max}} \end{aligned}$$

Where $f_{\text{NO}_x}(\cdot)$ and $f_q(\cdot)$ are the objective functions between the first five boiler operating variables listed in Table 4-1, and boiler outlet NO_x emissions and heat rate penalty, q , respectively. The optimization was constrained by fly ash unburned carbon, θ , to be below a prescribed maximum of 4 percent, and the operating input parameters to be between minimum and maximum levels, representing their operational upper limit and lower limit, as indicated in Table 4-1. Figures 5-21(a) to 5-21(d) show different stages of the GA optimization for minimum boiler NO_x and heat rate penalty. The parametric test database is shown in Figure 5-21(a). A sequence of data generation and best fitness selection is shown in Figures 5-21(b) to 5-21(d). Converged optimal solutions are presented in Figure 5-21(d) after the 30th generation. The heat rate penalty vs. SCR inlet NO_x trend in Figure 5-21(d) was fitted into a polynomial function to be used in the second step in the optimization.

The second step of the optimization consisted of minimizing an overall cost function that combines the costs of: (1) the heat rate penalty resulting from tuning of the boiler control settings to achieve an optimal boiler outlet or SCR inlet NO_x emissions rate; (2) reagent to produce the required SCR NO_x reduction performance; and (3) the heat rate penalty to operate the APH within the ABS deposition constraint, if necessary. Savings due to avoidance of APH washes was not included in the optimizable cost function. The second step optimization was defined by:

$$\begin{aligned} \min C_{\text{total}} &= k_1 C_1(\text{NO}_x) + k_2 C_2(\text{NH}_3) + k_3 C_3(D_{\text{APH}}) \\ \text{subject to: } d_{\text{ABS}} &\leq a_{\text{depth}} \\ \text{NO}_{x,\text{outlet}} &\leq a_{\text{NO}_x,\text{limit}} \\ \text{NO}_{x,\text{min}} &\leq \text{NO}_x \leq \text{NO}_{x,\text{max}} \\ \text{NH}_{3,\text{min}} &\leq \text{NH}_3 \leq \text{NH}_{3,\text{max}} \\ D_{\text{APH},\text{min}} &\leq D_{\text{APH}} \leq D_{\text{APH},\text{max}} \end{aligned}$$

Where the total cost C_{total} is composed of the fuel cost, C_1 , due to the boiler heat rate penalty; the NH_3 treatment cost, C_2 , and the heat rate penalty cost, C_3 , due to the manipulation of the APH bypass damper (D_{APH}). The coefficients, k_i , $i = 1, 2, 3$ were set with a value of 1.0. The deposition depth limit (d_{ABS}) was set $< a_{depth} = 2.75$ ft.

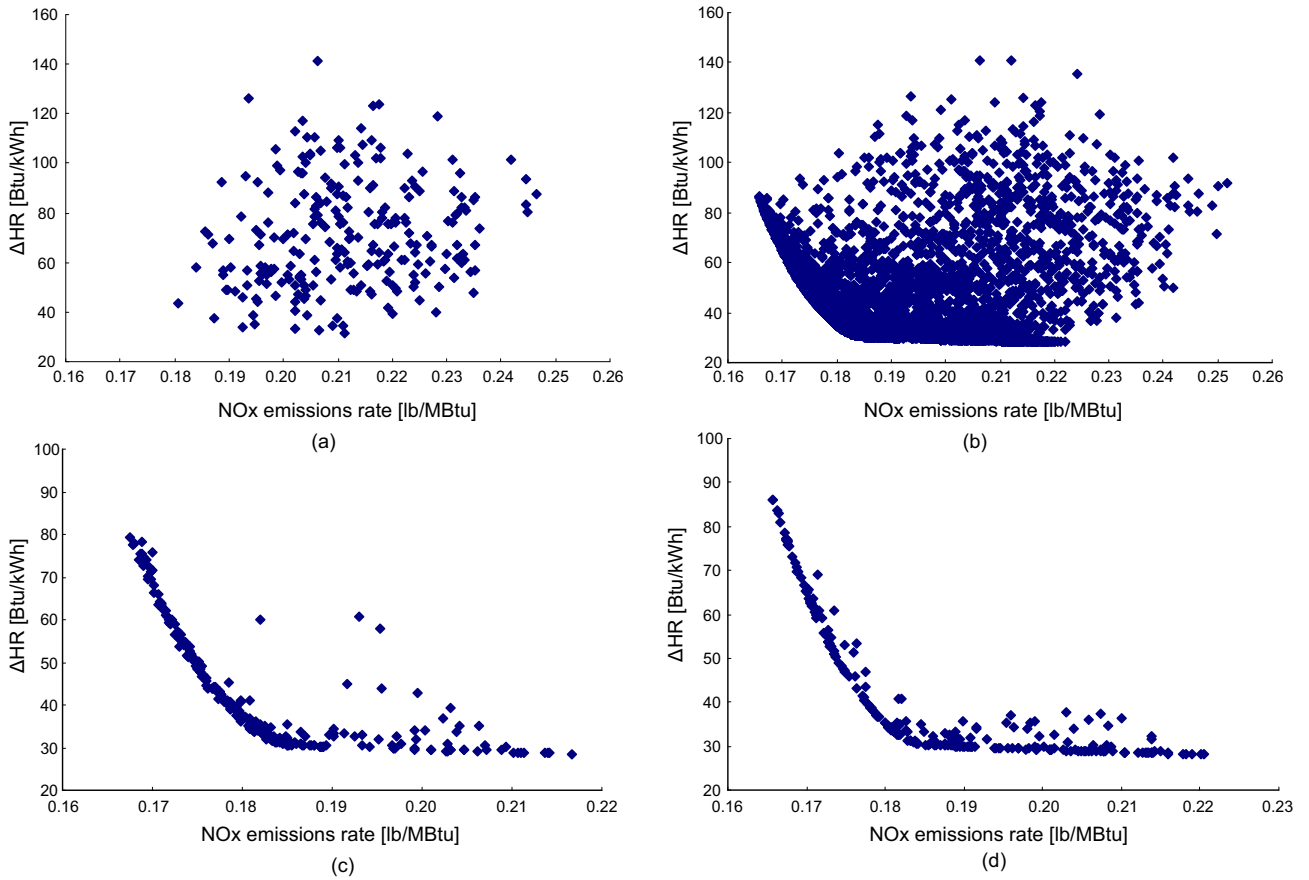


Figure 5-21: GA Optimization Results for Boiler Outlet NO_x – (a) Initialization Dataset, (b) 1st Generation, (c) 15th Generation, (d) 30th Generation.

The combined boiler/SCR/APH cost function was optimized using GAs. The following rates were used in the evaluation of the cost function: power generation cost of \$0.02/kWh and NH_3 cost of \$0.25/lb, to convert the objective function to units of dollars per hour. Figures 5-22(a) and 5-22(b) show a 3-D map of all searched solutions provided by the GA, expressed as differential costs with respect to baseline heat rate conditions. Also, included in these figures are the sets of SCR inlet NO_x , NH_3 injection rate and APH bypass damper positions that violate the ABS deposition distance constraint and the NO_x emissions rate limit. The set of feasible solutions, which satisfy both constraints are also shown in Figures 5-22(a) and 5-22(b). These solutions were obtained after the 22nd generation of the GA algorithm. Figure 5-22(a) shows on the z-axis that a low NH_3 injection rates the stack NO_x emissions constraint is violated, while at high NH_3 injection rates the ABS deposition constraint is violated. Optimal solutions that satisfy both

constraints are obtained in the NH₃ flow rate range between 120 and 195 lb/hr. The optimal solution for the lowest cost of compliance corresponds to the following control setting: O₂ = 3.2%, average SOFA register opening = 51% (both top- and mid-SOFA registers open equally), average burner tilt angle = -8 degrees, average SOFA tilt angle = +6 degrees, 1A1-Mill coal flow rate = 6 ton/hr, APH bypass damper = 0%, and an NH₃ injection rate = 125 lb/hr. The optimal NH₃ injection rate represents a reduction in NH₃ flow rate from baseline conditions of approximately 22 percent. The combination of optimal settings will result in NO_x emissions at the boiler outlet of 0.188 lb/MBtu, while complying with ABS deposition at less than 2.75 ft. and fly ash unburned carbon below 4 percent, at a differential cost of \$41.2/hr. Figure 5-23 shows costs associated with operation at optimal combinations of boiler control settings that result in a range of boiler outlet NO_x emissions levels. It can be inferred from Figure 5-23 that operation at the “knee” of the SCR inlet NO_x vs. heat rate penalty results in the lowest combined cost of operation. Operation at SCR inlet NO_x levels at the left of that knee results in a significant added cost, due to the contribution from the boiler heat rate penalty. Operation at the right of the knee results in a gradual moderate cost increase due to additional NH₃ consumption, until a point is reached (at around 0.25 lb/MBtu) where there is a need to manipulate the APH bypass damper to control the ABS deposition. This results in a steep heat rate penalty due to increased stack losses. As anticipated, the optimization model indicates that the total cost of compliance increases as the ABS deposition distance is tightly set, closer to the APH cold-end. A reduction in the ABS deposition depth setpoint below 2.5 ft. would require opening of the APH bypass damper, with the associated heat rate penalty from this component of the cost function.

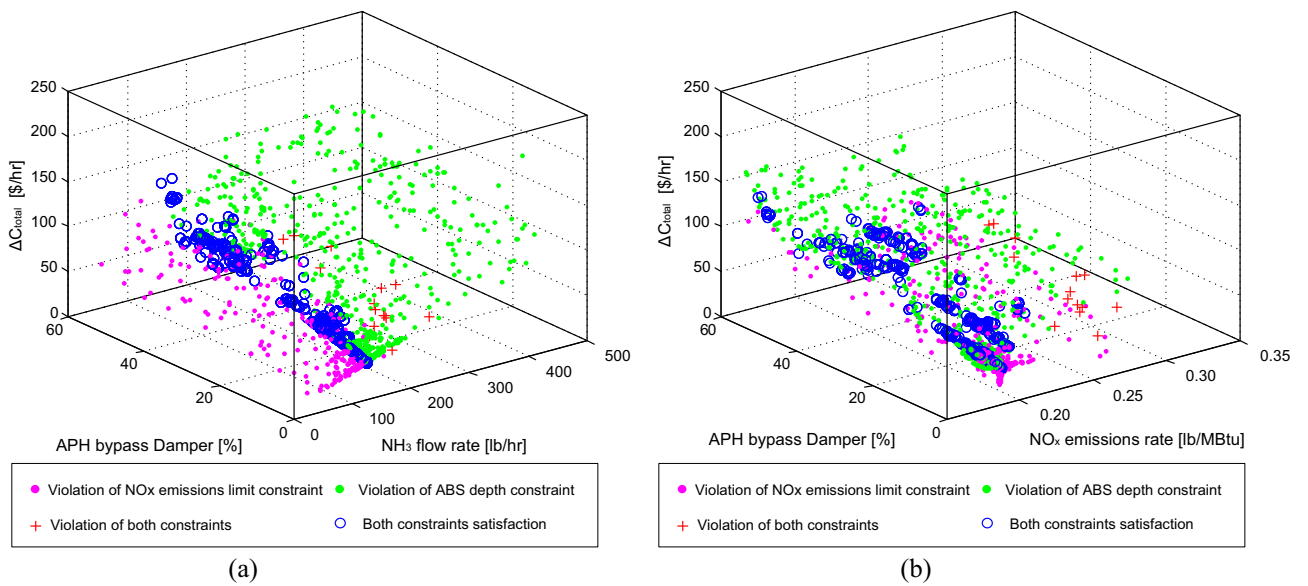


Figure 5-22: GA Optimization Solutions for the Total Cost Function.

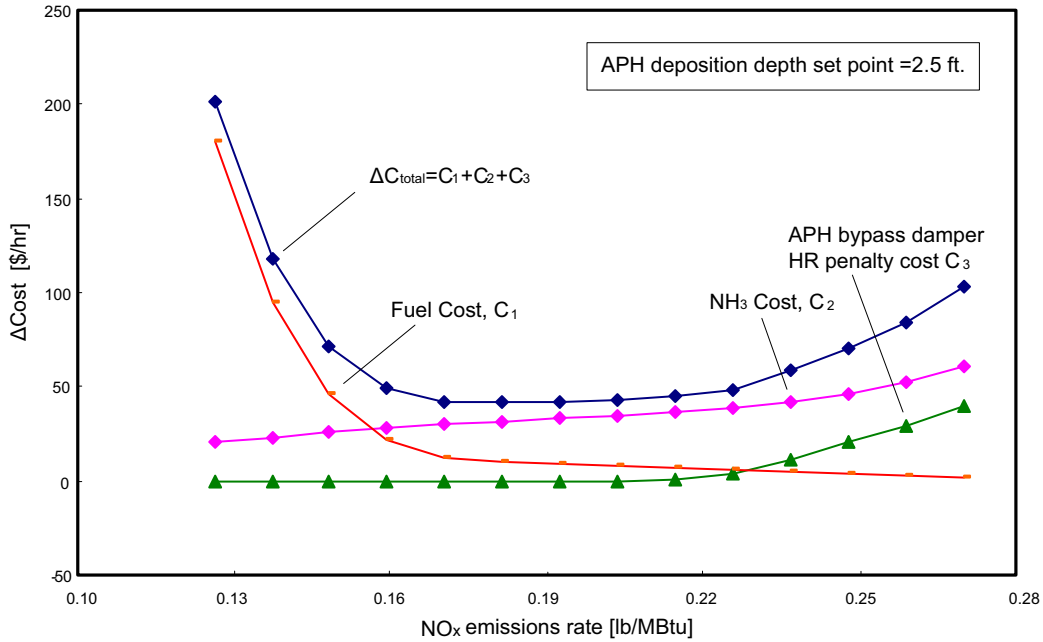


Figure 5-23: Cost Components as a Function of Boiler Outlet NO_x .

The constraints imposed for the stack outlet NO_x emissions level at < 0.095 lb/MBtu and for the APH to maintain the ABS axial deposition location in the APH at 2.75 ft. from the cold-end were found to be adequate to maintain Cayuga Station's NO_x allowances. The location of the ABS setpoint was chosen based on the known penetration distance of the APH sootblowers, which are located at the cold-end side of the APH. Any deposition of sticky ABS deposits on the APH baskets, beyond the chosen deposition setpoint, would have a lower probability of being removed by sootblowing, increasing the risk of gradual fouling of the APH and further loss of generation for APH washing. From the results of this work, it was determined that two options are available when the ABS deposition distance is beyond the reach of the sootblowers (exceeds the 2.75 ft. setpoint), viz, to lower the NH_3 injection rate to the lowest conditioning permitted to achieve the required outlet NO_x level, or manipulate the APH air bypass damper to increase the metal temperatures. Opening the APH bypass damper is the least preferred option, since it results in heat rate penalties, due to the increase in stack losses associated to higher flue gas temperatures exiting the boiler.

Section 6

UPGRADED SCR CONTROL STRATEGY

As part of this project, modifications to the SCR control logic were studied and proposed, aiming at developing an upgraded control strategy that incorporates feedback measurements and optimization results. The system composed by the boiler, SCR system and APH was considered for the upgrade (see illustration in Figure 6-1). The adopted upgraded control strategy consists in: (1) regulating pertinent boiler conditions (O_2 , SOFA registers, burner tilt, SOFA tilt and 1A1 mill coal flow) to minimize NO_x at the SCR inlet and maximize SCR efficiency; (2) regulating the NH_3 flow to control stack or continuous emissions monitoring (CEM) NO_x ; and (3) regulating the APH bypass damper to control ABS deposition depth within the APH. Since the ABS deposition depth is also affected by the NH_3 flow, an approach for integrated control of SCR and APH is discussed. The proposed control scheme includes a dual-loop control strategy for automatic boiler, NH_3 flow, and APH bypass damper control over the unit load range with the ultimate goal of minimizing boiler outlet NO_x emissions, minimizing stack NO_x emissions, minimizing NH_3 consumption (maximizing SCR efficiency), and minimizing unit heat rate penalties.

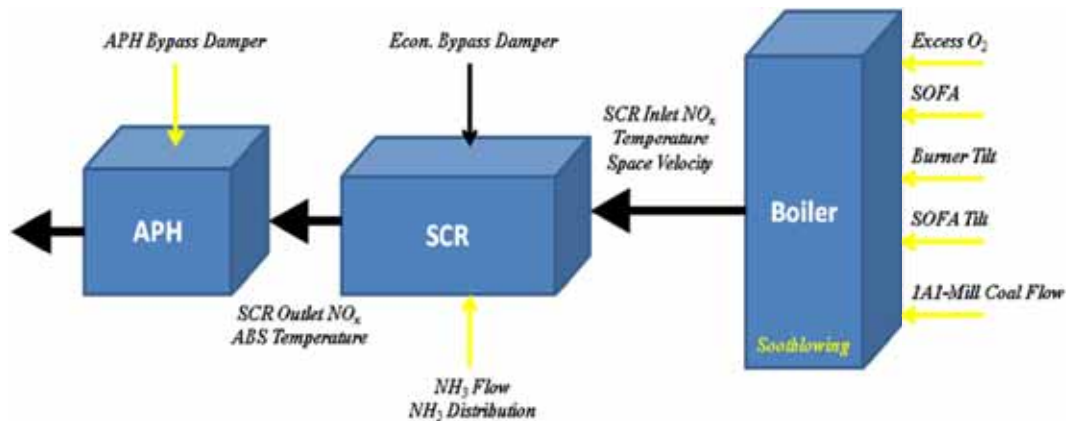


Figure 6-1: System Configuration Used for the Control Strategy Upgrade.

UPGRADED SCR/APH CONTROL SCHEME

SCR Control

The SCR control system provided by the manufacturer is shown in Figure 6-2. This control scheme is typical for SCR control in the industry. The objective of the feedback control loop is to regulate the efficiency of the SCR system at a predefined value given by η_{SCR} . The injection of NH_3 is dictated by this feedback loop but also by a feedforward controller, which makes the feedforward component of the NH_3 flow just proportional to NO_x_{in} . Although, this scheme guarantees a specific efficiency, it cannot guarantee a specific value of CEM NO_x .

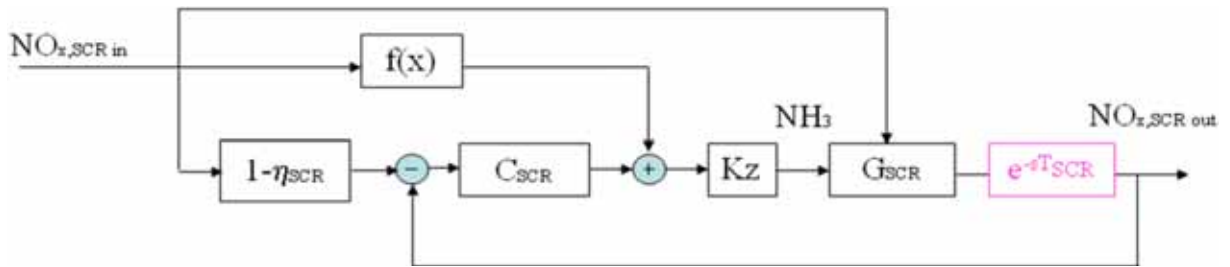


Figure 6-2: SCR Manufacturer's Typical Control Architecture. The term $NO_{x,SCR\ in}$ denotes the NO_x level at the SCR inlet (denoted as NO_{x_in} in the text). The term $NO_{x,SCR\ out}$ denotes the NO_x level at the SCR outlet (denoted as NO_{x_out} in the text).

By exploiting the availability of the continuous emissions monitoring system, it is possible to propose a different control approach where the ultimate goal is the regulation of the NO_{x_CEM} level at a predefined value. The approach, illustrated in Figure 6-3, also combines both feedforward and feedback loops. The variable "s" is used to denote the Laplace Transform variable in the system transfer functions.

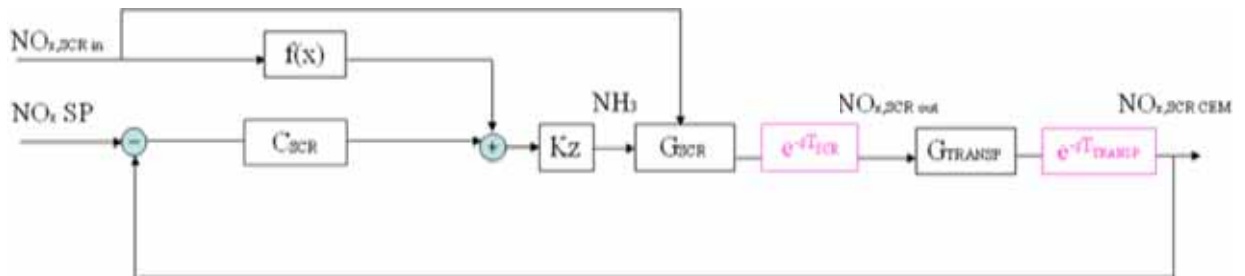


Figure 6-3: SCR Control Architecture Based on the CEM NO_x Input. The term $NO_{x,SCR\ CEM}$ denotes the NO_x level at the CEM (denoted as NO_{x_CEM} in the text). The term $NO_x\ SP$ denotes the setpoint value for NO_{x_CEM} (denoted as $NO_{x_CEM_setpoint}$ in the text).

Although, the controller in Figure 6-3 can in principle guarantee a specific level of NO_{x_CEM} , the time delays, both in the SCR system and in the transport channel (denoted in pink in both Figures 6-2 and 6-3) can significantly affect the performance of the control approach. Since the NO_x signal from the plant CEM is used to regulate NH_3 flow, a pure time delay, associated with the measurement of this parameter, needs to be dealt with. There are several control methods available to deal with time delays in feedback loops. Most of them, however, require a good knowledge, i.e., a model of the system, which is usually not the case in coal-based power plants. For this reason, it is proposed a non-model-based approach consisting in a multi-loop proportional–integral–derivative (PID) approach combined with optimal tuning. Information on the rate of change of NO_x at both, the SCR inlet and the SCR outlet is incorporated into the NH_3 flow feedback controller in order to overcome the effect of the time delay and eliminate oscillations present in both the CEM NO_x and NH_3 injection. In addition, not only positive but also negative feedback correction (bias) of the feedforward loop is allowed with the objective of eliminating the NH_3 slip that characterizes SCR operation, due to this control limitation. The proposed scheme is shown in Figure 6-4, where the

outer-loop controller $C_{SCR,OUT}$ is a PID controller, the inner-loop controller $C_{SCR,IN}$ is a proportional-derivative (PD) controller, and the feedforward controller $C_{SCR,FEED}$ is a pure derivative (D) controller:

$$C_{SCR_OUT}(s) = K_{P,OUT} + K_{I,OUT} \frac{1}{s} + K_{D,OUT}s, \quad C_{SCR_IN}(s) = K_{P,IN} + K_{D,IN}s, \quad C_{SCR_FEED}(s) = K_{D,FEED}s$$

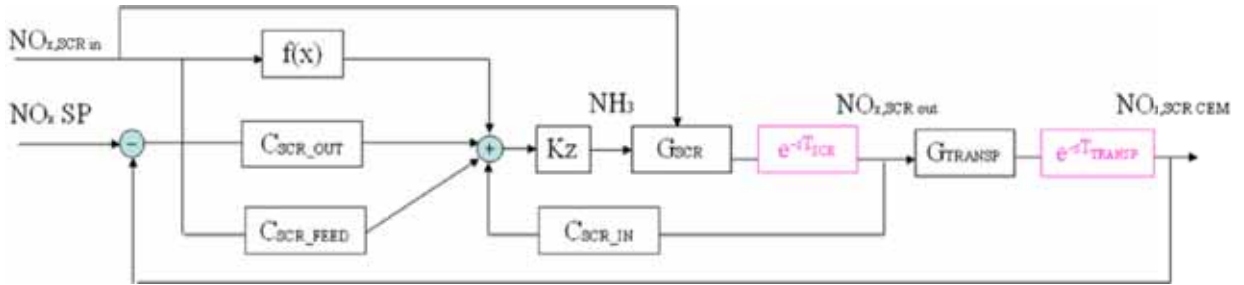


Figure 6-4: Multi-Loop SCR Control Architecture Based on CEM NO_x, SCR Inlet NO_x and SCR Outlet NO_x.

In order to compare the different control approaches, and also to optimally tune the controller parameters to cope with the time delays, simulations were carried out using MATLAB SIMULINK[®]. For that purpose, a simplified model of the SCR system was created. A diagram of the SIMULINK closed-loop system is illustrated in Figure 6-5.

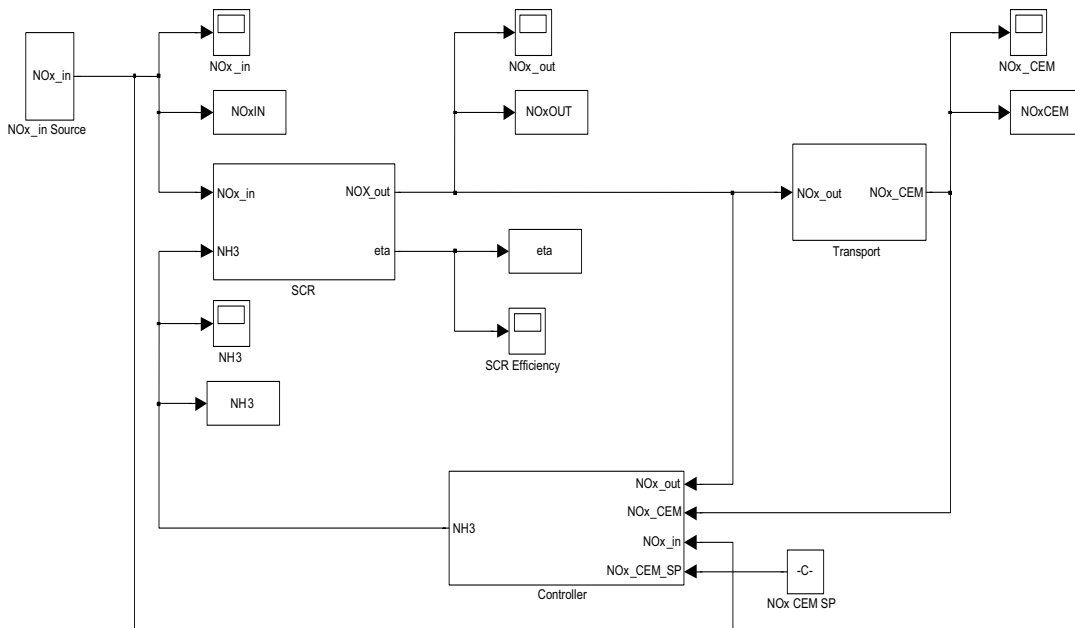


Figure 6-5: SIMULINK SCR Control Configuration.

As illustrated in Figure 6-6, the SCR system was modeled as:

$$NOx_out = e^{-sT_{SCR}} \frac{1}{\tau_{SCR}s + 1} n_{SCR}(NH_3/NOx_in)NOx_in,$$

Where $\eta_{SCR}(NH_3/NOx_in)$ is plotted in Figure 6-7.

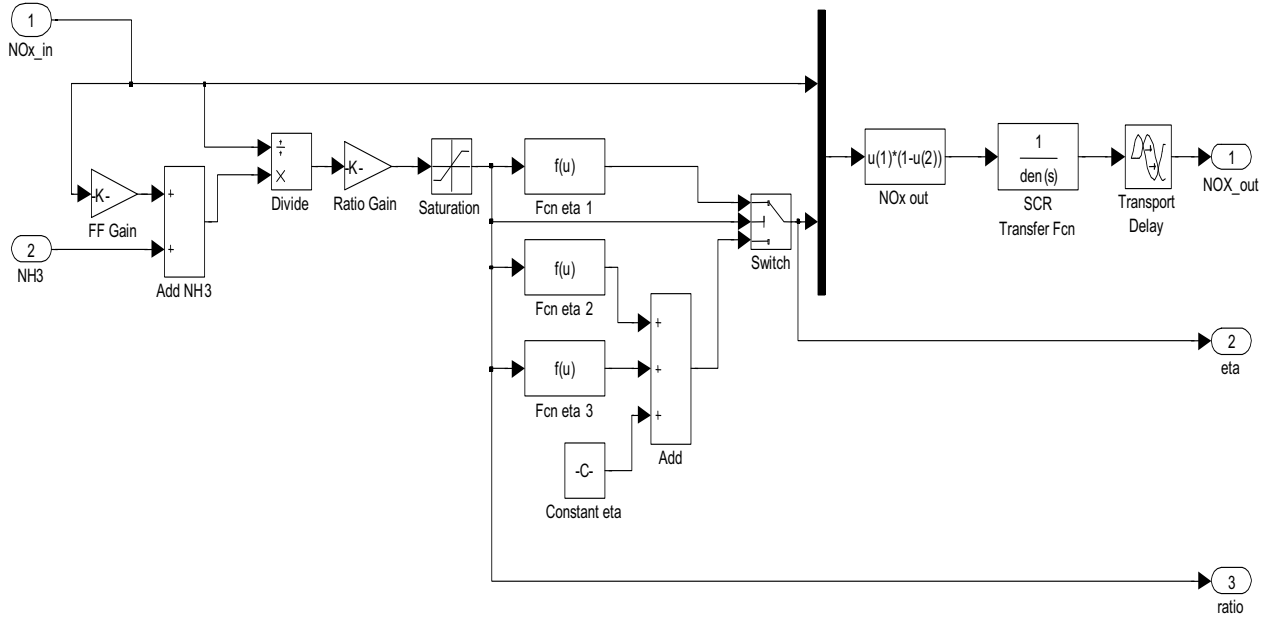


Figure 6-6: Simplified SCR Model.

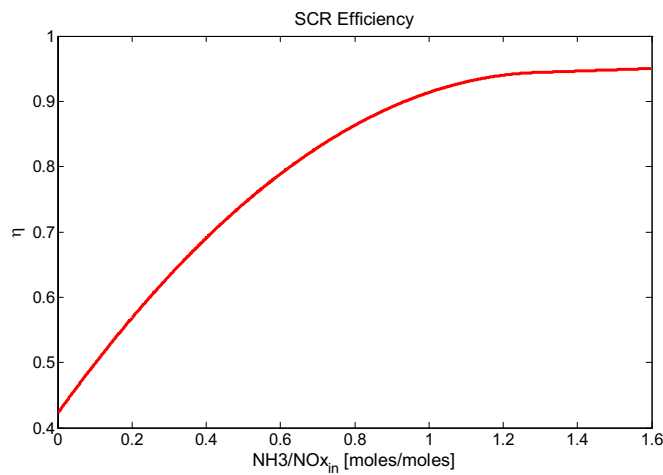


Figure 6-7: SCR Efficiency as a Function of NH₃/NO_x_{in} Ratio.

An extremum seeking optimization (see details below) was also carried out to optimally tune the gains of the controllers in the equation corresponding to Figure 6-4. The objective is to tune the controller gains in order to minimize the tracking error. Thus, we define the to-be-minimized cost function as:

$$J = \frac{1}{2} \int_{t_0}^t [NOx_CEM(t) - NOx_CEM_setpoint(t)]^2 dt$$

Figure 6-10 shows the evolution of the cost function as a function of the extremum-seeking iteration number. The evolution of the to-be-optimized parameters, $\theta_1=K_{P,OUT}$, $\theta_2=K_{I,OUT}$, $\theta_3=K_{D,OUT}$, $\theta_4=K_{P,IN}$, $\theta_5=K_{D,IN}$, and $\theta_6=K_{D,FEED}$ is shown in Figure 6-11. The optimization was stopped after 200 iterations because no significant further improvement of the cost function value was achieved. The chosen simulation parameters were: $T_{SCR}=30s$, $\tau_{SCR}=10s$, $T_{TRANSP}=60s$, $\tau_{TRANSP}=20s$. The resulting optimal gains were: $K_{P,OUT}=1.3182$, $K_{I,OUT}=1.1563$, $K_{D,OUT}=1.0564$, $K_{P,IN}=2.9020$, $K_{D,IN}=0.0170$ and $K_{D,FEED}=0.0572$.

To demonstrate the performance of the SCR controller, Figure 6-12(d) shows the time response of the SCR multi-loop system when NOx_{in} changes as illustrated in Figure 6-12(a). The feedback component for the NH_3 injection is showed in Figure 6-12(b). In Figure 6-12(c), it can be seen that SCR efficiency was not kept constant, because the ultimate goal is the regulation of NOx_CEM at the desired setpoint. Figure 6-12(d) shows that the controller successfully regulates the NO_x emissions level at the stack, rejecting changes in NOx_{in} .

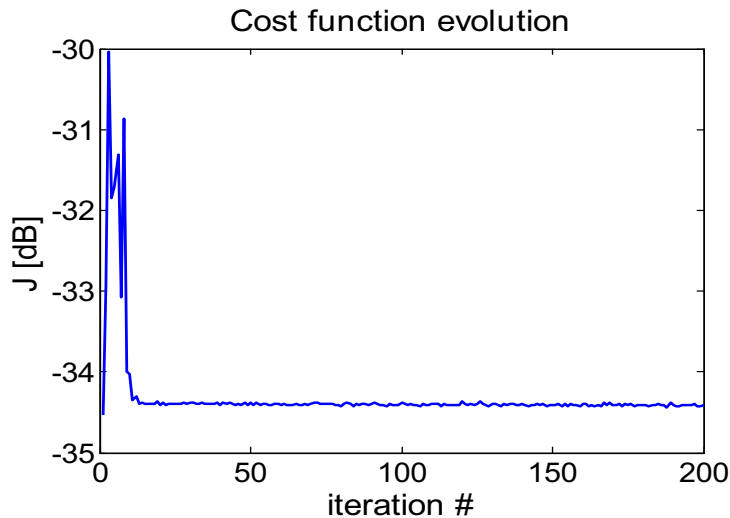


Figure 6-10: Evolution of the Cost Function.

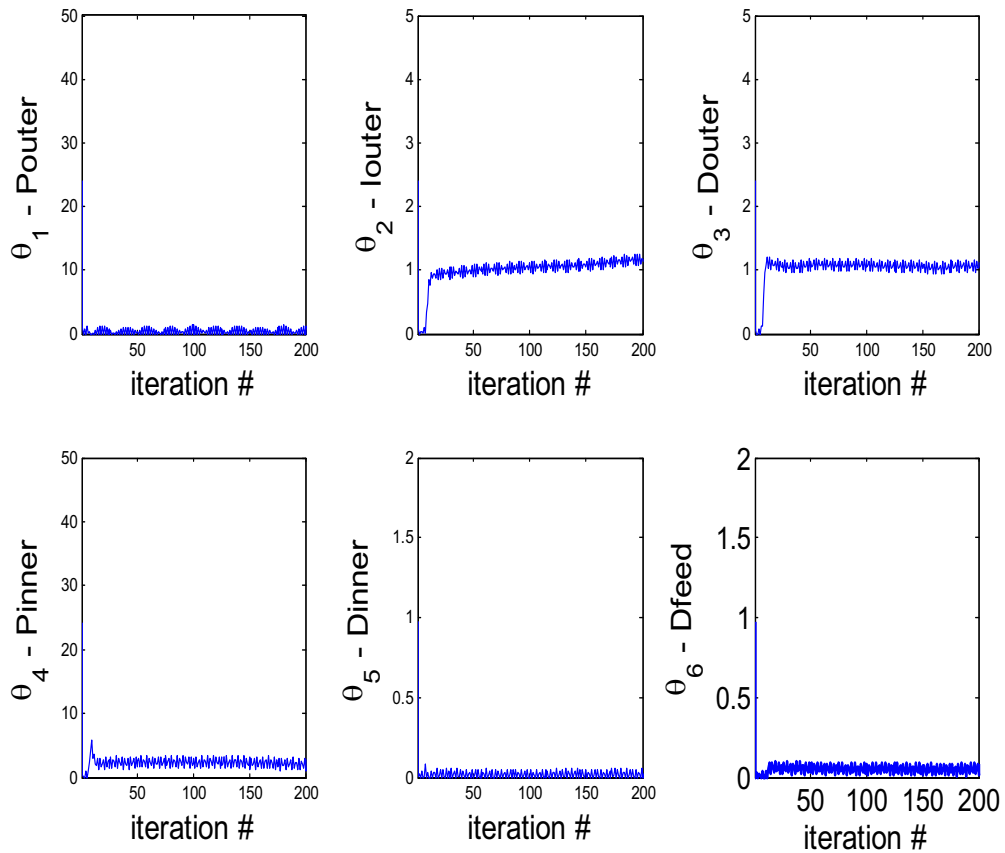


Figure 6-11: Evolution of the Controller Gains.

Air Preheater Control

The control logic at Cayuga Unit 1 was modified to include a scheme that incorporates the feedback measurements from the sensor implemented in this project (the AbSensor - AFP for ABS formation temperature and associated deposition location) and a control strategy provision for the APH air bypass damper. The ABS deposition location can be controlled by manipulating the APH matrix temperature and, consequently, the average cold-end APH temperature through the bypass damper with the ultimate goal of minimizing APH fouling.

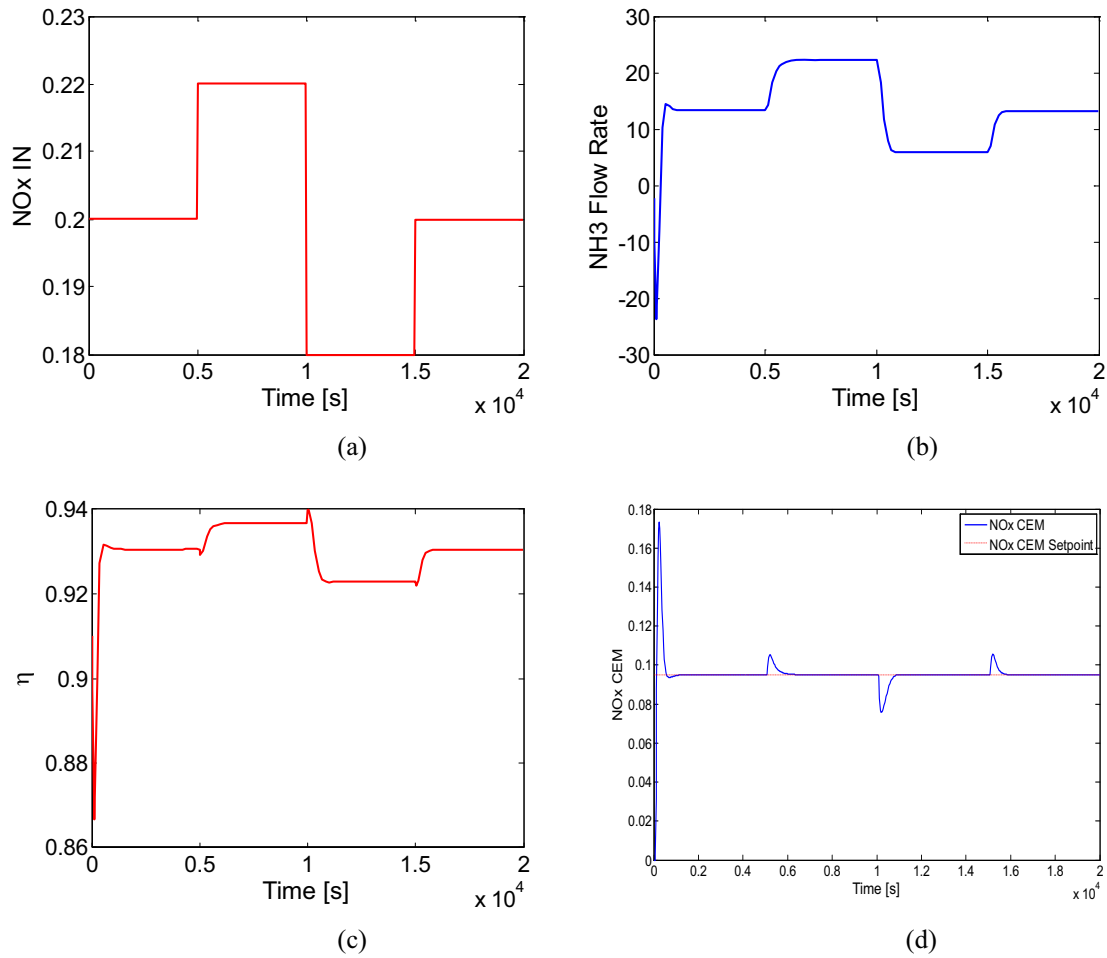


Figure 6-12: Illustration of the Time Response of the Optimized Multi-Loop Scheme.

Figure 6-13 illustrates the APH control configuration. The deposition depth can be estimated through the function $D(x)$ from the ABS formation temperature, which is also function of the NH_3/NO_x ratio and the APH temperature. The PID control $K_{\text{APH}} * C_{\text{APH}}$ regulates the deposition depth to a desired setpoint.

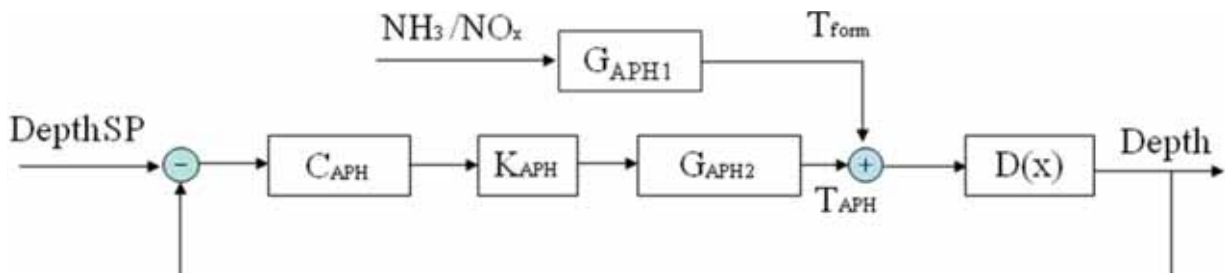


Figure 6-13: APH Control Configuration.

In order to simulate the APH closed-loop system performance, simulations were carried out using MATLAB SIMULINK[®]. For that purpose, a simplified model of the APH system was created. The SIMULINK closed-loop system is illustrated in Figure 6-14.

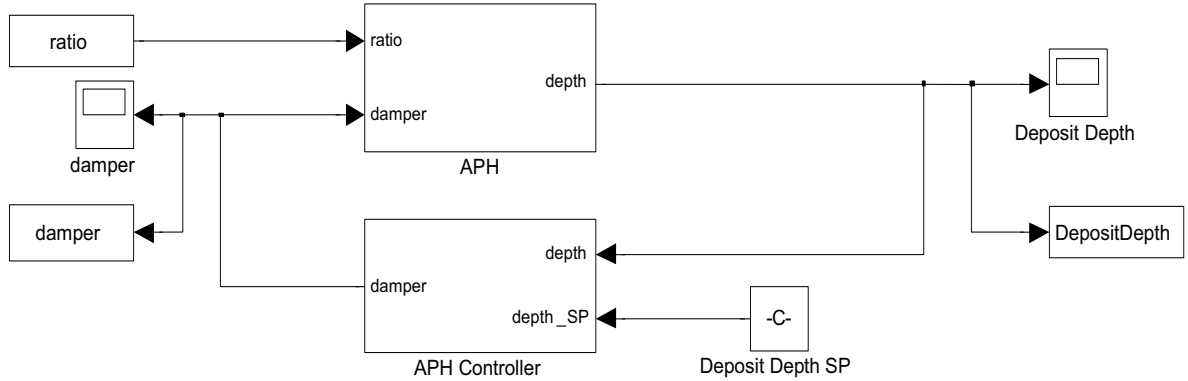


Figure 6-14: SIMULINK APH Control Configuration.

The simplified model for the APH dynamics is shown in Figure 6-15. The ABS deposition depth is determined by both the ABS formation temperature and the APH metal temperature. The APH response to the bypass damper manipulation is modeled as a simple first-order transfer function $G_{APH2}(s)=1/(s+1)$. The response of the formation temperature to the NH_3/NO_x in ratio is modeled as a first-order transfer function $G_{APH1}(s)=1/(2s+1)$ in series with the nonlinear function in Figure 6-16. Only the section of the curve in Figure 6-16 from 0.5 to 1.5 NSR is realistic and was used in the modeling. This specific function is modeled within the APH ABS block as illustrated in Figure 6-17. The APH controller has a PID structure as shown in Figure 6-18.

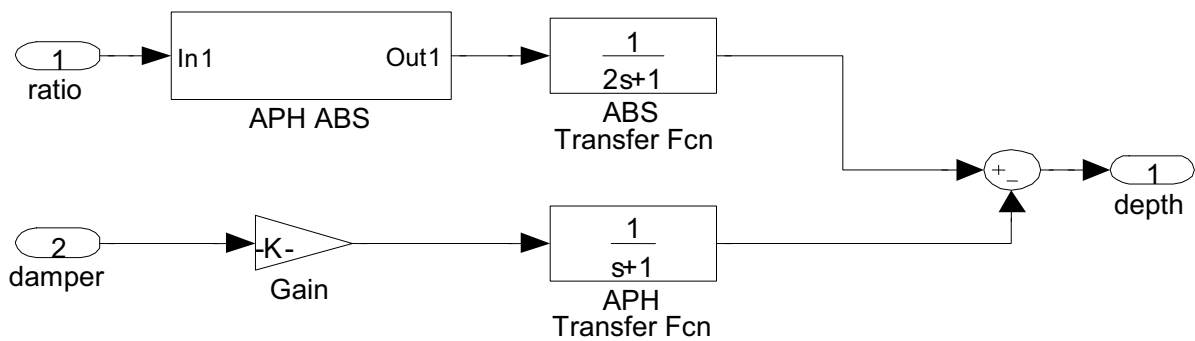


Figure 6-15: Simplified APH Model.

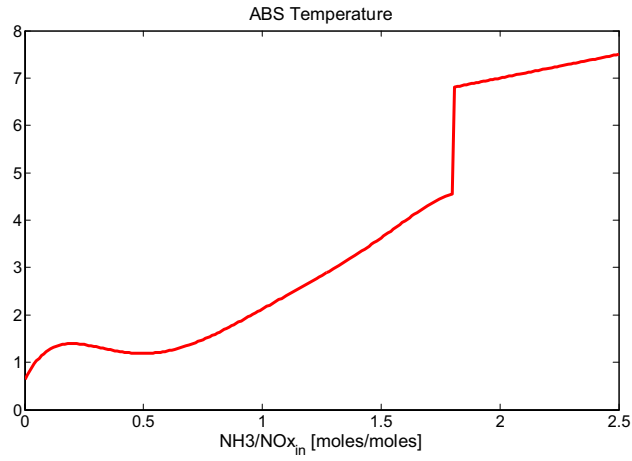


Figure 6-16: ABS Formation Temperature as a Function of $\text{NH}_3/\text{NO}_{x_{in}}$.

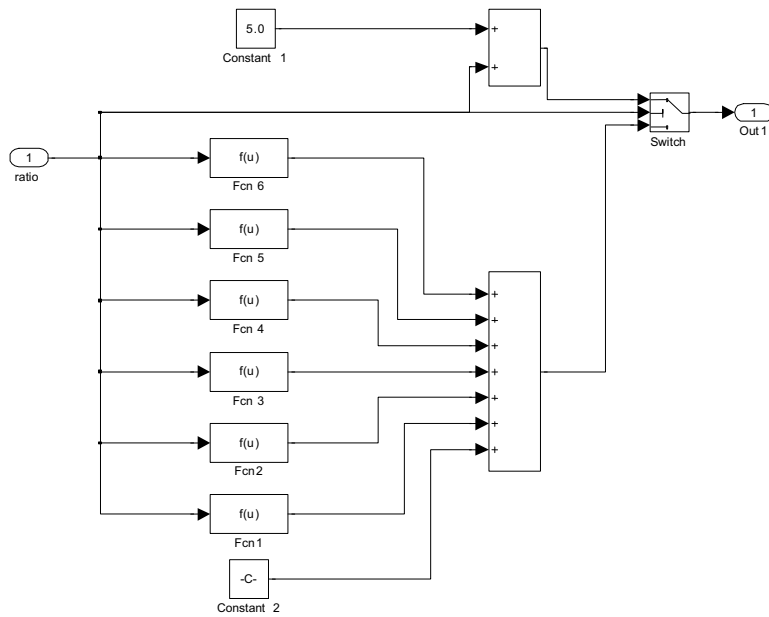


Figure 6-17: ABS Formation Temperature Simplified Model.

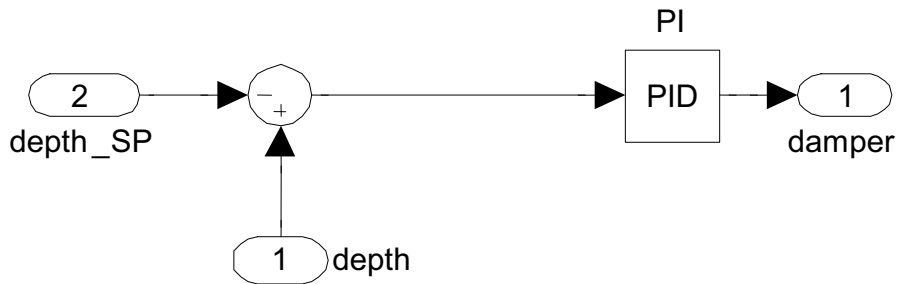


Figure 6-18: APH Deposition Depth Controller.

Integrated SCR/APH Control

ABS deposition depth can be controlled not only by regulating the APH bypass damper but also by modulating the NH_3/NO_x in ratio. For a given NO_x in, a decrease in NH_3 injection would result in a decrease in NH_3/NO_x in, and in turn, in the ABS formation temperature. Therefore, a decrease in NH_3 injection could prevent opening of the APH bypass damper and its associated heat rate penalty. However, a decrease in NH_3 injection would result in an increase in NO_x CEM. There is then a tradeoff between the NO_x emissions level at the stack and the heat rate penalty due to the opening of the APH bypass damper. If a small increase of NO_x CEM is tolerated, it can help control the ABS deposition depth by reducing the NH_3 flow rate, in lieu of opening the bypass damper. Figure 6-19 shows an ad hoc coordinated SCR and APH control scheme, where the block $E(x)$ modifies the setpoint for NO_x CEM as a function of the APH bypass damper opening, which is directly proportional to the APH heat rate penalty.

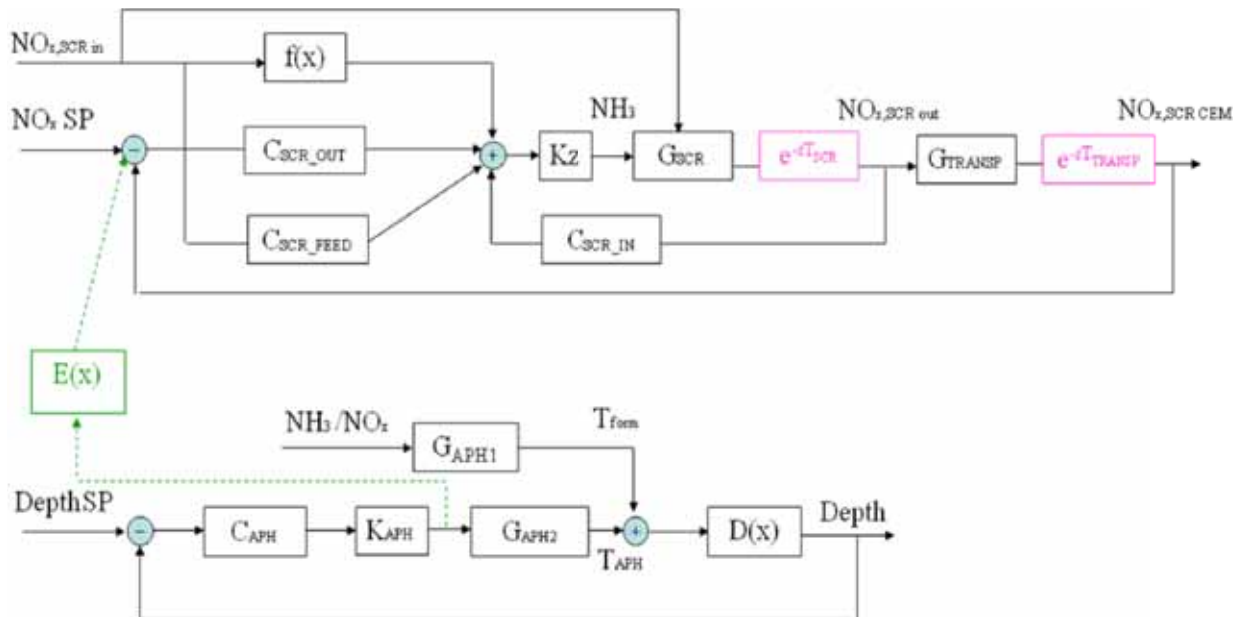


Figure 6-19: Coordinated SCR and APH PID-Based Control.

A MATLAB SIMULINK[®] version of the coordinated scheme is presented in Figure 6-20. It should be noticed that the SCR and APH control schemes are identical to those introduced in Figures 6-5 and 6-14. The “Coordinator” block is the only addition to the control architecture. This coordinator, shown in more detail in Figure 6-21, will not modify the setpoint for NO_x CEM as long as the APH bypass damper opening is smaller than a predefined threshold. When the APH bypass damper opening exceeds this threshold, the NO_x CEM setpoint is modified proportionally to the APH bypass opening.

Figure 6-22 illustrate the case where the threshold for coordination is zero. This means that the setpoint for NO_x_CEM will always be modified proportionally to the APH bypass damper. Figure 6-22(d) shows the modification of the NO_x_CEM setpoint to a higher value for which the NH_3 injection can be significantly reduced (see Figure 6-22(f)) and, consequently, the APH bypass damper opening required to regulate the APH deposition depth is also significantly reduced (see Figure 6-22(e)), minimizing in this way the APH heat rate penalty at the expense of a higher level of NO_x at the stack. Finally, the red lines in Figure 6-22 show an intermediate case where the threshold for the coordinator block is set at 40% of the APH bypass damper opening. Once the damper opening exceeds this value the setpoint for NO_x_CEM is modified. It should be noticed the slight increase in the setpoint in Figure 6-22(d) that allows reductions of both NH_3 injection and APH bypass damper opening if compared to the uncoordinated case (blue lines).

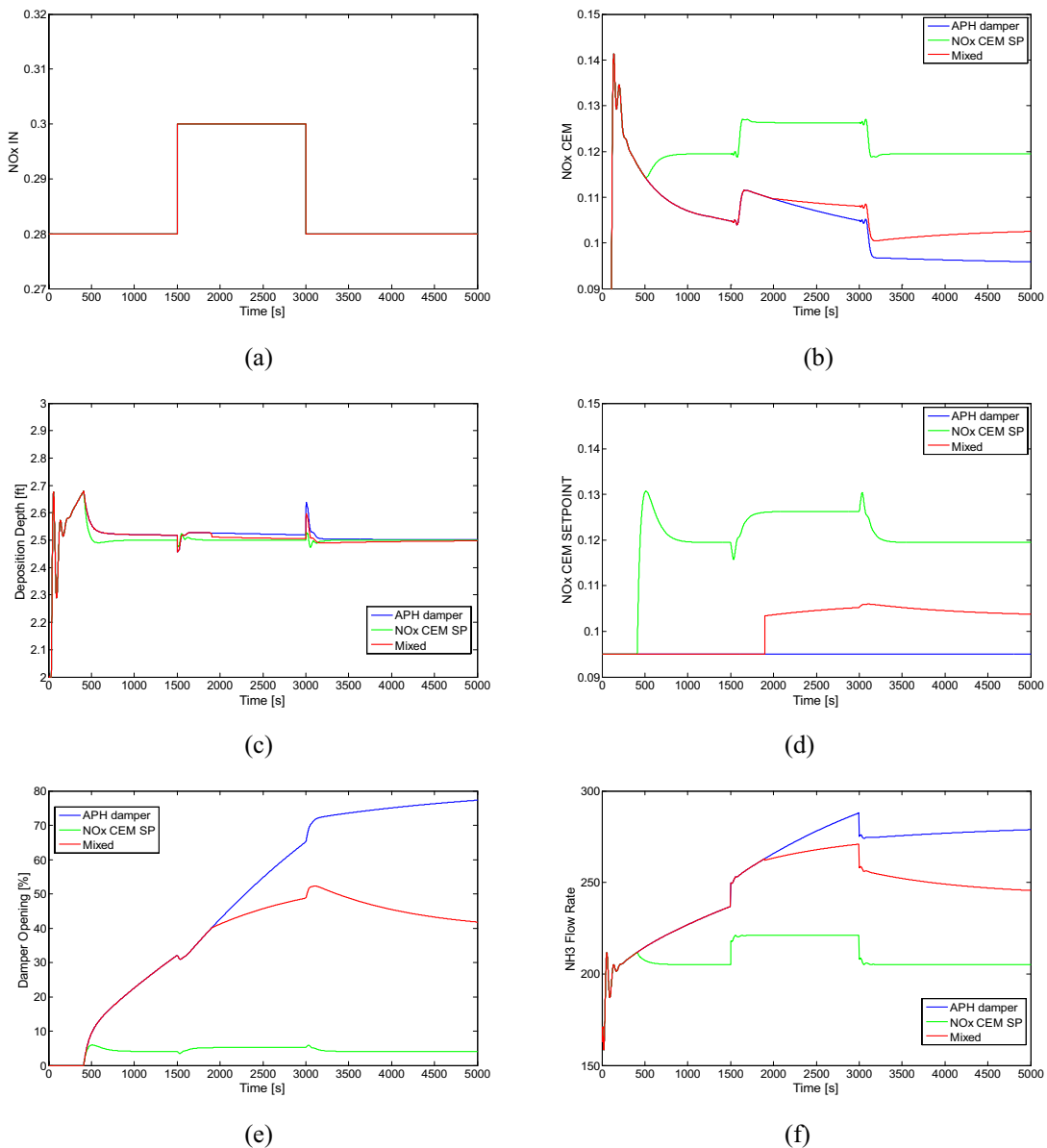


Figure 6-22: Effect of Modification of NO_x_CEM Setpoint.

NON-MODEL-BASED OPTIMAL ADAPTIVE CONTROL

In addition to the non-model-based approach presented in the preceding paragraphs and that includes multi-loop PIDs, a non-model-based optimal adaptive control strategy is also introduced for both the boiler and the SCR/APH systems. The proposed control scheme is based on extremum seeking and it includes a dual loop control strategy illustrated in Figure 6-23. The first non-model-based adaptive controller is proposed to regulate the boiler inputs (viz, excess O₂, SOFA registers, burner tilt, SOFA tilt, and 1A1 mill coal flow) to minimize both NO_x emissions at the SCR inlet and the boiler heat rate penalty. The second non-model-based adaptive controller is proposed to regulate NH₃ flow to the SCR system and the APH bypass damper opening in order to optimally control in real-time and in a coordinated fashion both the CEM NO_x and ABS deposition within the APH, avoiding NH₃ slip and minimizing the APH heat rate penalty. The effectiveness of extremum seeking adaptive controllers, in keeping the system at an optimal operation point in the presence of input disturbances and system changes (unit load, coal quality, firing system maintenance condition, SCR aging, etc.) was demonstrated through dynamic simulations.

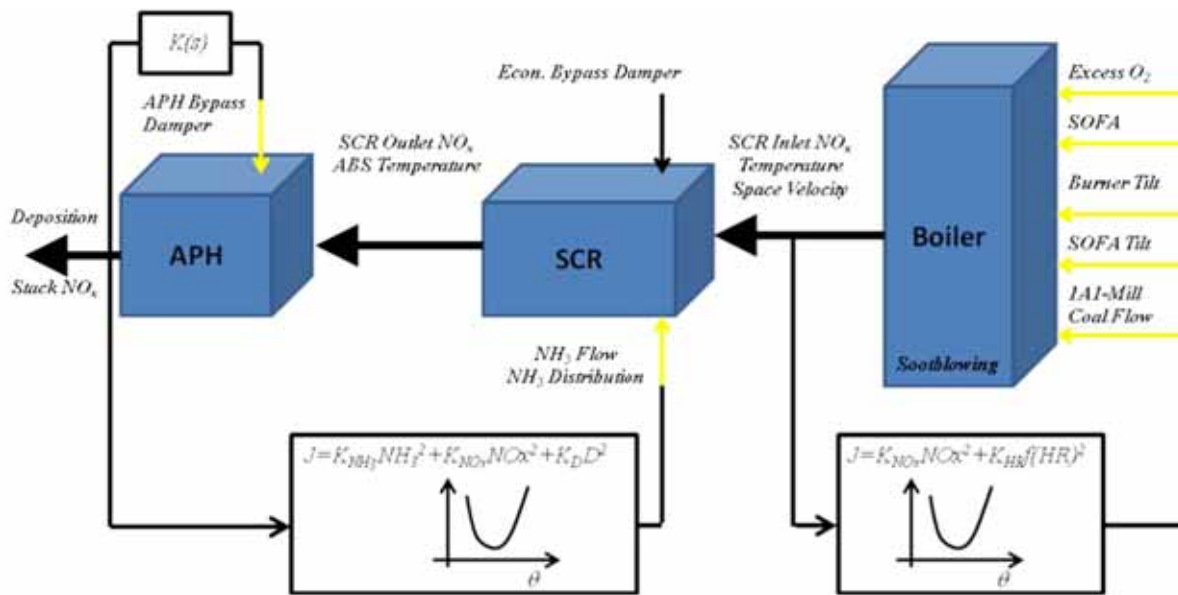


Figure 6-23: Two-Loop Adaptive Control Strategy with Extremum Seeking.

Extremum Seeking

Extremum seeking control (Ariyur, 200; Ariyur, 2003), a popular tool in control applications in the 1940-50s, has seen a resurgence in popularity as a real time optimization tool in different fields of engineering. In addition to being an optimization method, extremum seeking is a method of adaptive control, usable both for tuning set points in regulation/optimization problems and for tuning parameters of control laws. It is a non-model based method of adaptive control, and, as such, it solves, in a rigorous and practical way,

some of the same problems as neural networks and other intelligent control techniques. Aerospace and propulsion problems (Binetti, 2002), combustion instabilities (Schneider, 2000; Banaszuk, 2004), flow control (Wang, 2000), compressor rotating stall (Wang, 2000), automotive problems (anti-lock braking, engine mapping), bioreactors (Wang, 1999), and charged particle accelerators (Schuster, 2004) are among its applications. Extremum seeking is applicable in situations where there is a nonlinearity in the control problem, and the nonlinearity has a local minimum or a maximum. The nonlinearity may be in the plant, as a physical nonlinearity, possibly manifesting itself through an equilibrium map. Hence, extremum seeking can be used for tuning a setpoint to achieve an optimal value of the output. The parameter space can be multivariable. The discrete-time implementation (Choi, 2002) is depicted in Figure 6-24, where z denotes the Z -transform variable. The high-pass filter is designed as $0 < h < 1$, and the modulation frequency, ω , is selected such that $\omega = \alpha\pi$, $0 < |\alpha| < 1$, and α is rational. Without loss of generality, the static nonlinear block $J(\theta)$ is assumed to have a minimum J^* at $\theta = \theta^*$. The extremum seeking procedure guarantees that the estimation of θ , denoted as $\hat{\theta}$ in Figure 6-24, will converge to θ^* , minimizing J .

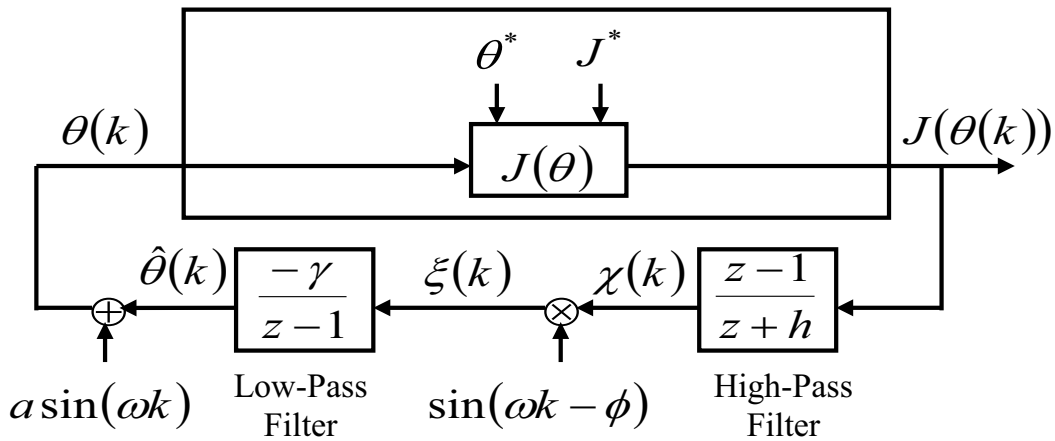


Figure 6-24: Extremum Seeking Approach.

The purpose of the extremum seeking optimization algorithm illustrated in Figure 6-24 is to use the gradient information of the static map $J(\theta)$ to drive θ to θ^* so that the cost functional $J(\theta)$ is driven to its minimum J^* . The variable $\hat{\theta}$ denotes the estimate of the unknown optimal parameter θ^* provided by the extremum seeking algorithm. The probing signal $a \sin(\omega t)$, with $a > 0$, added to the estimate $\hat{\theta}$ and fed into the plant helps to get a measure of the gradient information of the map $J(\theta)$. The high-pass filter preserves only the perturbation in the cost functional, J , caused by the perturbation in the θ parameter introduced by the probing signal. The demodulator picks the component of the filtered perturbed cost functional, χ , with the same frequency, ω , as the probing signal. The resulting signal, ξ , which can be seen as proportional to the gradient of the map $J(\theta)$, is used by the pure-integrator low-pass filter to update the θ parameter in order to drive the cost functional J closer to its minimum.

As an example, Figure 6-25 shows residual NO_x at the SCR outlet (as a percentage of inlet NO_x), NH₃ slip, and a cost function $J = K_{NOx_out} NOx_out^2 + K_{NH3} NH_3^2$ that can be computed in real-time from direct measurements of outlet NO_x and NH₃. The cost function J conciliates two competing objectives: simultaneous minimization of residual NO_x and NH₃ slip. By modifying the control inputs, the extremum seeking controller makes the system work at an operating point that corresponds to the minimum of the cost function J (minimum of the pink curve in Figure 6-25), independently of transients and disturbances. In this way, both NO_x and NH₃ slip can be minimized in real-time. The relative importance of NO_x_out and NH₃ can be defined by the operator through the selection of their corresponding weights K_{NOx_out} and K_{NH3} .

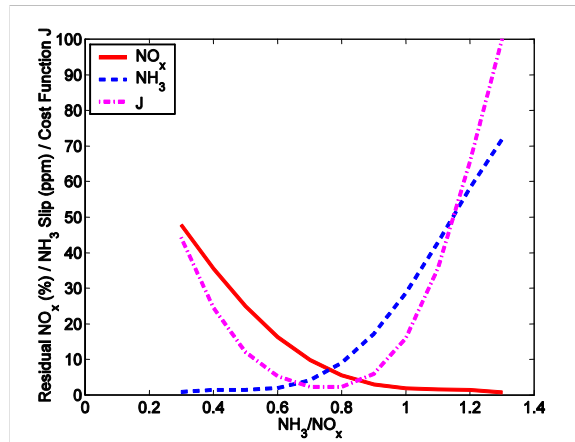


Figure 6-25: Example of Extremum Seeking Minimized Cost Function.

Real-Time Boiler Optimization

Dynamic Model Identification. In order to illustrate the potential of adaptive extremum-seeking control for minimization of both the level of NO_x at the boiler outlet and the corresponding heat rate penalty, it is necessary simulate the dynamics of the boiler. In contraposition to static models that are obtained from steady-state data, transient data is needed to identify dynamic models. Based on sampled measurements of the boiler variables, an ARMAX model is proposed:

$$A(q)y[k] = \sum_i B_i(q)u_i[k - nk_i] + C(q)e[k]$$

Where y denotes the measured output (level of NO_x at the SCR inlet, NOx_in), u denotes the measured inputs (excess O₂, SOFA registers, burner tilt, SOFA tilt, 1A1 mill coal flow), and e denotes non-measurable noise. The variable q denotes a time shift operator:

$$qy[k] = y[k + 1], \quad q^{-1}y[k] = y[k - 1],$$

where k denotes the sampling time. The polynomial $A(q)$ has order na , the polynomials $B_i(q)$ has order nb_i for $i=1, \dots, 5$, and $C(q)$ has order nc . The variable nk_i denotes the delay order for each of the inputs i . The coefficients of these polynomials are obtained by solving the following minimization problem:

$$\min_{A,B_i,C} (y^*[k] - y[k])^2$$

where $y[k]$ denotes the model-predicted output and $y^*[k]$ the real output obtained from direct measurement. The identified discrete-time dynamic model was converted to the continuous-time domain using a “tutsim” transformation. The resulting continuous-time dynamic model is written in terms of transfer functions in the Laplace domain and implemented in MATLAB SIMULINK[®] as shown in Figure 6-26.

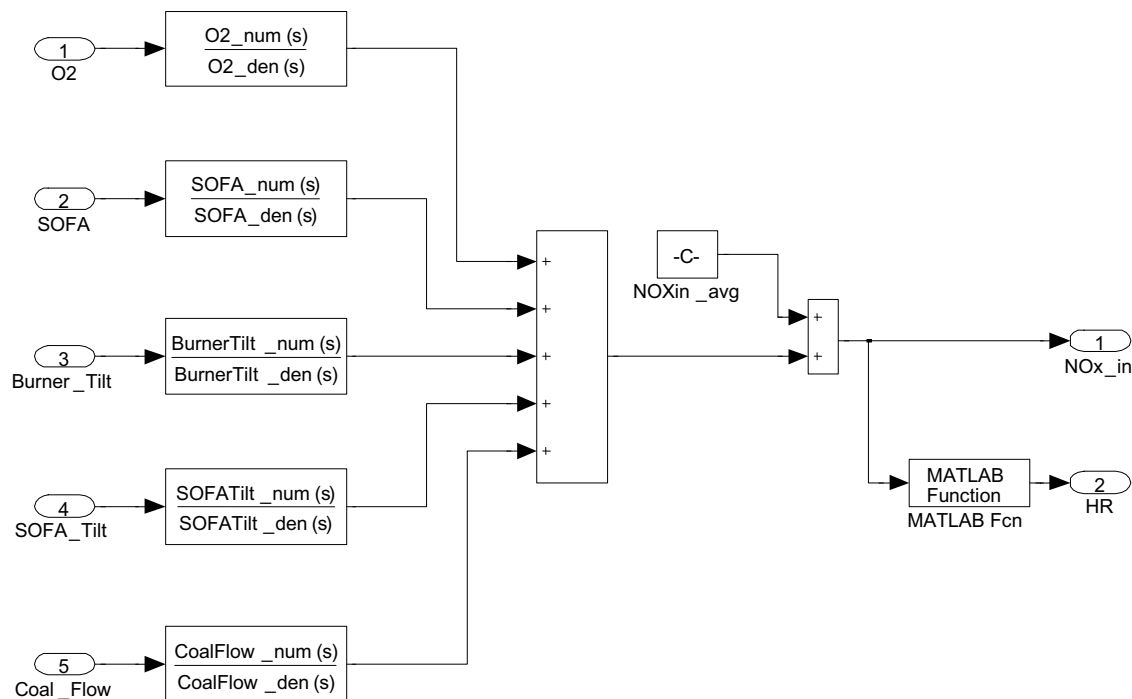


Figure 6-26: Simplified Boiler Dynamic Model.

Extremum Seeking Controller. From the parametric tests carried out during the project the parametric testing it is possible to infer the dependence of NOx_in and HR on excess O_2 level. By defining the following cost function:

$$J = K_{NOx_in} NOx_in^2 + K_{HR} HR^2,$$

where HR represents boiler heat rate penalty. This cost function is shown in Figure 6-27, where it can be noticed that there exists an optimal value of O_2 for which a minimum is achieved. By careful selection of

the coefficients K_{NO_x} and K_{HR} , different weights can be assigned to the competing objectives NO_x_{in} and HR .

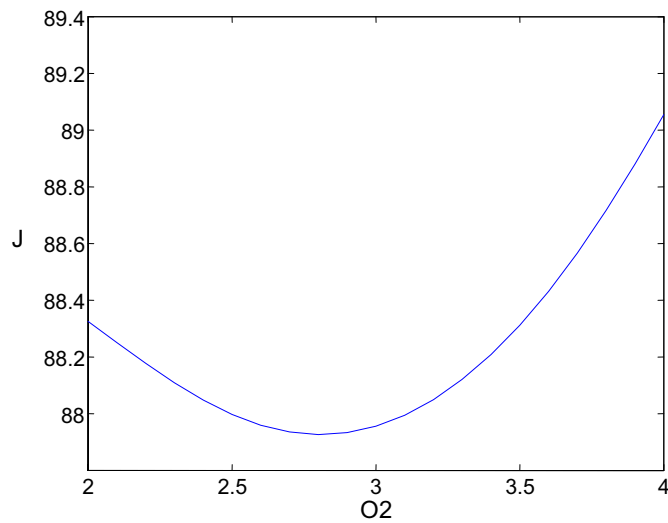


Figure 6-27: Cost Function of O₂ when SOFA = 0%, Burner Tilt = -4 degrees, SOFA Tilt = 1 degree and 1A1 Coal Flow = 15 ton/hr.

Given that static optimization will fall short in dealing with real-time changes in the cost function, extremum seeking allows real-time optimization by reacting to any change and keeping the system at an optimal operation point. Figure 6-28 shows a proposed extremum-seeking boiler control configuration. The value of the cost function J is fed into the extremum seeking block shown in Figure 6-29, where the real-time optimization is carried out to modify the value of O₂ in order to drive the value of the cost function J to its minimum. Only the variable O₂ is controlled in this example. It is worth mentioning that extremum seeking can handle multi-input systems. An example to illustrate the performance of the non-model-based adaptive extremum seeking controller is shown in Figure 6-30, where the time evolutions of NO_x_{in} and heat rate penalty predicted by the identified dynamic model are used to compute the cost function J . In this case, a step perturbation of magnitude 10 ton/hr for the 1A1 coal flow is introduced at $t=2,500$ min (Figure 6-30a). The level of SOFA registers, and burner and SOFA tilt are kept constant during the simulation. Before the coal flow step, the extremum seeking introduces a modification to the O₂ level (Figure 6-30b), in order to drive the system to the point where the cost function is minimized (Figure 6-30e). After the coal flow step, the extremum seeking reacts by modifying the O₂ level (Figure 6-30) in order to recover to a cost function minimum. It should be noticed that not only the minimizing values of O₂ are different, but also the cost function minimum values also differ. Figures 6-30c and 6-30d show how the NO_x and heat rate penalty values are changed by the extremum seeking controller. The potential of extremum seeking resides on its capability of computing the optimal value in real-time without the aid of a model.

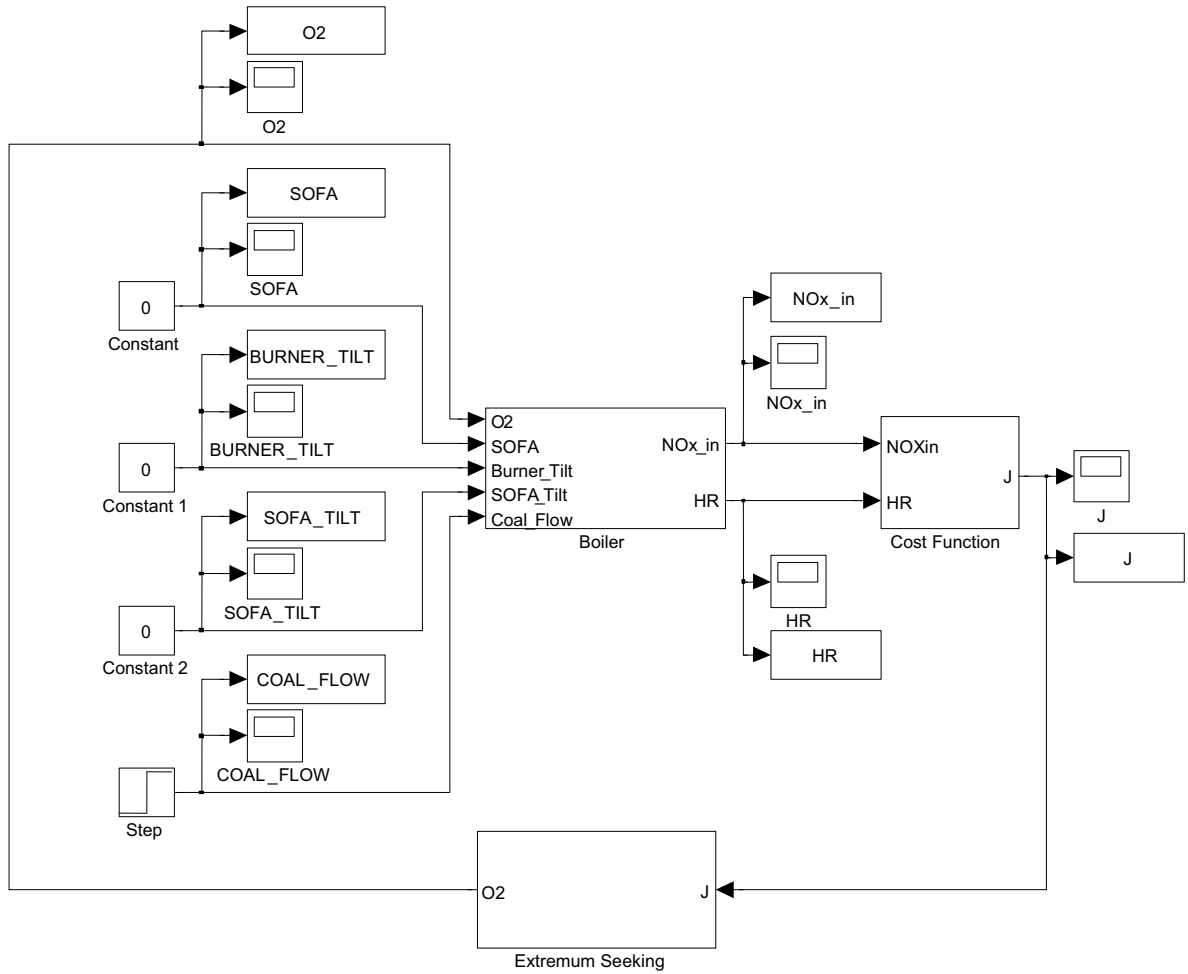


Figure 6-28: SIMULINK Extremum Seeking Boiler Control Configuration.

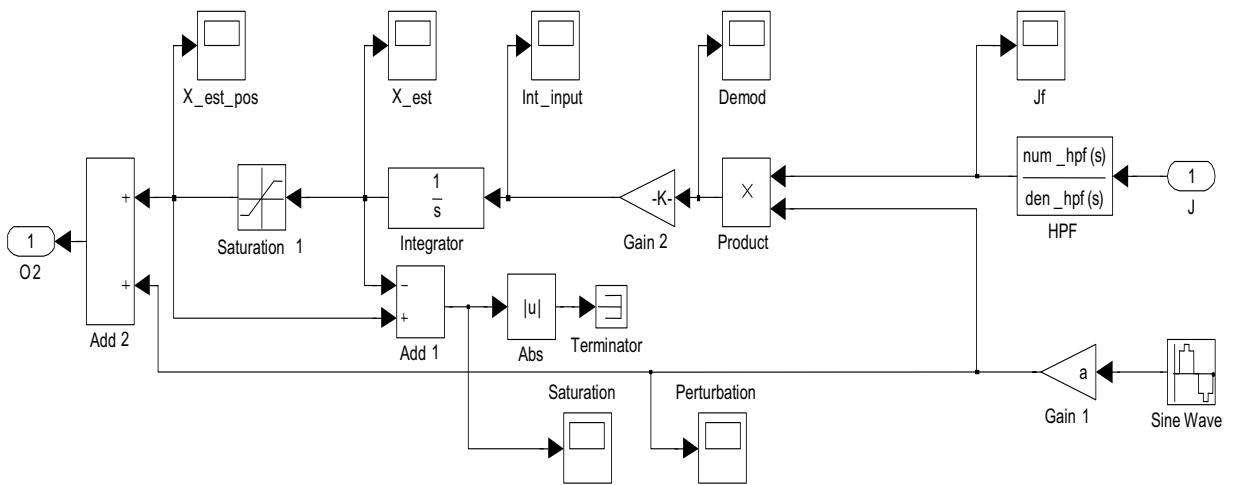


Figure 6-29: Extremum Seeking Implementation for Excess O₂ Optimal Modulation.

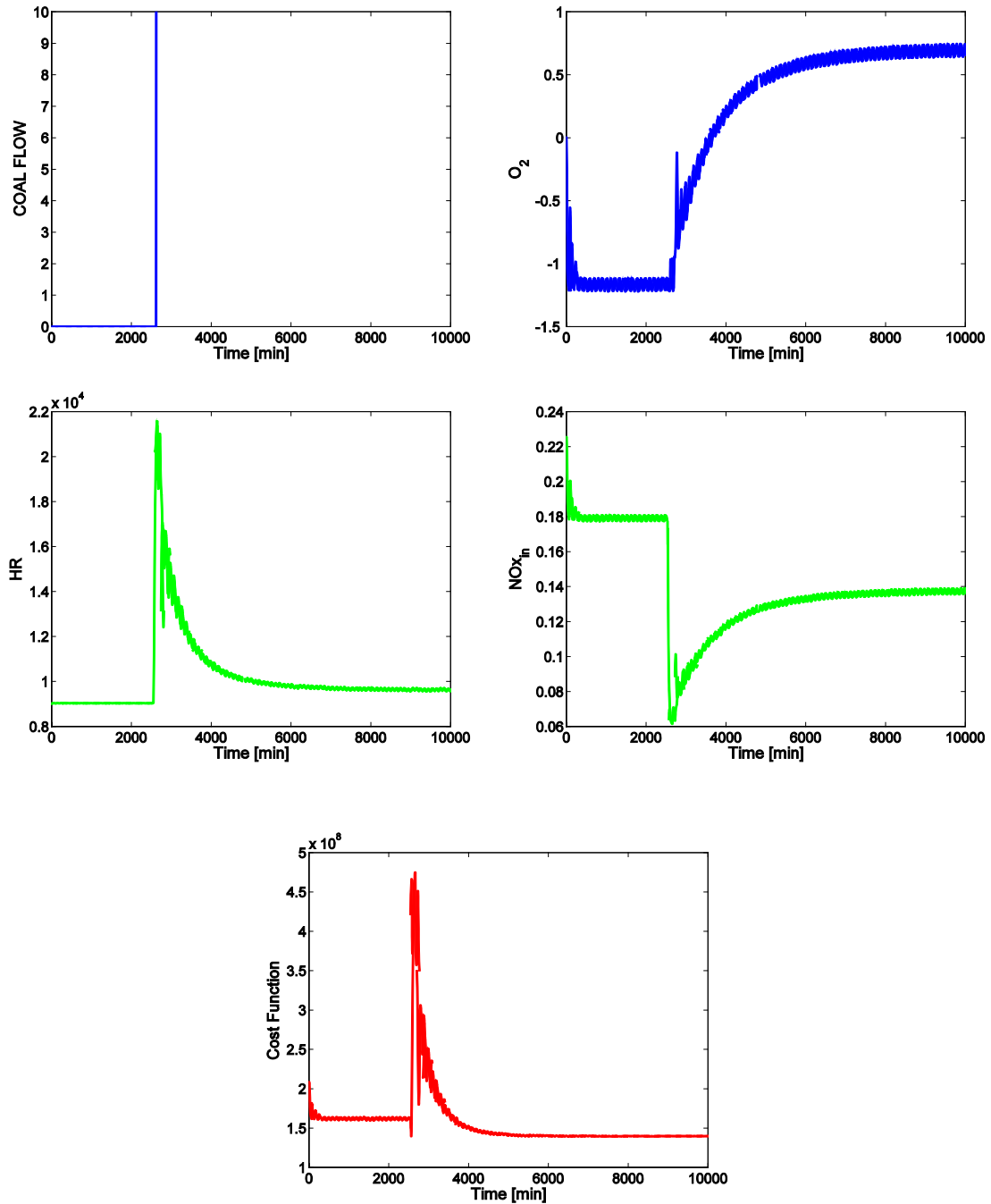


Figure 6-30: Extremum Seeking Simulation Results (a to e from left to right, top to bottom).

SCR/APH Real-Time Optimization. This section presents a combined extremum-seeking/PID control architecture as illustrated in Figure 6-31. It considers that while the NH_3 flow is directly controlled by an extremum-seeking controller, the APH bypass damper opening is controlled by a PID controller driven by a ABS deposition depth error. By defining the cost function as:

$$J = K_{NOx_CEM} NOx_CEM^2 + K_{NH3} NH3^2 + K_D D^2,$$

the extremum-seeking controller (shown in Figure 6-32) regulates NH₃ flow in order to minimize NO_x_CEM, NH₃ flow, and the APH bypass damper opening (D). Introduction of the APH bypass damper term in the cost function is a step forward in the efforts to coordinate the SCR and APH control loops. The user-defined weigh factors K_{NOx} , K_{NH3} and K_D regulates the tradeoff between NO_x_CEM minimization and NH₃ - D minimization.

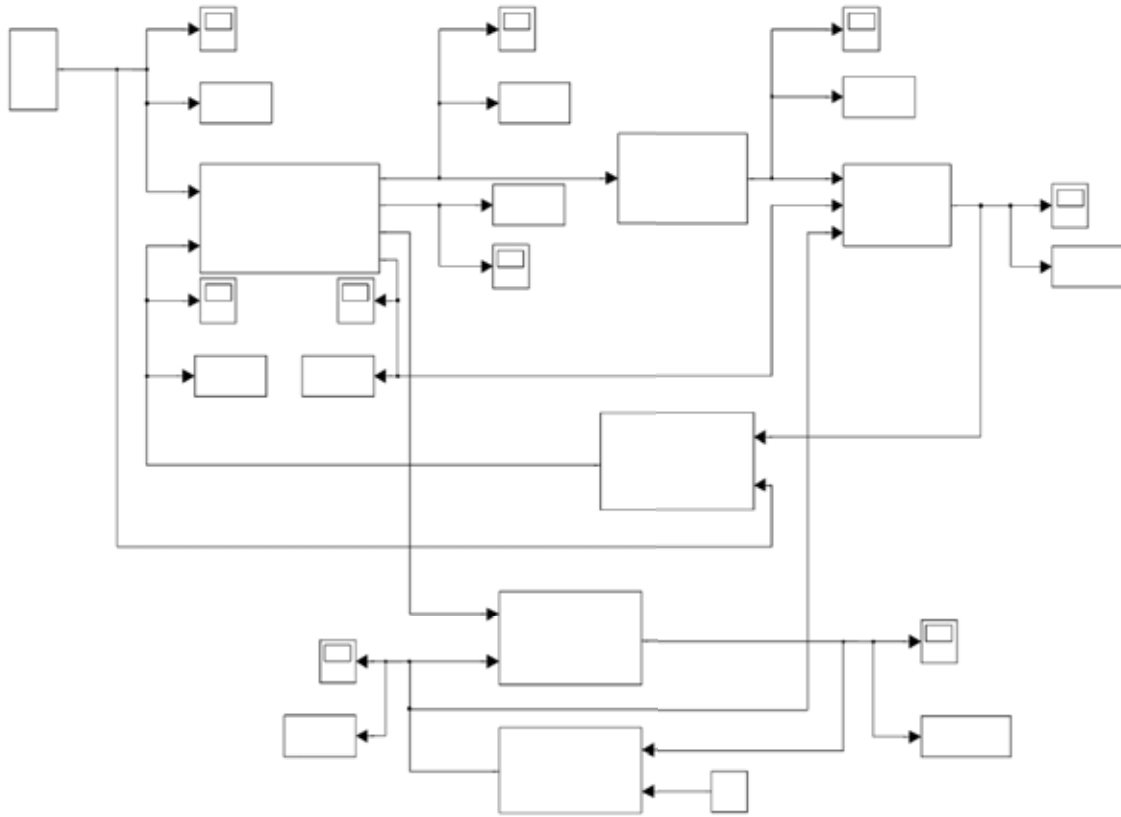


Figure 6-31: SIMULINK Extremum Seeking SCR/APH Control Configuration.

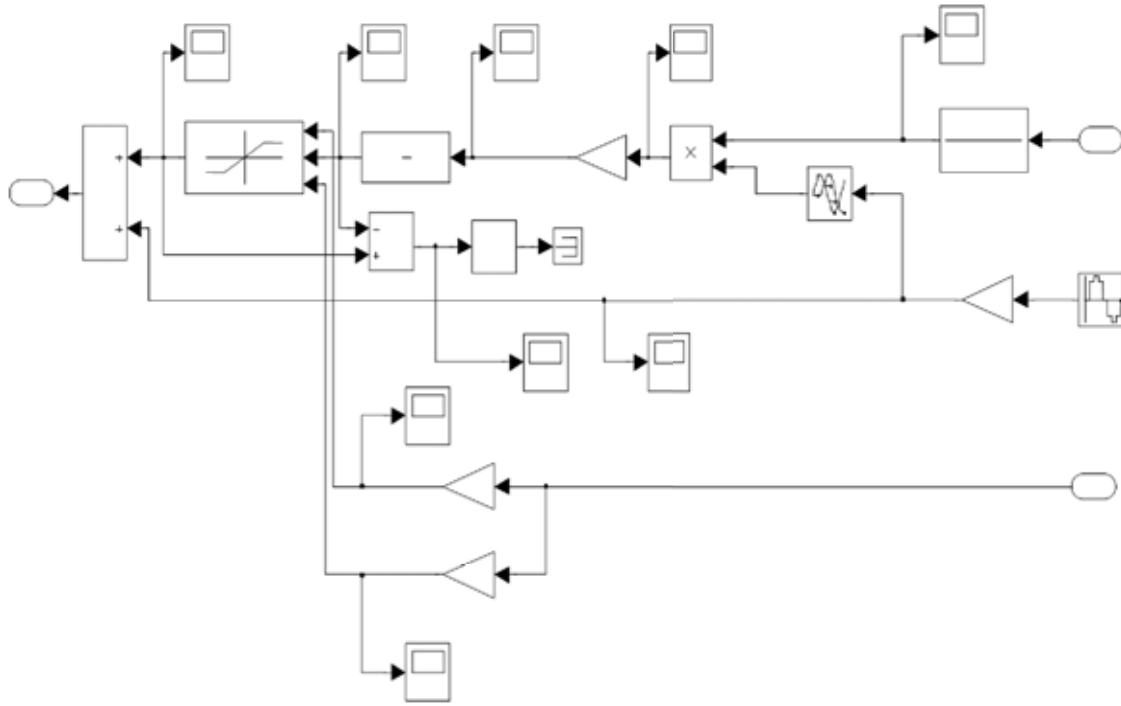
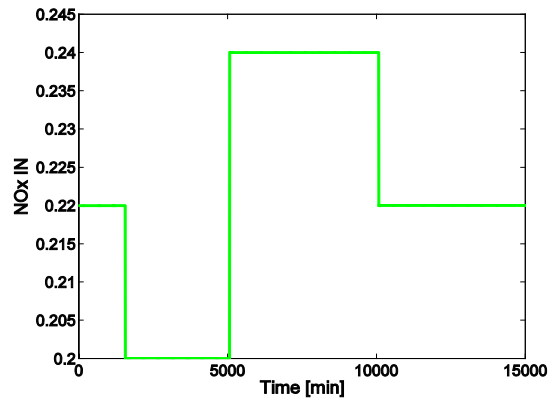
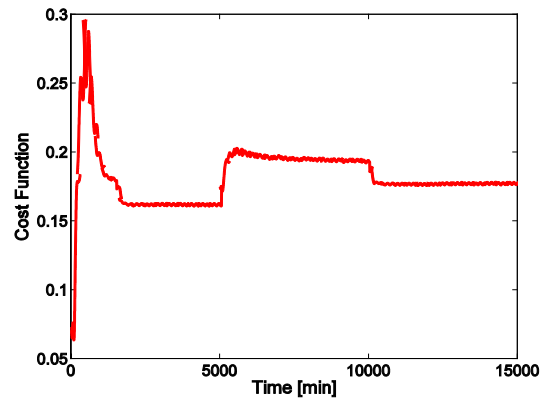


Figure 6-32: Extremum Seeking Implementation for NH₃ Optimal Modulation.

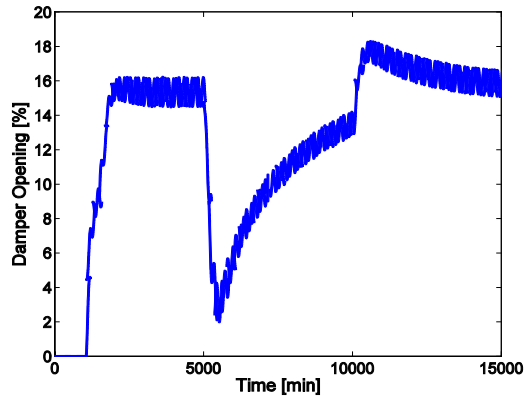
Simulation results for the controllers introduced in Figures 6-31 and 6-32 are included in Figure 6-33. The level of NO_x at the SCR inlet is varied as shown in Figure 6-33(a). While the ABS deposition depth (Figure 6-33(f)) is regulated by the PID at a fixed setpoint (2.5 ft), the level of CEM NO_x (Figure 6-33(e)) has the freedom to fluctuate in order to minimize the cost function J shown in Figure 6-33(b). The minimizing variable is the NH₃ flow rate shown in Figure 6-33(d). The APH bypass damper opening, shown in Figure 6-33(c) is kept at a relatively closed level.



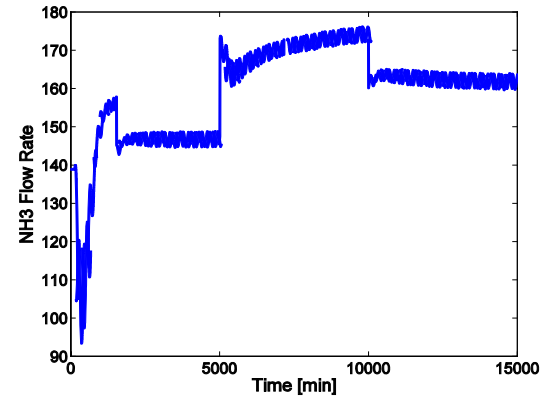
(a)



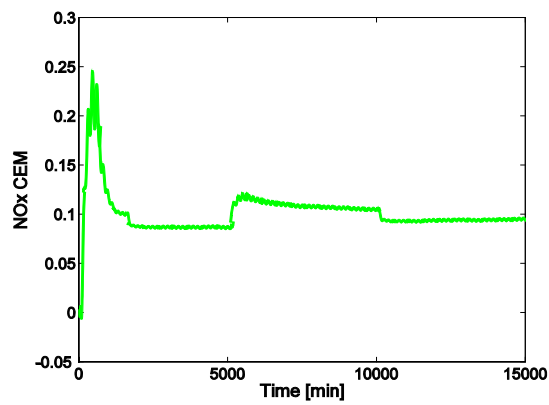
(b)



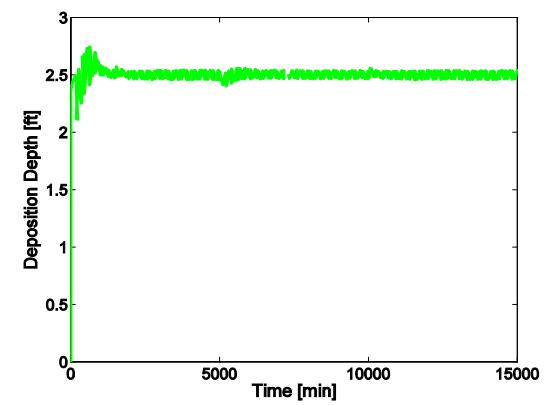
(c)



(d)



(e)



(f)

Figure 6-33: Extremum Seeking Simulation Results.

Section 7
EVALUATION OF BENEFITS

Based on the results of this project an evaluation was performed to assess the benefit of modifying the combined operation of the boiler, SCR system and APH for savings in fuel and SCR reagent. As part of this project, a new ABS fouling probe was retrofit to Cayuga Unit 1. This technology includes control capabilities to implement a new upgraded control strategy. Findings from this project have been made available to Cayuga Station, in terms of the adequacy of flue gas conditions to the SCR, trending relationships between boiler control settings and the parameters of interest (such as reduced NO_x emissions levels, SCR performance, unit heat rate deviations or penalties, and ABS formation and deposition in the APH), and sootblowing characterization and improved schedule. Recommendations were made to Cayuga Station regarding modified control settings for optimal boiler and combustion conditions, as well for operation of the NH₃ injection system and APH air bypass damper control. This section presents results of a simplified evaluation of the cost benefit from implementing these results. It should be mentioned that other indirect benefits would result from the implementation and improvements introduced by this study. These include reduction in fly ash NH₃ contamination and reduction of sulfur related problems, such as sulfuric acid corrosion and stack visible plume.

This section provides gross annual estimates associated with the benefit of implementing project results at Cayuga Unit 1 for an optimized operation of the boiler/SCR/APH system. These savings include only those savings related to reduction in reagent usage, catalyst life extension, unit thermal performance or fuel cost, and frequency and savings in APH wash. A capacity factor of 0.90 is used in the calculations.

Reduced Ammonia Usage. These savings total approximately \$69,000. The savings comes from an approximate 22 percent reduction in NH₃ usage due to modification in boiler and SCR control settings that result in reduced NO_x treatment levels and improved SCR performance efficiency. The NH₃ usage savings is calculated as the product of the following items:

1. Anhydrous NH₃ usage reduction (160 – 125 = 35 lb/hr)
2. Number of hours for year-round compliance (7,884 hrs)
3. Ammonia cost (\$500/ton)
4. Conversion factor (1 ton/2,000 lb)

Reduced Catalyst Replacement Frequency. These savings total approximately \$45,000. The savings comes from the increase in catalyst lifetime that is assumed that result from the better utilization of the SCR reaction process. It is assumed that over the course of 5 years, this will result in at least one decreased catalyst replacement event. The savings is equal to the product of the following items:

1. Catalyst requirement for SCR system (37 ft³/MW)
2. Catalyst cost (\$155/ft³ for honeycomb type catalyst)
3. Portion of catalyst saved by reducing replacement frequency (1/4)
4. Number of decreased replacement events over the course of catalyst replacement cycle (1/5 years)

Savings in Fuel. These savings total approximately \$151,000. The savings come from an estimated operation at minimal unit heat rate from manipulation of boiler control settings to avoid penalization from increased unburned carbon in the fly ash, stack losses due to increased excess air, and controllable losses due to off-design steam temperatures; and from minimal manipulation of the APH to prevent ABS deposition. This savings is the sum of combustion-related heat rate penalties and APH-related heat rate penalties:

1. Cost of fuel (\$0.02/kWh or \$2.22/MBtu)
2. Number of hours for year-round operation (7,884 hrs)
3. Estimated combustion and APH-related heat rate penalties avoidance (54 Btu/kWh or 0.60% from estimated baseline heat rate)

Savings in Air Preheater Cleaning. These savings total approximately \$483,000. The savings comes from an estimated reduction in excess NH₃ slip and, consequently, prevention of APH plugging that would have required unit shut down for water washing of the heater. Since implementation of the ABS fouling probe and associate controls, the frequency of APH wash at Cayuga Unit 1 has been reduced from approximately 4 per year (since start of SCR operation) to 1 so far in 2008. This savings is the sum of the cost of the washing services and the lost of unit availability:

1. Two-day outage to manipulate unit load and water-wash and dry the APH (\$258,000; it includes 3 washes)
2. Cost of APH water wash services (\$225,000; it includes 3 washes, \$5,000 labor cost (3 repairmen at 2-12 hr. shifts), \$68,000 water treatment cost (170,000 gallons treated at \$0.40/gallon), \$2,000 miscellaneous costs)

In summary, the estimated annual cost savings for Cayuga Unit, due to optimized instrumentation, optimized operation of the boiler/SCR/APH system and upgraded control is of the order of \$748,000. This estimated savings do not include other savings that may result from this type of optimization, such as improvements to the sootblowing operation. The estimates do not also consider that it might be practical for Cayuga to “over-control” NO_x to sell allowances into the NO_x allowance market, without compromising a side-effect-free operation of the SCR system.

Section 8

CONCLUSIONS AND RECOMMENDATIONS

A study funded by the New York State Energy Research and Development Authority (NYSERDA) and AES Cayuga was performed to investigate the feasibility of developing an optimization methodology and demonstrate the benefit of operating in an optimal mode that achieve maximum boiler NO_x emissions reductions, maximum selected catalytic reduction (SCR) system performance, minimal unit heat rate penalties, and lower cost of operation at Cayuga Unit 1. Cayuga Unit 1 is a 150 MW_{net} unit, equipped with a low-NO_x firing system and an anhydrous ammonia (NH₃)-based SCR system. Process optimization is a cost-effective approach to improve the cost of NO_x compliance at coal-fired boilers, while meeting other operational and environmental constraints. In boilers equipped with SCRs, this is a classic multi-objective optimization problem to balance boiler thermal performance, NO_x emissions, the cost of reagent and air preheater (APH) maintenance costs. The specific objectives of this study included:

- Provide upgraded instrumentation and control capabilities of ammonium bisulfate (ABS) fouling at the APH.
- Develop a methodology for a combined boiler combustion/SCR/APH optimization.
- Perform field testing at Cayuga Unit 1, and modeling and data analysis to support the demonstration of a combined optimization.
- Develop upgraded control strategy for minimum boiler NO_x emissions, optimal SCR operation, minimal NH₃ consumption, optimal APH operation and minimal overall cost of operation.

Long-term operation of a SCR system at optimal conditions should:

- Improve reagent utilization.
- Minimize catalyst deterioration and reduce operational and maintenance (O&M) costs.
- Operate at tighter stack NO_x levels with minimal standard deviation.
- Maintain SCR constraints such as design NH₃ slip and SO₂-to-SO₃ conversion.
- Minimize SCR impact on balance of plant equipment, such as ABS formation, and unit heat rate.

The following conclusions and recommendations were achieved from the results of this study:

- SCR tuning is an important aspect that should be considered when optimizing the operation of SCR systems. This involves the adjustment of the SCR injection grid

for uniform reagent treatment. However at Cayuga Unit 1, the as-found conditions and NH₃ injection tuning capability rendered this step unnecessary.

- A Breen Energy's AbSensor – Anti-Fouling Probe (AFP) was installed at one of the APH inlets at Cayuga Unit 1 for on-line monitoring of ABS and real-time determination of the ABS deposition axial location in the APH. This probe was found very reliable and an excellent tool to be used in an upgraded optimal SCR system operation.
- Parametric field tests were performed at Cayuga Unit 1. From these tests, it was found that economizer excess O₂, the top two separated overfire air (SOFA) register openings, burner tilt, SOFA tilt, the coal flow to the top pulverizer (1A1-Mill), and the NH₃/NO_x ratio, all have an impact on SCR inlet NO_x, NH₃ requirement for a target stack NO_x emissions level, SCR NO_x removal efficiency, net unit heat rate and ABS deposition. Lower flue gas temperatures were found to improve SCR performance; hence, manipulation of the economizer bypass damper was found ineffective to improve SCR performance at full load. It was found that increasing the NH₃ flow rate in excess of 130 lb/hr, increases the likelihood of exceeding a 2.75 ft. threshold distance from the APH cold-end for ABS deposition. Within this 2.75 ft. distance, ABS removal by sootblowing is greatly enhanced.
- Sootblowing tests were performed to investigate the impact of different sootblowing routines on the operation of the SCR system and associated NO_x reduction and NH₃ consumption. It is recommended a sootblowing schedule that introduces activation of wall blowers (Model IR) at the waterwalls every 10 minutes, alternating blowers from each ring (A, B and C), and retractable blowers (Model IK) every shift; as well as cleaning of the SCR once a shift, and of the APH three times per shift.
- Artificial intelligence techniques were used to model the test data and provide a tool for mathematical optimization. A modified accurate on-line support vector regression (AOSVR) was implemented on the parametric test data to built artificial intelligence-based, functional relationships between the boiler outlet or SCR inlet NO_x level and heat rate penalty. The prediction performance of proposed AOSVR model was adequate. Genetic algorithms (GAs) were used to solve the constrained multi-objective optimization problem with success. An optimal solution is recommended for the lowest cost of compliance, which corresponds to the following control setting: Economizer excess O₂ = 3.2%, average SOFA register opening = 51% (both top- and mid-SOFA registers open equally), average burner tilt angle = -8 degrees, average SOFA tilt angle = +6 degrees, top 1A1-Mill coal flow rate = 6 ton/hr, APH bypass damper = 0% open (completely shut) and an NH₃ injection rate = 125 lb/hr. The optimal NH₃ injection rate represents a reduction in NH₃ flow rate

from baseline conditions of approximately 22 percent. The combination of optimal settings should result in NO_x emissions at the boiler outlet of 0.188 lb/MBtu, while limiting ABS deposition to at less than 2.5 ft. from the APH cold-end, and producing fly ash unburned carbon below 4 percent, at a differential cost of \$41.2/hr. This is the lowest combined (heat rate penalty – and NH₃-related) cost of operation, as compared to a highest cost of close to \$200.00/hr. The savings in net unit heat rate from operation at optimal boiler and APH conditions equate to 54 Btu/kWh as 0.6% from the baseline net unit heat rate.

- A multi-loop control upgrade was proposed to enhance the boiler/SCR/APH control strategy. The multi-loop control approach was complemented with a systematic method for optimal tuning of proportional–integral–derivative (PID) control gains. The SCR control logic that was in use at Cayuga Unit 1 was partially modified to include a scheme that incorporates the feedback measurements implemented in this project (viz, real-time ABS monitoring and deposition tracking). The control system upgrade includes a control strategy provision for the APH bypass damper, by controlling the average cold-end APH temperature to minimize APH fouling/plugging. Additionally, simple dynamic models for the boiler, SCR system, and APH system were identified from the data and proposed to provide coordination of both the SCR and APH control systems to enhance the overall performance of the system. This coordination approach led to the definition of tradeoffs, resolved using extremum-seeking control techniques.
- For future work, two extremum-seeking loops are proposed for real-time optimization at Cayuga Unit 1. The first non-model-based adaptive extremum-seeking controller is proposed to regulate the boiler inputs (O₂, SOFA register opening, burner tilt, SOFA tilt, top mill coal flow) to minimize both NO_x at the SCR inlet and the boiler heat rate penalty. Non-model-based controllers learn from dynamic operating data of the process. This compares to model-based controllers that utilize dynamic models to obtain mathematical conditions between the controller design parameters and tuning rates. The second non-model-based adaptive extremum-seeking controller is proposed to regulate the NH₃ flow to the SCR system and the APH bypass damper opening in order to optimally control in real-time and in a coordinated fashion both, the NO_x at the stack and ABS deposition within the APH. Based on the results obtained during this project, the proposed approach has the potential for further reducing stack NO_x emissions, unit heat rate, NH₃ usage, and provide savings from reduced APH washing frequency.
- Based on the results of this study, it is indicated that modifying the combined operation of the boiler and SCR system can result in savings in reagent usage, heat

rate improvements, and corresponding O&M costs. Estimates were run to calculate the economic benefits of an optimal operation. In addition, other indirect benefits would result from these improvements. These include catalyst life extension, reduction in APH cleaning frequency and costs associated with the loss of unit availability. Other added benefits not considered in the evaluation of benefits include savings due to optimal sootblowing system operation, reduction in fly ash NH₃ contamination, and reduction of sulfur related problems, such as sulfuric acid corrosion and stack visible plume. The estimated annual cost savings for Cayuga Unit 1, due to optimized operation of the boiler/SCR/APH system is of the order of \$748,000. The estimates do not consider that it might be practical for utilities to “over-control” NO_x to sell allowances into the NO_x allowance market.

The results of this analysis are based on a single limited data set. However, these results indicate that there is a significant potential to optimize the combined operation of boiler combustion, SCR system and APH to achieve reduced operating costs.

Section 9
REFERENCES

Ariyur, K., and Krstic, M. Slope Seeking and Application to Compressor Instability Control. *2002 IEEE Conference on Decision and Control*, Las Vegas, Nevada, pp. 3690–3697, Dec. 2002.

Ariyur, K., and Krstic, M. Real-Time Optimization by Extremum Seeking Feedback. Wiley, 2003.

Banaszuk, A., Ariyur, K., Krstic, M., Jacobson, C.A. An Adaptive Algorithm for Control of Combustion Instability. *Automatica* 40 (2004) 1965 – 1972.

Binetti, P., Ariyur, K., Krstic, M., Bernelli, F. Control of Formation Flight Via Extremum Seeking. *2002 American Control Conference*, Anchorage, Alaska, pp. 2848–2853, May 2002.

Choi, J.-Y., Krstic, M., Ariyur, K., and Lee, J.S. Extremum Seeking Control for Discrete-time Systems. *IEEE Transactions on Automatic Control*, vol. 47, no. 2, pp. 318-323, 2002.

Jones, C. Consider SCR an Integral Part of the Combustion Process. *Power*, December 1993.

Breen Energy Solutions. AbSensor – AFP Condensable Anti-Fouling Probe Manual, 2008.

Eskenazi, D., Sarunac, N. and D’Agostini, M. User’s Guide for the HEATRT Code. ERC Report #93-500-1-1, January 1993.

Matlab – the Language of Technical Computing. The Math Works Inc., 1997.

Power Test Code PTC 6.1. The American Society of Mechanical Engineers, New York, 1985.

Romero, C., Li, Y and Bilirgen H. Using Boiler Operating Conditions for Mercury Emissions Control: A Feasibility Study. ERC Report #04-400-11-14, August 2004.

Sarunac, N. and Levy, E. RPHMT – Air Preheater Metal Temperature Code. EPRI Report RP1681/2153, 1989.

Schneider, G., Ariyur, K., Krstic, M. Tuning of a Combustion Controller by Extremum Seeking: A Simulation Study. *Conf. on Decision and Control*, Sydney, Australia, pp.5219–5223, Dec. 2000.

Schuster, E., Morinaga, E., Allen, C.K., and Krstic, M. Optimal Beam Matching in Particle Accelerators via Extremum Seeking. Submitted to the 44th IEEE Conference on Decision and Control, Seville, Spain, 12-15 December 2004.

Smola AJ, Schölkopf B. A Tutorial on Support Vector Regression. Statistics and Computing 2004; 14(4):199-222.

Srinivas N., Deb K. Multiobjective Optimization Using Nondominated Sorting in Genetic Algorithms. Evolutionary Computation 1994; 2(3):221-248.

Wang, H.-H., Krstic, M., and Bastin, G. Optimizing Bioreactors by Extremum Seeking. International Journal of Adaptive Control and Signal Processing, vol. 13, pp. 651–659, 1999.

Wang, H.-H., Yeung, S., Krstic, M. Experimental Application of Extremum Seeking on an Axial-Flow Compressor. IEEE Trans. on Control Systems Technology, vol. 8, pp. 300–309, 2000.

APPENDIX A
CALCULATION OF THE EFFECT OF BOILER
OPERATING CONDITIONS ON UNIT THERMAL PERFORMANCE FROM TEST DATA

BACKGROUND

- In parametric field tests (combustion optimization, boiler tuning, boiler performance tests), the effect of each parameter is typically investigated one at a time (excess O₂ level, damper position, mill bias, burner tilt angle, etc.).
- In addition to the parameter being tested, other operating parameters **unrelated** to the test, such as condenser pressure, make-up flow, cycle extractions, coal quality, slagging and fouling vary during the test.
- Changes in operating parameters **unrelated** to the test can mask the effect of the test parameter.

Parametric test data summarized in Table A-1 show variations occurring in typical parametric tests.

Table A-1: Parametric Test Data.

| Parameter | Test 1 | Test 2 | Test 5 | Test 19 |
|-------------------------------|----------|---------------------|---------------------|--------------------------|
| | Baseline | O ₂ Test | O ₂ Test | SOFA/O ₂ Test |
| P _g [MW] | 94.516 | 94.092 | 94.391 | 93.873 |
| P _{aux} [MW] | 5.066 | 5.102 | 4.869 | 5.060 |
| O ₂ [%] | 2.80 | 2.93 | 1.68 | 2.62 |
| SOFA [%] | 100 | 75 | 75 | 75 |
| CCOFA [%] | 0 | 46 | 46 | 47 |
| Burner Tilt [deg.] | 0 | 0 | 0 | 0 |
| LOI [%] | 8.7 | 11.4 | 19.6 | 18 |
| CO [%] | 11 | 4 | 47 | 7 |
| T _{APH,go} [°F] | 686 | 671 | 646 | 643 |
| M _{MST,Spray} [lb/h] | 1,625 | 2,357 | 1,231 | 4,634 |
| M _{RHT,Spray} [lb/h] | 1,418 | 3,052 | 4,153 | 4,471 |
| T _{MST} [°F] | 1,008.2 | 1,010.6 | 1,011.0 | 1,001.3 |
| T _{RHT} [°F] | 1,010.2 | 1,009.5 | 1,010.3 | 1,010.3 |
| P _{cond} [”Hg] | 1.52 | 1.54 | 1.49 | 1.58 |
| P _{throttle} [psia] | 1,468 | 1,463 | 1472 | 1,458 |
| M _{make-up} [lb/h] | 0 | 3,000 | 4,000 | 6,000 |
| M _{aux,extr} [lb/h] | 0 | 1,000 | 1,500 | 2,500 |

Note: See definition of terms in the List of Abbreviations.

Problem:

How to filter out the effects of extraneous parameters and accurately determine the effects of just the test parameter(s) on heat rate?

HEAT RATE DIFFERENCE METHOD

Description of the Method

To determine the effect of boiler test parameters on unit performance, baseline cycle performance data are corrected for deviations in **relevant** operating parameters (those affected by test parameters) from baseline conditions. This yields changes in heat rate from the baseline value due to the changes in test conditions, by using:

$$HR_{\text{cycle}} = HR_{\text{cycle,BL}} \times CF_{\text{Heat Rate}}$$
$$P_g = P_{g,BL} \times CF_{\text{Load}}$$

Where:

| | |
|-------------------------|---|
| HR_{cycle} | Actual (test) value of cycle heat rate due to change in a test parameter |
| P_g | Actual (test) value of gross unit load due to change in a test parameter |
| $HR_{\text{cycle,BL}}$ | Baseline value of cycle heat rate from turbine thermal kit or baseline test |
| $P_{g,BL}$ | Baseline value of gross unit load from turbine thermal kit or baseline test |
| $CF_{\text{Heat Rate}}$ | Product of correction factors for heat rate for relevant parameters |
| CF_{Load} | Product of correction factors for load for relevant parameters |

CALCULATION PROCEDURE

1. Calculate boiler efficiency from: $\eta_B = Q_{\text{Steam}}/Q_{\text{fuel}}$
2. Determine unit heat rate from: $HR_{\text{net}} = HR_{\text{cycle}} \times P_g / \eta_B (P_g - P_{\text{aux}})$
3. The absolute value of net unit heat rate determined by this approach might differ from the absolute actual net unit heat rate.
4. The relative changes in unit performance due to variations in test parameters are calculated accurately.

RELEVANT OPERATING PARAMETERS

The ASME PTC 6.1 code defines Group 1 and 2 corrections for cycle heat rate and gross unit load:

Cycle Operating Parameters in Group 1:

Top Terminal Temperature Difference
Extraction Line Pressure Drop
Desuperheat Spray
Reheat Spray
Auxiliary Extraction Steam Flow
Condenser Make-Up
Extraction Flow to the Feedwater Pump Turbine

Cycle Operating Parameters in Group 2:

Throttle Pressure
Throttle Temperature
Hot Reheat Temperature
Reheater Pressure Drop
Exhaust Pressure (Condenser Back Pressure)

Correction factors are calculated only for those cycle parameters that are affected by the changes in test parameters. Variations in other parameters, not related to the test, are disregarded. In particular, only the desuperheat and reheat sprays, throttle and hot reheat steam temperatures, and auxiliary steam extraction flow for preheating air entering an APH are affected by changes in test parameters in a combustion optimization test.

NUMERICAL EXAMPLE

- A series a combustion optimization tests is conducted at full load conditions where parameters such as excess oxygen level, SOFA and CCOFA damper settings, and burner tilt angle are parametrically varied one at the time.
- The station does not use a secondary air heater (steam or glycol coils) for inlet air preheating. Auxiliary extraction from cold reheat is used for supplying heat to the tank farm and for building heat.

- Need to determine the heat rate impact of individual test parameters.

Sample test data are presented in Table A-2. Baseline cycle performance is calculated from turbine thermal kit using the average value of main steam flow rate for all tests, $M_{MST,avg}$.

$$M_{MST,avg} = 656.85 \text{ klb/h}$$

Table A-2: Sample Test Data.

| Parameter | Reference Test | O ₂ Test (Test 2) | O ₂ Test (Test 5) | SOFA/O ₂ Test (Test 19) |
|-------------------------------|----------------|------------------------------|------------------------------|------------------------------------|
| O ₂ [%] | 2.80 | 2.93 | 1.68 | 2.62 |
| SOFA [%] | 100 | 75 | 75 | 75 |
| CCOFA [%] | 0 | 46 | 46 | 47 |
| Burner Tilt [deg.] | 0 | 0 | 0 | 0 |
| LOI [%] | 8.7 | 11.4 | 19.6 | 18 |
| CO [%] | 11 | 4 | 47 | 7 |
| T _{APH,go} [°F] | 686 | 671 | 646 | 643 |
| M _{MST,Spray} [lb/h] | 1,625 | 2,357 | 1,231 | 4,634 |
| M _{RHT,Spray} [lb/h] | 1,418 | 3,052 | 4,153 | 4,471 |
| T _{MST} [°F] | 1,008.2 | 1,010.6 | 1,011.0 | 1,001.3 |
| T _{RHT} [°F] | 1,010.2 | 1,009.5 | 1,010.3 | 1,010.3 |
| Boiler Efficiency | 0.8926 | 0.8906 | 0.8856 | 0.8860 |

For the average value of main steam flow rate ($M_{MST,avg}$), the baseline value of the turbine cycle heat rate is $HR_{cycle,BL} = 8,585 \text{ Btu/kWh}$. The baseline value of gross power output is $P_{g,BL} = 94.02 \text{ MW}$. Baseline turbine cycle conditions (from turbine thermal kit) are:

$$\begin{aligned}
 M_{MST,Spray,BL} &= 0 \text{ lb/h} \\
 M_{RHT,Spray,BL} &= 0 \text{ lb/h} \\
 T_{MST,BL} &= 1,010^\circ\text{F} \\
 T_{RHT,BL} &= 1,010^\circ\text{F} \\
 P_{throttle,BL} &= 1,465 \text{ psia} \\
 P_{cond,BL} &= 1.50 \text{ "Hg} \\
 M_{make-up,BL} &= 6,500 \text{ lb/h} \\
 M_{aux. extr,BL} &= 0 \text{ lb/h}
 \end{aligned}$$

Turbine cycle corrections for relevant test parameters and cycle performance (HR_{cycle} and P_g) at test conditions are summarized in Table A-3.

Table A-3: Turbine Cycle Corrections and Cycle Performance.

| Parameter | Reference Test | O ₂ Test Test 2 | O ₂ Test Test 5 | SOFA/O ₂ Test Test 19 |
|--|----------------|----------------------------|----------------------------|----------------------------------|
| Cycle Corrections for Heat Rate | | | | |
| CF for $M_{MST,Spray}$ | 1.0001 | 1.0001 | 1.0000 | 1.0002 |
| CF for $M_{RHT,Spray}$ | 1.0004 | 1.0009 | 1.0013 | 1.0013 |
| CF for T_{MST} | 1.0002 | 0.9999 | 0.9999 | 1.0011 |
| CF for T_{RHT} | 1.0000 | 1.0001 | 1.0000 | 1.0000 |
| CF _{Heat Rate} = ΠCF_i | 1.0007 | 1.0010 | 1.0012 | 1.0026 |
| HR_{cycle} [Btu/kWh] | 8,591 | 8,593 | 8,594 | 8,607 |
| Cycle Corrections for Unit Load | | | | |
| CF for $M_{MST,Spray}$ | 1.0002 | 1.0003 | 1.0001 | 1.0005 |
| CF for $M_{RHT,Spray}$ | 1.0013 | 1.0027 | 1.0037 | 1.0040 |
| CF for T_{MST} | 1.0003 | 0.9999 | 0.9999 | 1.0014 |
| CF for T_{RHT} | 1.0001 | 0.9998 | 1.0002 | 1.0001 |
| CF _{Load} = ΔCF_i | 1.0019 | 1.0027 | 1.0039 | 1.0060 |
| P_g [MW] | 94.195 | 94.271 | 94.384 | 94.582 |

RESULTS

Using the results from Table 3 and the expression for HR_{net} to calculate performance at test conditions. The results are summarized in Table A-4.

Table A-4: Effect of Boiler Test Parameters on Unit Heat Rate.

| Parameter | Reference Test | O ₂ Test Test 2 | O ₂ Test Test 5 | SOFA/O ₂ Test Test 19 |
|------------------------------------|----------------|----------------------------|----------------------------|----------------------------------|
| HR_{net} [Btu/kWh] | 10,172 | 10,201 | 10,232 | 10,264 |
| ΔHR_{net} [Btu/kWh] | 0 | 29 | 60 | 92 |

APPENDIX B
CAYUGA UNIT 1 TEST MATRIX

Table 1: Cayuga Unit 1 Test Matrix

| Test | Description | Load | Econ. O ₂ | TOP SOFA | | MIDDLE SOFA | | BOTTOM SOFA | | Top Mill (IA1) Loading | Economizer Bypass Damper Opening | Air-Preheater Bypass Damper Opening | NO _x | NH ₃ |
|---------|-------------------------------------|------|----------------------|----------|----|-------------|------|-------------|---|------------------------|----------------------------------|-------------------------------------|-----------------|-----------------|
| | | | | % | % | % | % | % | % | | | | | |
| BASE 1 | Baseline (12:15-13:15) | 150 | 3.27 | 1 | 10 | 74 | 15.9 | 1 | 0 | 0.222 | 159.8 | | | |
| BASE 2 | Baseline (9:45-10:45) | 150 | 3.30 | 1 | 10 | 75 | 15.9 | 1 | 0 | 0.234 | 161.4 | | | |
| TEST 3 | O ₂ Test (11:00 - 12:00) | 150 | 3.60 | 1 | 10 | 75 | 15.9 | 1 | 0 | 0.246 | 172.4 | | | |
| TEST 4 | O ₂ Test (13:30 - 14:30) | 150 | 3.00 | 1 | 10 | 75 | 16.0 | 1 | 0 | 0.214 | 149.9 | | | |
| TEST 5 | O ₂ Test (4:30 - 15:30) | 150 | 2.70 | 1 | 10 | 75 | 16.0 | 1 | 0 | 0.198 | 137.0 | | | |
| TEST 6 | O ₂ Test (15:30 - 16:30) | 150 | 2.85 | 1 | 10 | 75 | 15.9 | 1 | 0 | 0.202 | 140.1 | | | |
| BASE 7 | SOFA Test (8:30 - 9:30) | 150 | 3.24 | 1 | 11 | 76 | 14.9 | 0 | 1 | 0.211 | 138.0 | | | |
| TEST 8 | SOFA Test (11:00 - 12:00) | 150 | 3.30 | 99 | 97 | 3 | 15.0 | 0 | 0 | 0.174 | 109.8 | | | |
| TEST 9 | SOFA Test (12:00 - 12:20) | 150 | 3.27 | 75 | 75 | 3 | 15.0 | 0 | 0 | 0.172 | 109.8 | | | |
| TEST 10 | SOFA Test (13:00 - 14:20) | 150 | 3.31 | 49 | 50 | 4 | 15.0 | 0 | 0 | 0.187 | 117.9 | | | |
| TEST 11 | SOFA Test (14:00 - 14:50) | 150 | 3.22 | 23 | 23 | 4 | 14.9 | 0 | 0 | 0.226 | 148.9 | | | |
| TEST 12 | SOFA Test (14:50 - 15:50) | 150 | 3.27 | 1 | 1 | 4 | 14.9 | 0 | 0 | 0.268 | 183.7 | | | |
| TEST 13 | SOFA Test (15:50 - 16:30) | 150 | 2.96 | 2 | 2 | 5 | 14.9 | 0 | 0 | 0.251 | 173.7 | | | |
| TEST 14 | SOFA Test (16:30 - 17:05) | 150 | 3.03 | 25 | 25 | 5 | 14.9 | 0 | 0 | 0.214 | 143.5 | | | |
| TEST 15 | SOFA Test (17:05 - 17:45) | 150 | 2.96 | 51 | 49 | 5 | 14.8 | 0 | 0 | 0.179 | 113.4 | | | |
| TEST 16 | SOFA Test (17:45 - 18:50) | 150 | 3.02 | 98 | 97 | 5 | 14.8 | 0 | 0 | 0.165 | 99.3 | | | |

Table 1: Cayuga Unit 1 Test Matrix (Cont.)

| Test | Description | Load | Econ. O ₂ | TOP SOFA | MIDDLE SOFA | BOTTOM SOFA | Top Mill (IAI) Loading | Economizer Bypass Damper Opening | Air-Preheater Bypass Damper Opening | NO _x | NH ₃ |
|---------|-----------------------------------|--------------------------|----------------------|----------|-------------|-------------|------------------------|----------------------------------|-------------------------------------|-----------------|-----------------|
| | | MW | % | % | % | % | t/h | % | % | lbs/MMBtu | kbs/h |
| BASE 17 | Baseline (7:20 - 8:45) | 150 | 3.32 | 1 | 10 | 75 | 15.4 | 0 | 0 | 0.230 | 160.3 |
| TEST 18 | Air-Preheater Bypass Damper Tests | 150 | 3.29 | 2 | 10 | 75 | 15.5 | 0 | 28 | 0.223 | 157.9 |
| TEST 19 | | 150 | 3.36 | 2 | 10 | 75 | 15.8 | 0 | 50 | 0.221 | 152.8 |
| TEST 20 | | 150 | 3.35 | 2 | 10 | 75 | 15.5 | 0 | 75 | 0.218 | 153.3 |
| TEST 21 | | 150 | 3.27 | 2 | 10 | 75 | 15.6 | 0 | 14 | 0.221 | 155.1 |
| TEST 22 | | 150 | 3.44 | 69 | 70 | 5 | 15.5 | 0 | 0 | 0.183 | 122.5 |
| TEST 23 | | 150 | 3.34 | 69 | 70 | 5 | 15.6 | 0 | 15 | 0.181 | 119.3 |
| TEST 24 | | 150 | 3.49 | 69 | 70 | 5 | 15.5 | 0 | 25 | 0.183 | 119.6 |
| TEST 25 | | 150 | 3.34 | 69 | 70 | 5 | 15.5 | 0 | 50 | 0.175 | 116.8 |
| TEST 26 | | 150 | 3.48 | 68 | 70 | 5 | 15.5 | 0 | 75 | 0.182 | 119.5 |
| BASE 27 | | Baseline (12:30 - 12:45) | 150 | 3.34 | 1 | 10 | 75 | 15.5 | 0 | 0 | 0.223 |
| TEST 28 | Burner+SOFA Tilt (12:50 - 13:15) | 150 | 3.27 | 1 | 10 | 75 | 15.4 | 0 | 0 | 0.217 | 157.8 |
| TEST 29 | Burner+SOFA Tilt (13:15-13:40) | 150 | 3.22 | 1 | 10 | 75 | 15.3 | 0 | 0 | 0.215 | 156.9 |
| TEST 30 | Burner+SOFA Tilt (13:42-14:15) | 150 | 3.21 | 1 | 10 | 75 | 15.5 | 0 | 0 | 0.219 | 160.8 |
| TEST 31 | Burner+SOFA Tilt (14:20-14:55) | 150 | 3.34 | 70 | 70 | 5 | 15.6 | 0 | 0 | 0.178 | 126.8 |
| TEST 32 | Burner+SOFA Tilt (15:00-16:15) | 150 | 3.31 | 70 | 69 | 5 | 15.7 | 0 | 0 | 0.180 | 126.7 |
| TEST 33 | Burner+SOFA Tilt (16:15-16:45) | 150 | 3.42 | 70 | 69 | 4 | 15.8 | 0 | 0 | 0.188 | 129.9 |
| TEST 34 | Burner+SOFA Tilt (16:45-17:10) | 150 | 3.83 | 70 | 69 | 4 | 15.7 | 0 | 0 | 0.194 | 132.1 |
| TEST 35 | Burner+SOFA Tilt (15:15-17:40) | 150 | 3.65 | 70 | 69 | 4 | 15.7 | 0 | 0 | 0.192 | 134.7 |
| TEST 36 | Burner+SOFA Tilt (17:49-18:10) | 150 | 3.71 | 70 | 69 | 4 | 15.6 | 0 | 0 | 0.185 | 131.9 |

Table 1: Cayuga Unit 1 Test Matrix (Cont.)

| Test | Description | Load MW | Econ. O ₂ % | TOP SOFA % | MIDDLE SOFA % | BOTTOM SOFA % | Top Mill (1A1) Loading t/h | Economizer Bypass Damper Opening % | Air-Preheater Bypass Damper Opening % | NO _x lbs/MMBtu | NH ₃ klbs/h |
|---------|--|------------|------------------------------|------------------|---------------------|---------------------|-------------------------------------|---|--|------------------------------|---------------------------|
| | | | | | | | | | | | |
| BASE 37 | Baseline (11:00 - 11:45) | 150 | 3.28 | 1 | 9 | 74 | 15.9 | 0 | 0 | 0.214 | 157.5 |
| TEST 38 | Burner+SOFA Tilt (11:45-12:15) | 150 | 3.36 | 1 | 9 | 73 | 15.9 | 0 | 0 | 0.215 | 156.8 |
| TEST 39 | Burner+SOFA Tilt (12:15-12:45) | 150 | 3.51 | 69 | 70 | 1 | 15.9 | 0 | 0 | 0.194 | 135.0 |
| TEST 40 | Burner+SOFA Tilt (12:45-12:53) | 150 | 3.87 | 69 | 70 | 1 | 15.8 | 0 | 0 | 0.213 | 143.7 |
| TEST 41 | Burner+SOFA Tilt (13:50-14:15) | 150 | 3.55 | 69 | 70 | 1 | 15.8 | 0 | 0 | 0.180 | 120.5 |
| TEST 42 | Burner+SOFA Tilt (14:15-15:10) | 150 | 3.59 | 69 | 70 | 1 | 15.9 | 0 | 0 | 0.193 | 137.8 |
| TEST 43 | Burner+SOFA Tilt (15:10-15:55) | 150 | 3.50 | 69 | 70 | 1 | 15.6 | 0 | 0 | 0.180 | 121.6 |
| TEST 44 | Burner+SOFA Tilt (15:58-16:50) | 150 | 3.56 | 69 | 70 | 1 | 16.1 | 0 | 0 | 0.182 | 124.5 |
| TEST 45 | Mill Bias (21:30 - 22:30) | 150 | 3.33 | 69 | 71 | 1 | 10.1 | 0 | 0 | 0.168 | 107.6 |
| TEST 46 | Mill Bias (23:30 - 24:00) | 150 | 4.28 | 69 | 71 | 2 | 0.2 | 0 | 0 | 0.141 | 71.5 |
| BASE 47 | Baseline (8:35 - 9:30) | 150 | 3.52 | 2 | 11 | 74 | 16.2 | 0 | 0 | 0.212 | 148.1 |
| TEST 48 | Low-NO _x Baseline (9:30 - 10:00) | 150 | 3.58 | 69 | 69 | 1 | 16.0 | 0 | 0 | 0.184 | 128.8 |
| TEST 49 | Econ. Bypass (10:00 - 10:30) | 150 | 3.51 | 69 | 69 | 1 | 15.9 | 5 | 0 | 0.182 | 123.6 |
| TEST 50 | Econ. Bypass (10:30 - 11:00) | 150 | 3.61 | 70 | 70 | 1 | 15.9 | 15 | 0 | 0.188 | 125.7 |
| TEST 51 | Econ. Bypass (11:00-11:30) | 150 | 3.57 | 70 | 70 | 1 | 15.8 | 28 | 0 | 0.189 | 122.3 |
| TEST 52 | Econ. Bypass (11:50 - 12:20) | 150 | 3.56 | 70 | 70 | 1 | 16.3 | 40 | 0 | 0.202 | 128.4 |

Table 1: Cayuga Unit 1 Test Matrix (Cont.)

| Test | Description | Load MW | Econ. O ₂ % | TOP SOFA % | MIDDLE SOFA % | BOTTOM SOFA % | Top Mill (1A1) Loading t/h | Economizer Bypass Damper Opening % | Air-Preheater Bypass Damper Opening % | NO _x lbs/MMBtu | NH ₃ klbs/h |
|---------|---|------------|------------------------------|------------------|---------------------|---------------------|-------------------------------------|---|--|------------------------------|---------------------------|
| | | | | | | | | | | | |
| TEST 53 | Econ. Bypass (12:25-13:45) | 150 | 3.54 | 70 | 70 | 1 | 15.8 | 0 | 0 | 0.177 | 118.7 |
| TEST 54 | Econ. Bypass (13:58-14:45) | 150 | 3.38 | 70 | 70 | 0 | 15.7 | 40 | 0 | 0.192 | 120.1 |
| TEST 55 | Coal Air Temp. (14:25 - 15:30) | 150 | 3.30 | 70 | 70 | 0 | 15.9 | 0 | 0 | 0.177 | 113.6 |
| TEST 56 | Coal Air Temp. (15:30 - 16:15) | 150 | 3.40 | 70 | 70 | 0 | 15.4 | 0 | 0 | 0.175 | 112.6 |
| TEST 57 | Coal Air Temp. (16:20 - 17:05) | 150 | 3.46 | 70 | 70 | 0 | 15.4 | 0 | 0 | 0.173 | 113.8 |
| TEST 58 | Sootblowing (17:10 - 18:35) | 150 | 3.38 | 70 | 70 | 0 | 15.5 | 0 | 0 | 0.176 | 116.9 |
| BASE 59 | Sootblowing (8:50 - 9:30) | 150 | 3.32 | 2 | 10 | 75 | 15.5 | 0 | 0 | 0.216 | 150.9 |
| TEST 60 | Sootblowing (9:30-10:35) | 150 | 3.29 | 69 | 70 | 0 | 15.3 | 0 | 0 | 0.174 | 116.2 |
| TEST 61 | Sootblowing (10:51 - 13:30) | 150 | 3.32 | 69 | 69 | 0 | 15.5 | 0 | 0 | 0.173 | 111.9 |
| TEST 62 | Sootblowing (14:28 - 16:10) | 150 | 3.27 | 69 | 69 | 0 | 15.4 | 0 | 0 | 0.174 | 109.5 |
| TEST 63 | Sootblowing (16:28 - 18:15) | 150 | 3.34 | 69 | 68 | 1 | 15.4 | 0 | 0 | 0.185 | 116.8 |
| BASE 64 | Baseline (8:50 - 9:50) | 150 | 3.21 | 1 | 11 | 73 | 18.8 | 0 | 0 | 0.201 | 109.7 |
| TEST 65 | Bottom Mill O/S (9:53 - 10:40) | 150 | 3.08 | 70 | 70 | 0 | 18.9 | 0 | 0 | 0.163 | 80.0 |
| TEST 66 | Sootblowing (11:10 - 15:10) | 150 | 3.22 | 70 | 70 | 0 | 15.5 | 0 | 0 | 0.175 | 107.9 |
| BASE 67 | Baseline (11:00 -11:30) | 150 | 3.1 | 1 | 10 | 73 | 15.6 | 0 | 1 | 0.214 | 145.1 |
| TEST 68 | Low-NO _x Baseline (11:30-12:00) | 150 | 3.3 | 70 | 69 | 1 | 15.5 | 0 | 1 | 0.186 | 117.6 |
| TEST 69 | Sootblowing (12:00-16:15) | 150 | 3.3 | 70 | 69 | 1 | 15.5 | 0 | 1 | 0.181 | 114.6 |

Table 1: Cayuga Unit 1 Test Matrix (Cont.)

| Test | Description | Load MW | Econ. O ₂ % | TOP SOFA % | MIDDLE SOFA % | BOTTOM SOFA % | Top Mill (LA1) Loading t/h | Economizer Bypass Damper Opening % | Air-Preheater Bypass Damper Opening % | NO _x lbs/MMBtu | NH ₃ klbs/h |
|---------|---------------------------------------|------------|------------------------------|------------------|---------------------|---------------------|-------------------------------------|---|--|------------------------------|---------------------------|
| | | | | | | | | | | | |
| BASE 70 | Baseline (8:15 - 8:30) | 150 | 3.4 | 1 | 11 | 73 | 15.9 | 0 | 0 | 0.205 | 130.4 |
| TEST 71 | Low-NOx Baseline (8:00-9:00) | 150 | 3.3 | 70 | 69 | 1 | 15.9 | 0 | 0 | 0.175 | 107.4 |
| TEST 72 | Mill Bias+O2 (19:45-10:00) | 150 | 3.2 | 70 | 69 | 1 | 12.1 | 0 | 0 | 0.164 | 101.5 |
| TEST 73 | Mill Bias+O2 (10:40-10:55) | 150 | 3.0 | 70 | 69 | 1 | 11.8 | 0 | 0 | 0.160 | 95.7 |
| TEST 74 | Mill Bias+O2 (11:45-12:00) | 150 | 3.0 | 70 | 69 | 1 | 9.0 | 0 | 0 | 0.156 | 92.3 |
| TEST 75 | Mill Bias+O2 (12:00-13:00) | 150 | 3.3 | 70 | 69 | 1 | 8.9 | 0 | 0 | 0.162 | 96.5 |
| TEST 76 | Mill Bias+O2 (13:00-14:00) | 150 | 3.4 | 70 | 70 | 1 | 6.4 | 0 | 0 | 0.160 | 96.2 |
| TEST 77 | Mill Bias+O2 (14:00-15:00) | 150 | 3.1 | 70 | 70 | 1 | 6.4 | 0 | 0 | 0.157 | 92.8 |
| TEST 78 | Sootblowing (16:10-18:30) | 150 | 3.3 | 70 | 70 | 1 | 15.7 | 0 | 0 | 0.178 | 110.9 |
| BASE 79 | Baseline (7:45-8:00) | 150 | 3.1 | 1 | 11 | 75 | 16.2 | 0 | 0 | 0.216 | 144.8 |
| TEST 80 | Sootblowing (8:10-13:20) | 150 | 3.3 | 70 | 69 | 0 | 16.2 | 0 | 0 | 0.182 | 115.4 |
| BASE 81 | Baseline (22:30-24:00) | 100 | 4.29 | 2 | 25 | 0 | 10.9 | 33 | 43 | 0.258 | 163.1 |
| TEST 82 | O ₂ +SOFA (0:00 - 1:00) | 100 | 4.35 | 24 | 25 | 0 | 10.9 | 33 | 49 | 0.259 | 152.5 |
| TEST 83 | O ₂ +SOFA (1:00 - 1:45) | 100 | 4.16 | 25 | 25 | 0 | 10.7 | 33 | 45 | 0.255 | 146.6 |
| TEST 84 | O ₂ +SOFA (1:45 - 2:45) | 100 | 4.31 | 1 | 1 | 0 | 10.5 | 32 | 48 | 0.258 | 163.7 |
| TEST 85 | O ₂ +SOFA (2:45 - 4:00) | 100 | 4.42 | 1 | 1 | 0 | 0.4 | 32 | 58 | 0.258 | 126.1 |
| TEST 86 | O ₂ +SOFA (4:00 - 5:00) | 100 | 4.40 | 24 | 25 | 0 | 0.4 | 32 | 58 | 0.258 | 108.8 |

Table 1: Cayuga Unit 1 Test Matrix (Cont.)

| Test | Description | Load MW | Econ. O ₂ % | TOP SOFA % | MIDDLE SOFA % | BOTTOM SOFA % | Top Mill (LA1) Loading t/h | Economizer Bypass Damper Opening % | Air-Preheater Bypass Damper Opening % | NO _x lbs/MMBtu | NH ₃ klbs/h |
|----------|---|------------|------------------------------|------------------|---------------------|---------------------|-------------------------------------|---|--|------------------------------|---------------------------|
| | | | | | | | | | | | |
| TEST 87 | O ₂ ⁺ SOFA (22:15-23:15) | 100 | 4.40 | 49 | 49 | 0 | 0.2 | 33 | 52 | 0.259 | 92.9 |
| TEST 88 | O ₂ ⁺ SOFA (23:15 - 24:00) | 100 | 4.10 | 49 | 49 | 0 | 0.2 | 34 | 52 | 0.253 | 91.2 |
| TEST 89 | O ₂ ⁺ SOFA (0:00 - 0:30) | 100 | 4.13 | 49 | 49 | 0 | 0.3 | 49 | 50 | 0.253 | 91.2 |
| TEST 90 | O ₂ ⁺ SOFA (0:30 - 1:30) | 100 | 4.11 | 49 | 49 | 0 | 0.3 | 25 | 53 | 0.254 | 91.4 |
| TEST 91 | O ₂ ⁺ SOFA (1:30 - 2:30) | 100 | 4.46 | 14 | 14 | 1 | 0.4 | 33 | 50 | 0.259 | 103.7 |
| TEST 92 | O ₂ ⁺ SOFA (2:30 - 3:30) | 100 | 4.49 | 1 | 0 | 1 | 0.4 | 33 | 47 | 0.260 | 111.3 |
| BASE 93 | Baseline (23:30 - 23:45) | 75 | 5.46 | 1 | 2 | 0 | 0.1 | 100 | 0 | 0.275 | 142.7 |
| TEST 94 | O ₂ ⁺ SOFA (0:00 - 0:45) | 75 | 5.26 | 5 | 5 | 0 | 0.3 | 100 | 1 | 0.271 | 141.7 |
| TEST 95 | O ₂ ⁺ SOFA (1:25 - 2:10) | 75 | 5.22 | 11 | 10 | 0 | 0.3 | 100 | 1 | 0.271 | 139.9 |
| TEST 96 | O ₂ ⁺ SOFA (2:30 - 3:15) | 75 | 5.27 | 14 | 15 | 0 | 0.3 | 100 | 1 | 0.272 | 136.3 |
| TEST 97 | O ₂ ⁺ SOFA (3:40 - 4:25) | 75 | 5.22 | 15 | 15 | 0 | 0.3 | 100 | 1 | 0.272 | 132.5 |
| BASE 98 | Baseline (22:45 - 23:50) | 75 | 5.85 | 1 | 1 | 0 | 0.0 | 100 | 0 | 0.279 | 139.3 |
| TEST 99 | O ₂ ⁺ SOFA (00:30 - 2:15) | 75 | 5.07 | 2 | 2 | 0 | 0.0 | 100 | 0 | 0.267 | 149.1 |
| TEST 100 | O ₂ ⁺ SOFA (3:04 - 3:45) | 75 | 5.15 | 16 | 15 | 0 | 0.0 | 100 | 0 | 0.267 | 141.4 |
| TEST 101 | O ₂ ⁺ SOFA (4:00 - 4:25) | 75 | 5.14 | 20 | 19 | 0 | 0.0 | 100 | 0 | 0.268 | 139.1 |
| TEST 102 | O ₂ ⁺ SOFA (4:26 - 5:10) | 75 | 5.31 | 24 | 25 | 0 | 0.0 | 100 | 0 | 0.270 | 141.1 |

For information on other
NYSERDA reports, contact:

New York State Energy Research
and Development Authority
17 Columbia Circle
Albany, New York 12203-6399

toll free: 1 (866) NYSERDA
local: (518) 862-1090
fax: (518) 862-1091

info@nysesda.org
www.nysesda.org

**OPTIMIZATION OF SCR CONTROL TECHNOLOGY FOR REDUCED NO_x
EMISSIONS, IMPROVED PERFORMANCE AND REDUCED OPERATING EXPENSES**

FINAL REPORT 09-09

**STATE OF NEW YORK
DAVID A PATERSON, GOVERNOR**

**NEW YORK STATE ENERGY RESEARCH AND DEVELOPMENT AUTHORITY
VINCENT A. DEIORIO, ESQ., CHAIRMAN
FRANCIS J. MURRAY, JR., PRESIDENT, AND CHIEF EXECUTIVE OFFICER**

